QUANTUM DISSIPATION FROM PHONONS; METALLIC HYDROGEN; ELECTRON-ION MIXTURES

A Dissertation

Presented to the Faculty of the Graduate School

of Cornell University

in Partial Fulfillment of the Requirements for the Degree of

Doctor of Philosophy

by

Adriaan Anthony Louis

January 1998

QUANTUM DISSIPATION FROM PHONONS; METALLIC HYDROGEN;

ELECTRON-ION MIXTURES

Adriaan Anthony Louis, Ph.D.

Cornell University 1998

This thesis covers a number of different topics: atomic tunneling with dissipation, the metallization of liquid hydrogen, universality of electron-ion structure factors and non-linear response theory:

Chapter 2 discusses how a phonon environment can *qualitatively* change the tunneling behaviour of an atom.

Chapter 3 gives an overview of theoretical questions related to dense fluid metallic hydrogen, as recently discovered by Bill Nellis and co-workers.

Chapter 4 shows how and why the response of a single atom in an electron gas is well approximated by linear plus second order response.

Chapter 5 demonstrates that electron-ion correlations functions $S_{eI}(k)$ fall either into the *low valence* or *high valence* classes for liquid metals.

Chapter 6 establishes some exact results for pseudo-atom densities and effective ion-ion potentials.

Biographical Sketch

I was born in Utrecht, the Netherlands, to Marijke Eva and Adriaan Mels Louis, who soon took me to Africa, the most beautiful continent on earth. There I attended Bongolo Alliance School on an isolated little mountain in the pristine Gabon rain-forest. For high school I first attended Ivory Coast Academy, Cote d'Ivoire, where I majored in soccer, initiation pranks and having fun, and finished up at the (smore academically challenging) International School of Beverweerd (in a 14th century Dutch castle!). My Drs. degree at the Rijks Universiteit Utrecht was in theoretical physics and soon afterwards I set foot on US soil (August 1992) and have lived in Ithaca ever since. After a long-awaited 3-month trip around the world, mainly visiting friends I've made at Cornell[1], I'm returning to the old world as a post-doc at Cambridge U, (UK) in January 1998.

[1] but also, perhaps to atone for the forest of trees devoured by the endless drafts of this thesis, a one-month stint working for Gabon Vert, an enviromental consulting company specializing in preservation of African rain-forests (pour un environnement en forme)

Dedicated to my parents,

Acknowledgements

"I give you thanks, Creator and God, that you have given me this joy in thy creation, and I rejoice in the works of your hands. See I have now completed the work to which I was called. In it I have used all the talents you have lent to my spirit."

–Johannes Kepler[2] –

"Science is the most jealous of mistresses!"

–Isaac Pomeranchuk[3]–

Writing acknowledgments is like trying to describe an excellent red wine. Myriads of well worn phrases exist, but just as words never fully capture the experience of a luscious Bordeaux, so our feeble acknowledgments of thanks but dimly reflect what people have meant in our lives. The last 5 years at Cornell have been among the happiest in an otherwise blissful life. The reason for this is not the Ithaca weather or even the beautiful scenery, but the multitudes of kind, friendly and stimulating people that crossed my path here. Expressing that in words is frustrating, they always fall short. On the other hand, acknowledgments are the only part of a thesis most people read, so here goes:

I've had the privilege of working with three different advisors, each of whom brought just what I needed at that stage in my career:

First and foremost, I'd like to thank my thesis advisor Neil Ashcroft. I feel very honored to have been his advisee and profit from his seemingly inexhaustible knowledge of condensed matter physics, his sharp insights, his generosity, and his careful and tactful guidance ("Let's see Ard, what's the physics here?"). I always looked forward to our Monday morning discussions which taught me about much more of the world than physics alone, and hope we can continue to collaborate together from Cambridge.

[2] Cited in Christopher Kaiser, *Creation and the History of Science* (Eerdmans, Grand Rapids (1991)), p127.

[3] Cited in Yuri Orlov, *Dangerous Thoughts: Memoirs of a Russian Life*, (William Morrow and Company, New York (1991)), p112

Jim Sethna infected me with some of his boundless enthusiasm for physics, taught me a great deal about how to understand complicated problems in simple terms, and showed me how to have fun doing research. His guidance during my first two years here was exactly what I needed at that time, and I am very grateful for all his input and support.

Daan Frenkel was my first mentor in physics and I spent a very exciting and enjoyable few months working in his group in Amsterdam, trying to prove that entropy was really everything and getting my feet wet in that delightful process of generating new knowledge we call research. I look back with special fondness on our many late afternoon sessions in front of the white-board, where Daan taught me that asking the right questions is as important as knowing their answers.

I've also appreciated John Reppy's patience and good humor and thank him for serving on my special committee, and the Material Science Center through which the NSF funded me at Cornell (grant DMR96-24-8330).

Bill Nellis very kindly offered me the opportunity to write a paper with him on the fluid metallic phase of hydrogen that he discovered. I thoroughly enjoyed working with him, and thank him for his hospitality on my visit to Livermore. I also thank Bill Magro for teaching me much about hydrogen and path integral Monte Carlo. I thank Peter Edwards for reading through my thesis and for his useful advice. Karsten Jacobsen was also a great help on the project that fills the last three chapters of this thesis and I thank him for that.

Before I came to the US, an eminent American physics professor I hoped to work for advised me to go to the best school possible because I'd learn more from my fellow students than from anything else. Whether he said this out of altruism or to tactfully get rid of me remains to be seen, but I took his advice and came to Cornell. He was right, and I'd like to thank the many denizens of Clark and it's environs for creating such a stimulating (sorry ... using that word again), environment. Andone, Bill W, Bill E, Byard, Bruce, Dave, Iya, Jan von Delft, Geoff, Ivan, Jane', Jeff, Karen, Kurt, Lisa, Matej, Olga, Shashi and Tom immediately spring to mind. And of course thanks to my officemates, Alex, Badri, Mike and Wei-Jing, who provided many pleasant distractions, and helped make 535 the happening place to be. Special thanks go to Wei-Jing for being a good friend, consistently providing the office with food, and for being such a good sport when I threw him into the swimming pool and booby-trapped the bridal suite at his wedding.

But life here has been much more than physics alone. At the risk of missing some key people, I still would like to thank:

Prof. Dick Baer for the animated discussions about everything under the sun during many pleasant lunches at his house. The many members of the Cornell International Christian Fellowship (CICF) for all their love and support (and all the CICF alumni I'm visiting around the world in the next few months for their willingness to host me). I think especially of the new servant team: Keithanne, June, Lynette, Poline, Tak and Wayne, and also Simeon, Cattyann and Romulus. I thank Edith for always opening her house and heart to us, and Chuck Tompkins for all his support and encouragement. I thank Ned Hale for inviting me to share our CICF vision and experience at many I-student conferences around the country. I also thank the many members of GradIV for their friendship and the HGC for all their care and friendship, and for teaching me how to clap on the right beat and appreciate soul food. Special thanks go to my close friends Dave H, Nathan, Peter, Paul, Sebastian, Jarvis, Rod, Kazuo, and Tak with whom (at different times in my stay here) I met with on a regular basis to my great benefit. Thanks to Peter for dragging me to El-Salvador and Jamaica for great bike trips, and for being such a good friend. Jarvis has been a great friend, I think back with special fondness on being a tag team in all the discussions and Bible-studies we led on racial-reconciliation and much more. I will definitely miss Tak, Sebastian Rod and Nathan, after I leave, and look forward to seeing Kazuo in Japan, and being re-united with Paul in England. Thanks also to my housemates, Keithanne, Paul, Seb, Nancy, Dwight, Greg, Jarvis ... for making 303 such a warm and pleasant home. Special thanks also to Sarah Strzelec for her friendship and for being so fun. And lastly, to my sister Imke, all my love and thanks for her support, friendship and entertainment, and to my parents, for always believing in me, supporting me, but best of all being an example of all I could aspire to, in character, in actions and faith in God.

Table of Contents

List of Tables

List of Figures

Chapter 1

Introduction and Overview

In this thesis I discuss a number of different topics: atomic tunneling with dissipation, the metallization of liquid hydrogen, universality of electron-ion structure factors and non-linear response theory:

Chapter 2 discusses how a a phonon environment can *qualitatively* change the tunneling behaviour of an atom.

Chapter 3 gives an overview of theoretical questions related to dense liquid metallic hydrogen, as recently discovered by Bill Nellis and co-workers.

Chapter 4 shows how and why the response of a single atom in an electron gas is well approximated by linear + second order response.

Chapter 5 demonstrates that electron-ion correlations functions $S_{eI}(k)$ fall either into the *low valence* or *high valence* classes for liquid metals.

Chapter 6 establishes some exact results for pseudo-atoms and effective ion-ion potentials.

Chapter 2

Atomic Tunneling from a STM/AFM Tip: Dissipative Quantum Effects from Phonons

2.1 Introduction

We study the effects of phonons on the tunneling of an atom between two surfaces[1]. In contrast to an atom tunneling between two positions in the bulk material, the phonons couple very strongly to the atom, qualitatively changing the tunneling behavior. This is the first example of dissipative *ohmic* coupling from phonons for a two-state system. We propose an experiment in which an atom tunnels from the tip of an STM, and show how its behavior would be similar to the Macroscopic Quantum Coherence behavior predicted for SQUIDS. An ability to tune and calculate many parameters would lead to detailed tests of the standard theories[1].

[1] A general introduction for non-specialist can be found on the web at: http://www.lassp.cornell.edu/ ardlouis/dissipative/QAtunneling.html.

The fascinating experiments carried out by Eigler and colleagues[2, 3, 4, 5] have demonstrated that scanning tunneling microscopy can be used not only for imaging, but also to directly demonstrate fundamental aspects of quantum mechanics. Inspired by their success, we propose an experiment to test the effect of a dissipative environment on a quantum mechanical system. While often ignored in many applications of quantum mechanics, the environment can have important effects on a simple quantum system. In fact, from the dawn of quantum mechanics, the collapse of the wavefunction has been attributed to the interaction of a quantum system with a macroscopic environment[6]. Numerous authors have shown how interactions with an external environment can wipe out measurable effects of off-diagonal elements of the density matrix and as such give a plausible mechanism for the wave-function collapse process. In its modern form this idea is called decoherence[7] and is currently receiving renewed interest in its applications to the study of quantum computing. However, this in no way solves the measurement problem as many authors assert. Even if one were to solve the quantum mechanics of a sub-system interacting with a measuring device (for example a two-state system with two states, up and down), this leaves unanswered the question: why did measurement A produce an up-state and measurement B a down-state; what broke the symmetry? This in contrast to the spontaneous breaking of symmetry in a classical system (for example an Ising model with no external field) which could always (in principle) be traced back to a thermal fluctuation. With this caveat in mind, it is clear that understanding how an environment "collapses" a wave-function is still of great importance to understanding the measurement problem – but it doesn't solve it, it only pushes back the boundary of ignorance. As recently emphasized by Leggett[8], condensed–matter physics provides a natural laboratory for studying this: how does the surrounding macroscopic crystalline environment change the behavior of an embedded quantum system to which it is coupled? In particular, what can realistic models of the environment tell us?

A tantalizing view of the importance of the environment is given by the "overlap catastrophe"[9]. In a metal, the conduction electrons must be rearranged when a quantum subsystem changes state: the initial and final electron ground–state wavefunctions are so different that the bath of conduction electrons can force the subsystem to dissipate energy during each transition, or even keep the transition from occurring at all. In this chapter, we show that phonons, an environment even more ubiquitous than conduction electrons, can also cause an overlap catastrophe. In particular, we demonstrate that quantum tunneling behavior between two surfaces can be dramatically altered by the coupling to phonons. We show how detailed calculations of the macroscopic quantum coherence (MQC) community [10] could be tested experimentally in an admittedly microscopic system using the tunneling of atoms onto and off of the tip of a scanning tunneling microscope (STM) or atomic force microscope (AFM).

2.2 An Atom Between a Tip and a Surface feels a Double Well Potential

Eigler and collaborators report on an "atomic switch", in which a Xe atom is reversibly transfered from a Ni(110) surface to the W tip, as well as on "transfer near contact" processes in which an STM tip is brought so close to a surface that the absorbed Xe atom spontaneously hops to it[3, 4, 11]. Several theories have been put forth to explain the atomic switch experiment[12, 13, 14, 15, 16]. The potentials calculated for the Xe-tip-surface system have a double well shape as depicted in figure 2.1, and bringing the tip just slightly closer to the surface than the switch operating conditions can give significant tunneling amplitudes, even for a heavy atom like Xe[17]. Of course the exponential dependence of the tunneling amplitude Δ on system parameters and the precise shape of the potential makes it very difficult to accurately predict its magnitude from first principles. The point is more that because the atom can be brought arbitrarily close to where it sticks to the surface, the tunneling rate can be made arbitrarily large.

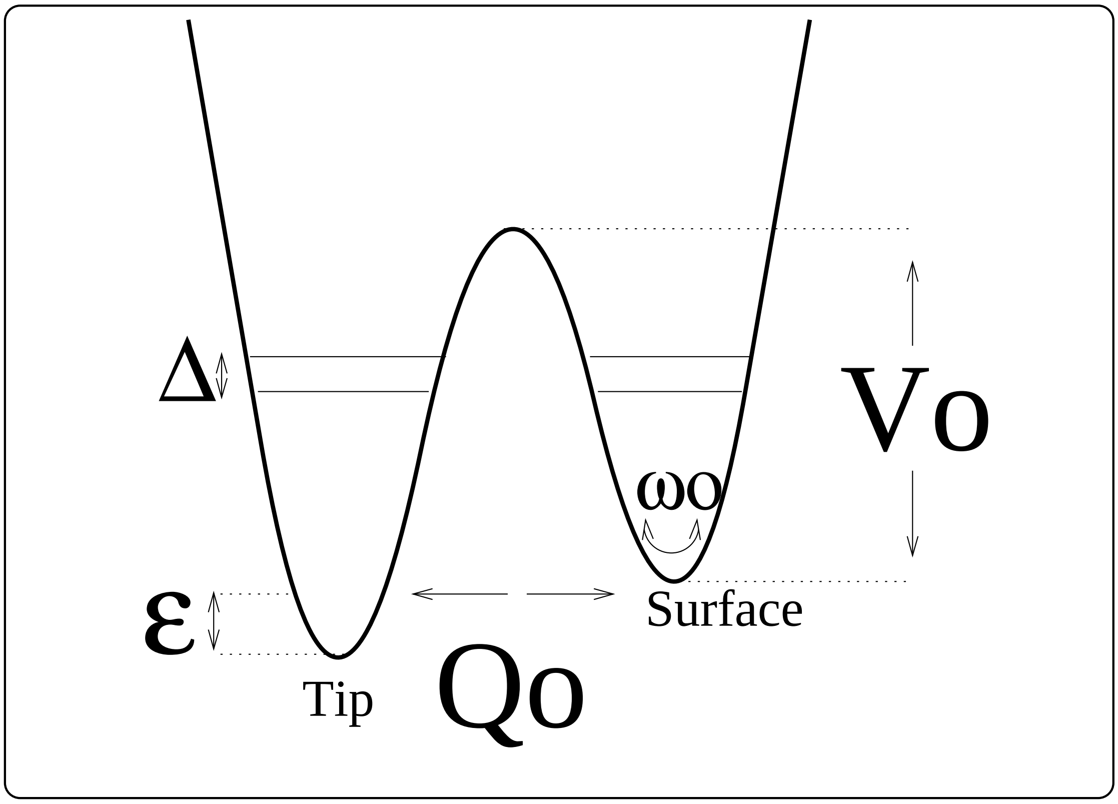

Figure 2.1: **Double-Well potential for the Tunneling Atom**
The atom tunnels from the STM/AFM tip to the substrate surface and back under the influence of a potential like the one shown above. For temperatures: $k_B T << \hbar\omega_0/2 < V_0$, the tunneling is between the lowest harmonic oscillator type states in each well. The tunneling amplitude Δ gives the energy splitting of the symmetric and anti-symmetric superpositions of tip + surface states, and is determined by the barrier height V_0, the effective distance Q_0, the mass of the particle, as well as the possible asymmetry energy ϵ. The small oscillation frequency ω_0 is determined by the same parameters.

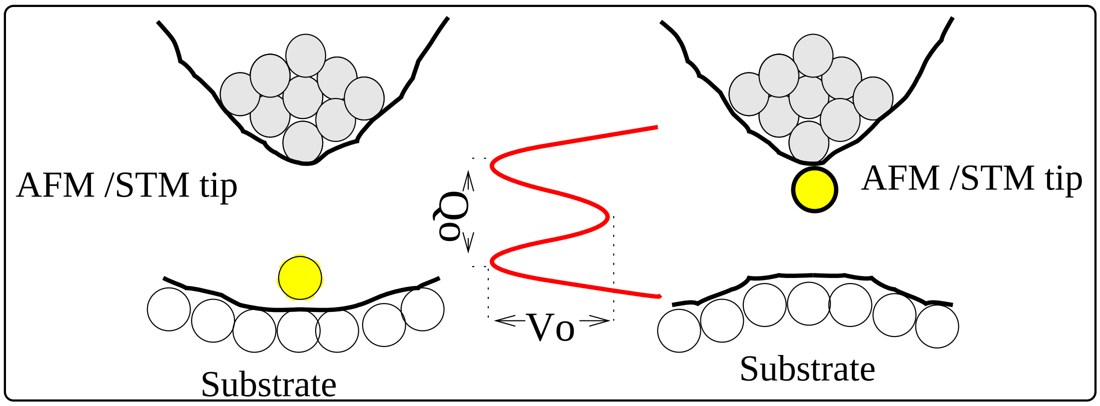

Figure 2.2: **Schematic drawing of the STM/AFM + atom system** The tunneling of the atom couples to phonons via the response of the substrate to the external force $\pm\Delta\mathbf{F}/2$ that depends on the position of the atom. The coupling to an environment drastically alters the tunneling behavior. For small coupling and low temperature, the tunneling is coherent with a renormalized tunneling frequency. For larger coupling, and zero temperature, there is no tunneling at all, while at finite temperature there is incoherent tunneling with a power-law dependence on temperature.

2.3 The Effect of the Phonon Environment: Ohmic Dissipation

We now proceed to the main part of this chapter: the effect of the phonon environment on our quantum tunneling system, and consider temperatures such that $k_B T << \hbar\omega_0/2 < V_0$, allowing us to truncate the Hilbert space to two states, one for each well[18].

As depicted in figure (2.2), the AFM/STM + atom system will exert a different force $\pm\Delta\mathbf{F}/2$[2] on the surface depending on where the atom is. The phonons will relax, switching their equilibrium positions in response to the atom being on the tip or the surface. This can be modeled by a Hamiltonian for the two-state system

[2] The use of the word force is an unfortunate misnomer: force is a purely classical concept. Instead this should be the gradient of the potential. However, in keeping with common conventions in the literature, we continue to use the word force.

with the displaced phonons:

$$H = \frac{\hbar\Delta}{2}\sigma_{\mathbf{x}} + \frac{\epsilon}{2}\sigma_{\mathbf{z}} + \sum_{\mathbf{k}\sigma}\left[\frac{1}{2}m_{\mathbf{k}\sigma}\dot{x}^2_{\mathbf{k}\sigma}\mathbf{1} + \frac{1}{2}m_{\mathbf{k}\sigma}\omega^2_{\mathbf{k}\sigma}\left(x_{\mathbf{k}\sigma}\mathbf{1} + q_{\mathbf{k}\sigma}\sigma_{\mathbf{x}}\right)^2\right]. \tag{2.1}$$

The $\{x_{\mathbf{k}\sigma}\}$ are the normal coordinates for a given polarization σ and wavevector $\mathbf{k}$. The masses of the normal coordinate particles are denoted by $m_{\mathbf{k}\sigma}$, and the phonon angular frequency by $\omega_{\mathbf{k}\sigma}$. The $\{q_{\mathbf{k}\sigma}\}$ are the new equilibrium positions in the presence of the force $\pm\Delta\mathbf{F}/2$.

In the absence of phonons, the probability of finding the atom at the tip at time t, given that it was started there at time $t = 0$, oscillates back and forth with the usual form $P(t) = \sin^2(\Delta t)$. For a potential of the form:

$$V(q) = V_0\left(1 - (\frac{2q}{Q_0})^2\right)^2, \tag{2.2}$$

the bare tunneling amplitude Δ can be found in WKB approximation or by an instanton analysis; namely:

$$\Delta = 2\sqrt{3}\omega_0(\hbar S_I/\pi)^{1/2}\exp[-\frac{S_I}{\hbar}] \tag{2.3}$$

$$S_I = \int_{-\frac{q_0}{2}}^{\frac{q_0}{2}}(2mV(q))^{1/2}dq, \tag{2.4}$$

where S_I is the instanton action. The prefactor comes from Gaussian fluctuations in the instanton approach so that for our potential:

$$S_I = \frac{2}{3}(2mV_0q_0^2)^{1/2} = \frac{8\sqrt{2}}{3}\left(\frac{V_o}{\omega_0}\right) \tag{2.5}$$

$$\Delta \approx 3.80(\hbar\omega_0V_0)^{1/2}\exp\left[-3.77\left(\frac{V_0}{\hbar\omega_0}\right)\right] \tag{2.6}$$

The tunneling amplitude Δ is roughly the geometric mean of the zero point energy and the barrier height times the exponential of their ratio.

What is now the effect of the phonons (environment) on the behavior of the atom (embedded quantum system)? Is there a *qualitative* change of behavior? For atoms tunneling between two states in the bulk, an approach often taken to account for the environment is calculating the overlap integral of the atom in state one (plus phonons) with the atom in state two (plus phonons). The new renormalized tunneling amplitude is just the bare amplitude multiplied by a Frank-Condon phonon-overlap factor. The atom still oscillates back and forth, but now with a reduced rate. If one assumes that the phonons are all in their ground states (Gaussians) then their effect on Δ can easily be calculated to be:

$$\begin{aligned} \Delta_r &= \Delta e^{-W} \\ W &= \sum_k \frac{\lambda_k^2 Q_0^2}{4\hbar m \omega_k^3} \end{aligned} \tag{2.7}$$

where λ_k is the coupling parameter given by:

$$\lambda_k = \left(\frac{m_k \omega_k^2 q_k}{Q_0} \right) \tag{2.8}$$

(the polarization index σ has been suppressed). For atoms tunneling in the bulk, this approach gives good qualitative results[19, 20]. However, for an atom tunneling between surfaces, the situation is quite different as can be seen by considering the "force" exerted by the atom on its environment (or more precisely, how the atom couples to the phonon environment through the gradient of the potential). While the defect tunneling in a solid only exerts a *dipole* force, resulting in $q_k \sim k^{-1}$[19], the external tip plus atom system exerts a *monopole* "force" on the surface, resulting in $q_k \sim k^{-2}$[21]. The external case has therefore a stronger coupling at low frequencies, and a naive calculation of the Frank-Condon factor gives an infrared divergence, a tell-tale sign that the adiabatic approximation breaks down. This "overlap catastrophe" is not the real physical picture though, and Leggett and co-workers have worked out a more sophisticated scheme that splits up the

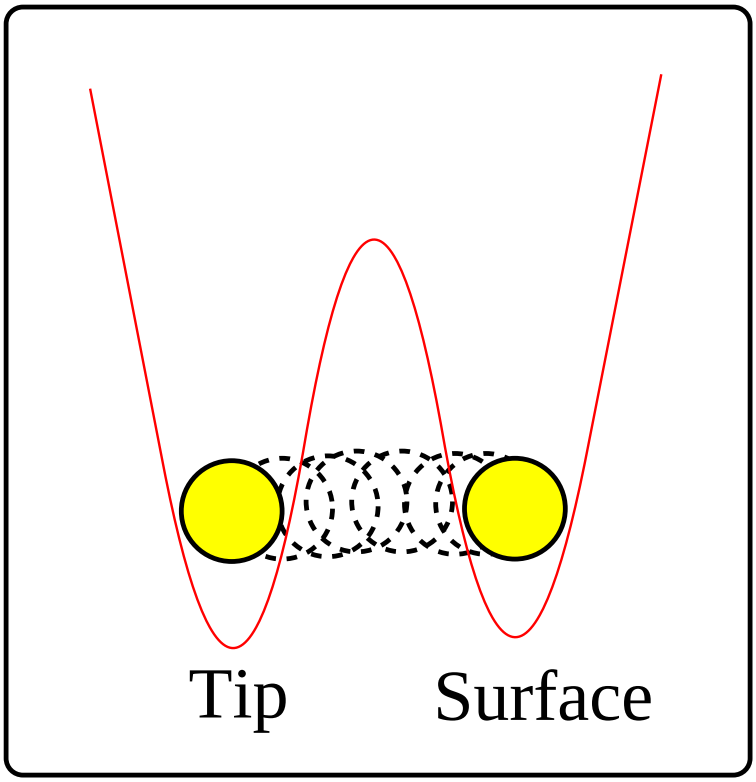

Figure 2.3: **Effect of long-frequency phonons on tunneling**
High frequency phonons simply renormalize the tunneling frequency Δ. However, the adiabatic approximation implicit in such a Frank-Condon factor approach breaks down for long-wavelength phonons with frequencies $\omega_k \leq \Delta$. In fact these phonons, which cause an infrared divergence in a simplistic Frank-Condon overlap integral, can safely be ignored.

effects of high and low frequency oscillators(phonons)[10]. They replace Δ by a "renormalized" tunneling element:

$$\Delta \to \Delta_r = \Delta \exp\left(\frac{-q_0^2}{2\pi\hbar}\int_{\Delta_r}^{\infty}\frac{J(\omega)}{\omega^2}d\omega\right), \tag{2.9}$$

where

$$J(\omega) = \frac{\pi}{2}\sum_k \frac{\lambda_k^2}{\omega_k m_k}\delta(\omega - \omega_k) \tag{2.10}$$

is the "spectral density". The lower-limit frequency cutoff is explained in figure (2.3). Eq(2.9) is then iterated to self-consistency. Leggett *et al.* find that the "renormalized" tunnel splitting becomes:

$$\Delta_r = \Delta \left(\frac{\Delta}{\hbar\omega_c} \right)^{\alpha/(1-\alpha)}, \tag{2.11}$$

where the ω_c is a cutoff frequency $\Delta << \omega_c << \omega_0$ used to separate high and low frequency oscillators and drops out of most relevant calculations. The effect of the environment can now be characterized by a dimensionless coupling parameter α defined as:

$$\alpha = \frac{\eta Q_0^2}{2\pi\hbar}, \tag{2.12}$$

with η equivalent to the friction coefficient in the macroscopic limit[22]. The case of tunneling between surfaces corresponds to "ohmic" dissipation in the language of the Macroscopic Quantum Tunneling (MQT) literature, as opposed to the bulk case, where the dissipation is of the "superohmic" variety[10]. The tunneling element is renormalized to Δ_r for $\alpha < 1$, and is zero for $\alpha > 1$. More sophisticated renormalization group calculations confirm this simple picture[23]. In other words, for small coupling parameter α, the effect of the phonons is *quantitative* only, reducing the tunneling frequency, while if α crosses 1 the effect is *qualitative*: there is a transition to no tunneling at all! This fascinating effect is the phonon analogue of Anderson's "overlap catastrophe " in an electron gas[9]. We emphasize that this would be the first case in which an overlap catastrophe is caused by phonons[24].

Having established that an atom tunneling from an STM/AFM tip to a surface undergoes "ohmic dissipation" from the phonon environment, we arrive at the question: Is the dimensionless coupling parameter α in an interesting regime? Assuming a point force $\Delta F/2$ on an semi-infinite isotropic medium with a linear (Debye) dispersion we find:

$$\alpha = \frac{1}{64\pi^2\hbar\rho c_t^3} G(\sigma)(\Delta F)^2, \tag{2.13}$$

where ρ is the density in $kg\ m^{-3}$, c_t is the transverse sound velocity, and $G(\sigma)$ is a tabulated function of Poisson's ratio $\sigma = (3\lambda + \mu)(6(\lambda + \mu))$, with roughly equal contributions from the acoustic bulk and Rayleigh modes[25][3] The critical $\Delta\mathbf{F}$ for which $\alpha = 1$ ranges from about 3 nanoNewtons(nN) for W, to 0.3 nN for Pb. Another order of magnitude reduction can be obtained for some organic materials. At the short distances needed for atomic tunneling, the typical force of a tip on a surface is of the order of a nN per Å separation[26], putting us right into the interesting regime[27]!

[3] For a more detailed discussion of Rayleigh modes, and why they produce *ohmic* coupling, see Appendix **B**.

2.4 Proposed Experimental Measuring Schemes

We envisage a number of realizations of the atom-surface tunneling experiments. First, it has been calculated that for $k_B T \geq \hbar\Delta/\pi\alpha$ the coherent oscillations are destroyed[28, 29], and there is only incoherent tunneling with a rate[10]:

$$\tau^{-1} = \Delta_r \frac{\Gamma(\alpha)}{\Gamma(\alpha+1/2)} \frac{(\pi)^{2\alpha+1/2}}{2} \left(\frac{k_B T}{\hbar\Delta_r}\right)^{2\alpha-1}, \tag{2.14}$$

from which the parameter α could be extracted and compared to our predictions[30, 31]. We believe this would be the first quantitative test of the α parameter, giving valuable insight into the validity of the linear coupling model of a dissipative environment. By varying the distance between the tip and the surface or by varying the position within the surface unit cell, the force $\Delta\mathbf{F}$, and thus the coupling parameter α, could be tuned. Of course simultaneously, this would heavily affect the tunneling frequency Δ by changing the potential barrier. However, one could still see the qualitative change in temperature dependence of the rate. Of particular interest would be the crossover of the rate from *decreasing* with increasing temperature to *increasing* with increasing temperature when α crosses $1/2$ from below[32] (See figure 2.4 for a quick summary of the regimes described above). An STM with sufficient control to manipulate atoms that can also vary temperature from $7K$ to $300K$ has already been built[33]!

Second, a more ambitious experiment might test the coherence predictions: observing the tunneling turn off as α is increased. Coherent oscillations, one of the goals of the MQC community[10], will occur if $T < \hbar\Delta/k_B\pi\alpha$, and $\alpha < 1/2$[34]. For experimentally accessible temperatures (say $1K$) with $\alpha = 0.1$ this means a tunneling rate of at least $10GHz$. Recent developments in high-speed STM have achieved a time resolution of picoseconds[35], and we envisage a direct measurement of the

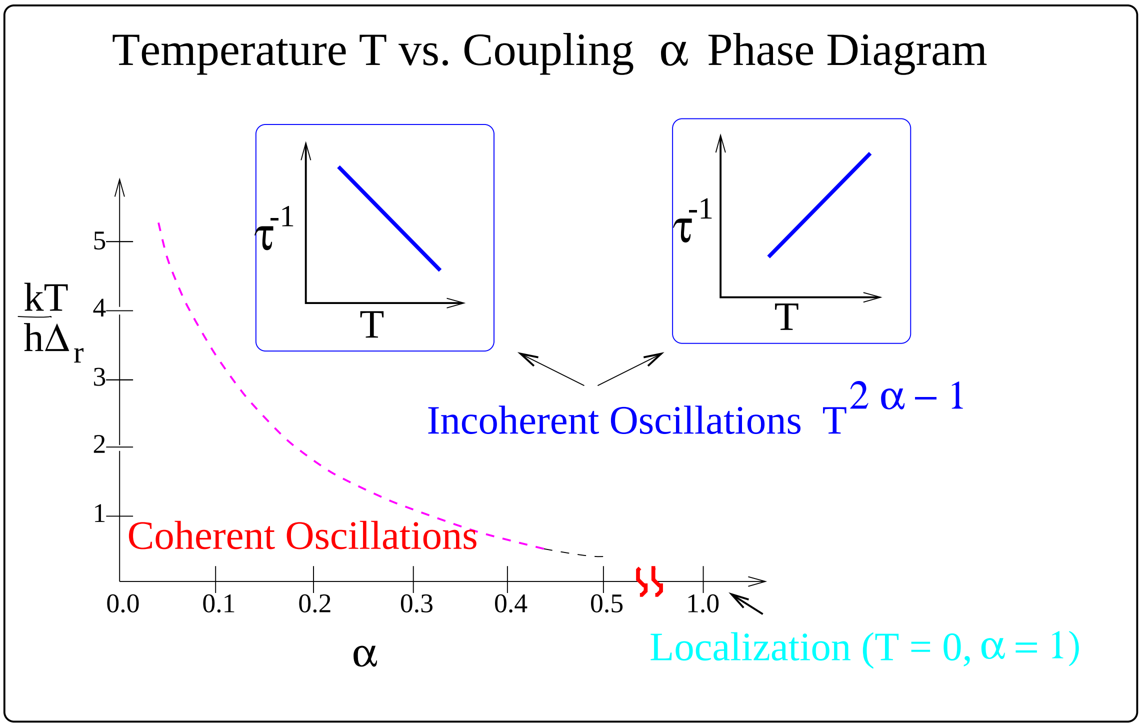

Figure 2.4: **Temperature T v.s. α Phase diagram**

The two parameters of interest are the temperature T (normalized by the renormalized tunneling frequency Δ_r) and the coupling constant α. At zero temperature the coherent oscillations are expected to disappear for $\alpha \geq 0.5$ and localization sets in for $\alpha \geq 1$. The coherent oscillations initially persist, as the temperature is raised, slowly becoming more and more damped until they cross over to incoherent behavior. What's particularly interesting is that the oscillation frequency has a *qualitatively* different power-law dependence on T when α crosses $\frac{1}{2}$. At even higher temperatures we anticipate Arrhenius behavior[4].

correlations by sending in pairs of voltage pulses[36]. This could be accomplished by a low-temperature STM coupled to picosecond lasers that generate the voltage pulses(as was done in Refs.[35]). By comparing with the temporal Bell Inequalities described in Appendix **A**, these correlations could be tested for quantum coherence. Varying the intra-pair time by $\pi/2\Delta$ will give an oscillation of the integrated current that reaches a maximum of 40% of the current difference between the atom on the tip and the surface for a slightly biased well with $\epsilon = \Delta$. The inter-pair time must be much greater than the intra-pair time, and the pairs must be long compared to the electron tunneling time (which is on the order of fs). These would be the first measurements of the coherent oscillations of a single entity with ohmic dissipation, and while the atom is not "macroscopic", our proposed experiment should be a fertile testing ground of new measurement schemes, and may shed light on the even more difficult problem of observing MQC in SQUIDS[37].

2.5 Conclusions for Atomic Tunneling with Dissipation

In summary, we have shown how the phonons couple in a fundamentally different way to an external particle at a surface than to an interstitial particle in a bulk, and can cause an "overlap catastrophe", just as electrons can. More precisely, the coupling of an atom to phonons at the surface produces ohmic dissipation, and *qualitatively* changes the tunneling behavior, in contrast to the well-known case of tunneling in the bulk where the effect of phonons is only *quantitative.* We have proposed an experiment with an atom tunneling between an STM/AFM tip and a surface, and show how this could test theories of MQC, albeit in a microscopic setting. Because the parameters Δ, ϵ and α can all be varied by changing the tip-surface position and the bias, many different regimes of the theories of two-state systems with ohmic dissipation can be put to the test.

Bibliography

[1] A.A. Louis and J. P. Sethna Phys. Rev. Lett. **74** ,1363 (1995).

[2] D.M. Eigler and E.K. Schweizer, Nature **344**, 524 (1990).

[3] D.M. Eigler, C.P. Lutz, and W.E. Rudge, Nature **352**, 600 (1991)

[4] J.A. Stroscio and D.M. Eigler, Science **254**, 1319 (1991).

[5] M.F. Crommie, C.P. Lutz, and D.M. Eigler, Nature **363**, 524 (1993), Science **262**, 218 (1993).

[6] see for example K. Gottfried in *Quantum Mechanics*, (Benjamin, Reading, MA (1966) pp 185-189 (see also the Special Preface to the 1989 Addison Wesley reissue where Gottfried calls the problem of the reduction (collapse) of the wave-function a "red herring"), or H. D. Zeh, in *Foundations of Quantum Mechanics.* B. D'Espagnat, Ed. Academic Press, New York (1970);

[7] See for example, W.H. Zurek, Phys. Rev. D **24**, 1516 (1981) R. Omnés, Rev. Mod. Phys. **64**, 339 (1992). (for a general introduction see: W.H. Zurek Phys. Today **44**, No 10, 36 (1991))

[8] A. J. Leggett in *Quantum Tunneling in Condensed Media*, eds. Yu. Kagan and A.J. Leggett, (Elsevier Science, Amsterdam, 1992)

[9] P.W. Anderson, Phys. Rev. Lett. **18**, 1049 (1967)

[10] See: A. J. Leggett *et al.*, Rev. Mod. Phys. **59**, 1 (1987) and references therein.

[11] Other workers have also succeeded in transferring for example Si atoms reversibly to a Si surface: I.-W. Lyo and P. Avouris *Science*, **253**, 173 (1991).

[12] S. Gao, M. Perrson, and B.I. Lundqvist, Solid State Commun. **84**, 271 (1992).

[13] R.E. Walkup, D.M. Newns, and Ph. Avouris, Phys. Rev. B **48**, 1858 (1993); *J. Elec. Spectroscopy* **64/65**, 523 (1993).

[14] M. Brandbyge and P. Hedegård, Phys. Rev. Lett. **72**, 2919 (1994).

[15] J.J. Sáenz and N. García, Phys. Rev. B **47**, 7537 (1993).

[16] F. Flores *et al.*, Il Nuovo Cimento D **15**, 451 (1993); P.L. de Andres *et al.*, J Phys: Condens. Matter **5**, A411 (1993).

[17] A number of authors have calculated well parameters. If we take for example some parameters from reference [16] for Xe on Ni(110) ($V_0 = 7meV, Q_0 = 0.6\text{Å}$), we can obtain tunneling elements up to $\hbar\Delta/k_B \sim 0.5K$! In this paper, we use the example of Xe simply because a lot is know about that system. Of course lighter elements such as He would have even larger tunneling amplitudes. By adding an electric field, the wells can be biased in either direction quite sensitively as was shown in reference [13], so that by varying the tip position and the bias, both Δ and ϵ can be varied independently.

[18] A.T. Dorsey, M.P.A. Fisher, and M. Wartak, Phys. Rev. A **33**, 1117 (1986)

[19] J. P. Sethna Phys. Rev. B **24**, 698 (1981); **25**, 5050 (1982)

[20] A similar effect is at work in the small-polaron problem, where the phonon-overlap integral lowers the hopping rate of an itinerant electron.

[21] This can be seen by the following argument: $q_{\mathbf{k}i} \sim D(k)^{-1}_{ij} \sum_l \Delta F_j(\mathbf{r}_l) e^{-i\mathbf{k}\cdot\mathbf{r}_l}$, where $D(k)_{ij}$ is the dynamical matrix which goes as $\sim k^2$ for small k. Thus $q_k \sim k^{-1}$ for a dipole force, and $q_k \sim k^{-2}$ for a monopole force.

[22] A.O. Caldeira and A. J. Leggett, Ann. Phys. (N.Y.) **149**, 374; **153**, 445(E) (1984)

[23] S. Chakravarty, Phys. Rev. Lett. **49**, 681 (1982); A.J. Bray and M.A. Moore, Phys. Rev. Lett. **49**, 1546 (1982), also S. Chakravarty and A. Schmid, Phys. Rep. **140**, 193 (1986).

[24] Ohmic coupling from one-dimensional phonons has been postulated for an escape problem by L.S. Levitov, A.V. Shytov, and A. Yu. Yakovets, "Quantum Breaking of an Elastic String" preprint cond-mat/9406117 (1994).

[25] The dimensionless function $G(\sigma)$ varies monotonically from 6.36 for $\sigma = 0$ to 2.35 for $\sigma = 0.5$. For a different symmetry (say cubic), the calculation becomes very difficult to do analytically. One must resort to numerical procedures such as slab calculations of the phonon dispersion and density of states (see for example R.E. Allen, G.P. Alldredge, F.W. de Wette, Phys. Rev. B **4**, 1661 (1971)). However, we don't expect the value of α to change very much from the isotropic result as it depends only on the long-wavelength elastic behavior (which is independent of any local details) and $\mathbf{\Delta F}$, which can be independently measured with an AFM.

[26] U. Durig *et al.* Phys. Rev. Lett. **57**, 2403 (1986); **65**, 349 (1990), C.J. Chen *Introduction to Scanning Tunneling Microscopy*, New York: Oxford University Press (1993).

[27] Note that we have ignored the phonons in the tip. Although they are part of the environment, their effect is expected to be small. On the one hand, if we approximate the tip as another flat surface, the total coupling will just be sum of the α's from each surface. As the tip is usually made of tungsten or some other stiff material, it will typically have an α an order of magnitude smaller than the α from the substrate surface. On the other hand, if we approximate the tip as a $1-d$ vertical line of atoms, the coupling will be *sub-ohmic*, and the tunneling will be quenched at all coupling strengths. We have also ignored possible coupling to electron hole pairs. Of course for an insulator they won't matter, and for example in the case of Xe on Ni(110), the electron- hole pair dissipation is typically a factor 100 smaller than the phonon dissipation[12]. When it is not negligible, it will give an additive contribution to α. An estimate of the force difference ΔF can be obtained from *ab-initio* total energy pseudopotential calculations quite accurately with standard techniques (Thomás Arias, private communication).

[28] Anupam Garg, Phys. Rev. B **32**, 4746 (1985).

[29] C.H. Mak and D. Chandler, Phys. Rev. A **44**, 2352 (1991); R. Egger and U. Weiss, Z. Physik B **89**, 97 (1992).

[30] An AFM operating in non-contact mode can measure the oscillations by the force modulation of $\pm\mathbf{\Delta F}/2$. The tunneling current of an STM is significantly larger when the atom is on the tip than when it is on the surface[3].

[31] Beautiful experiments (B. Golding, N.M. Zimmerman and S.N. Coppersmith, Phys. Rev. Lett. **68**, 998 (1992); K. Chun and N.O. Birge, Phys. Rev. B **48**, 11500 (1993)) on individual two-state tunneling defects coupled to conduction electrons in mesoscopic metals, and on SQUIDS (S. Han, J. Lapointe, and J. E. Lukens, Phys. Rev. Lett. **66**, 810 (1991)) have confirmed this powerlaw behavior of the (incoherent) rate with temperature. However, in contrast to our system, these experiments do not allow one to vary α, or calculate it from first principles.

[32] We note in passing that adding an oscillating electric field in the incoherent regime would bring us into the very interesting regime of *Quantum Stochastic Resonance*, recently discovered by Löfsted and Coppersmith(R. Löfsted and S. N. Coppersmith, Phys. Rev. Lett. **72**, 1947 (1994); AT&T Bell Labs preprint (1994)) as well as a host of other effects relating to driven quantum systems with dissipation.

[33] B.C. Stipe, M.A. Rezai, W. Ho, S. Gao, M. Perrson, and B.I. Lundqvist, Phys. Rev. Lett. **78**, 4410 (1997).

[34] Although the transition to no tunneling only occurs for coupling $\alpha > 1$, the tunneling in the region $1/2 \leq \alpha < 1$ is expected to be incoherent[10].

[35] S. Weiss *et al.* Appl. Phys. Lett **63**, 2567 (1993), G. Nunes and M. R. Freeman, *Science* **262**, 1029 (1993).

[36] There have been an extensive discussion of the problems of measuring coherent oscillations in the MQC literature (see for e.g. A.J. Leggett and Anupam Garg, Phys. Rev. Lett. **54**, 857 (1985); **54**, 2724 (1985); **59**, 1621 (1987); L.E. Ballentine Phys. Rev. Lett. **59**, 1493 (1987); C. D. Tesche Phys. Rev. Lett. **64**, 2358 (1990); Juan Pablo Paz and Günter Mahler, Phys. Rev. Lett. **71**, 3235 (1993)). For example, Peres (Asher Peres, Phys. Rev. Lett. **61**, 2019 (1988)) has claimed that non-invasive measurements are impossible in this case: a measurement introduces and energy of order $\hbar\omega_0$. This has been disputed by Leggett and Garg (A.J. Leggett and Anupam Garg, Phys. Rev. Lett. **63**, 2159 (1989)), and in fact, we find that the uncertainty in momentum P caused by measuring the position to better than $Q_0/2$ is $(\Delta P)^2/2 \geq \hbar\omega_0(\hbar\omega_0/64V_0)$ which gives a sizable window for the direct measurement we propose. More specifically for the case of Xe on Ni(110) theories for the switch experiment estimate that for a bias voltage greater than $\hbar\omega_0$, about one in 2000 electrons will inelastically scatter and excite the atom into a higher vibrational state[13]. For a current of $\sim 0.1nA$ the atom would be excited on average about once every μs. Thus an STM in imaging mode can only measure oscillations if $1/\Delta << 1\mu s$, a rate that is easily reached for close enough tip-surface separation[17]. If the bias is less than $\hbar\omega_0$, excitations can only occur through multiple electron transitions, so the excitation rate will be much smaller and lower oscillation rates can be measured.

[37] Coherent oscillations with ohmic coupling have been observed by H. Wipf *et al* Europhys. Lett., **4** 1379 (1987) for Hydrogen tunneling in Niobium. In this case, the measurement is in frequency space on a large number of trapped H atoms interacting with conduction electrons. Recent calculations (Daniel S. Fisher and Aris L. Moustakas, "On the Localization of Heavy Particles in Metals", Harvard preprint HU-AM-94-001 (1994)) have shown that simultaneous tunneling of the atom and electrons will inhibit localization caused by the conduction electron bath that gives ohmic dissipation in the aforementioned experiments[31, 37] and thus a phonon bath may be the only experimentally accessible route to this effect.

Chapter 3

Metallization of Fluid Hydrogen

3.1 Introduction to Metallic Hydrogen

3.1.1 Some background on dense hydrogen

Hydrogen, out of it the Universe evolved,
every atom and leaf, marine iguana

and apricot-smelling chanterelle. But my, my,
what alchemy: nondescript H_2

–Diane Ackerman[1]–

Hydrogen, a deceptively simple mixture of electrons and protons in equal concentration, is commonly thought of as a group I element, a correspondence which helped motivate the classic 1935 paper by Wigner and Huntington[1] in which they predicted that pressures above about 25 GPa would be sufficient to break the diatomic bond, leading to one electron per unit cell, and within a standard band-theory picture, metallic behavior. Since then hydrogen has often been viewed as

[1] Taken from "Jupiter", in *The Planets A Cosmic Pastoral*, Diane Ackerman, William Morrow and Company Inc. New York (1976)

the prototypical (MIT) system and has been intensely studied; experiment and theory revealing a remarkably rich phase behavior.

A joint intertwining of strong Coulomb interactions and quantum mechanics produces a robust molecule[2], and in the solid phase heroic attempts to metallize it and to eventually rupture the bond have not yet been successful. Instead, at low temperatures, solid paired hydrogen undergoes a number of phase transitions with increasing density, each of which seems to open the energy gap in such a way that it stays insulating up to 10-fold compression[2, 3, 4] and pressures an order of magnitude higher than originally predicted by Wigner and Huntington.

This persistence of pairing suggests that hydrogen is perhaps better described as a group VII element[5], with one electron short of a filled shell. Like the halogens, it condenses into a diatomic insulating solid, and, as was predicted 20 years ago[6, 7], it can become metallic in the diatomic phase by a band overlap transition. Iodine is a good example of this; it becomes metallic by a band-overlap transition at about 16Gpa[8], before the diatomic bonds are broken at slightly higher pressures.

The quest for metallic hydrogen has been motivated in part by the hope that understanding the (MIT) in this "simple" system would lead to new understanding of the phenomenon in more complex materials. However, hydrogen is far from a simple material. Instead, experiments consistently surprise, leading repeatedly to an overhaul of theoretical models. There are several reasons for this: first, hydrogen has no core-electrons, there is no pseudo-potential to soften the electron-ion interaction from its bare Coulomb form, and so higher order scattering effects quickly become relevant. Second, the low mass of the protons implies substantial zero-point motion (around $0.25eV$ per proton at 10-fold compression) which is difficult

[2] The energy required to separate the free molecule into atoms is $\sim 4.5eV$.

to treat theoretically. Mainly for these two reasons (there are more) dense hydrogen research consistently stretches the limits of our calculations and theoretical models, resulting in a deeper and more complete understanding of the theory of rarefied and condensed matter.

Besides the fundamental interest as a model system, dense hydrogen is crucial to the understanding of the giant planets. For example Jupiter and Saturn contain almost 400 earth masses of hydrogen, most of which is in a dense (hot) fluid phase. Details of the MIT transition can profoundly influence theories of the interior of these planets. For example, convective motion in metallic hydrogen produces large, observable magnetic fields through a dynamo effect[9], and the recent experiments demonstrating metallization of fluid hydrogen[10] have interesting implications for the interior of Jupiter[11]. Also, Jupiter-size planets now being discovered close to nearby stars[12] probably contain massive amounts of hydrogen as well, and the interiors of these giant planets are likely to be at high pressures and high temperatures and therefore in the fluid state[13].

3.1.2 What (When) is a metal?

..., instead of having a cosy arrangement in which each ion has its 'own' electron bound tightly to it, we have a sort of communist society ..."

–J.M. Ziman[3]–

The electrical resistivity of the elements can range anywhere from $\rho =\sim 1\mu\Omega cm$ for copper to $\rho \sim 10^{18}\mu\Omega cm$ for sulphur, 18 *orders of magnitude!*, arguably one the largest natural variation of any material property at normal equilibrium con-

[3] J.M Ziman in *Electrons in Metals: A Short Guide to the Fermi Surface*, London, Taylor and Francis (1964)

ditions[4] Materials with low resistivity are typically called metals, materials with high resistivity are typically called insulators. With that the question: *"What is a metal?* would seem closed, but this optimistic assessment breaks down when external conditions such as temperature, pressure or composition are are varied: many materials transform from metals to insulators and vice-versa under the action of varying an external parameter. These metal-insulator transitions have spectacular consequences for the resistivity, they have been described as "turning copper into wood"[5], but the phenomenon remains poorly understood, still standing as one of the premier intellectual challenges of our day. In the words of P.P. Edwards and M.J. Sienko; "The two questions: 'What is a metal?' and 'When does a metal transform to an insulator?' are indeed inseparable"[14].

The traditional understanding of "What is a metal?" is based on a one-electron approximation (band-theory) and crystalline order. In fact, "the conductivity of a perfect periodic crystal is infinite"[6], the electrons are in stationary Bloch states, with all effects of the periodic lattice taken into account. Certain symmetries may also preclude conductivity: If there are for example two electrons per unit cell and thus no readily accessible states for conduction, a material is a perfect insulator[15]. At the level of band-theory (and at $T = 0$) all matter is classified into perfect metals and perfect insulators. For metallic systems any residual resistivity must therefore arise through deviations from perfect crystallinity: phonons, defects, grain-boundaries etc.., and one intuitively expects greater disorder to induce larger resistivities.

---

[4] If we extend this point to compounds, fused quartz has a resistivity even higher than sulphur, namely $10^{26}\mu\Omega cm$!

[5] C.N.R. Rao, private communication to P.P. Edwards

[6] See [57] page 215. Of course this holds for partially filled bands only.

In the light of this, the recent shock-compression experiments of Nellis et al[10], which claim to metallize hydrogen in the (disordered) fluid state at pressures and densities for which the (periodic) solid is still in the insulating phase, are all the more surprising. This new fluid state straddles the borders of plasma physics and solid-state physics, as well as the borders of the classical statistical mechanics of a correlated molecular liquids and the quantum physics of correlated electron liquids. A theoretical discussion of these experiments will necessarily explore and illuminate multiple aspects of the twin questions "What is a metal" and "When is a metal", and this forms the focus of the present chapter.

3.1.3 Short historical retrospective on the metal-insulator transition and the definition of a metal*

"He [Sommerfeld] didn't even care terribly much why electrons were free, which I thought was a very important thing to know"

–H. A. Bethe†

A few years after J.J. Thompson's 1897 discovery of the electron, P. Drude[20] put forth the first theory capable of describing metallic behavior from quasi-microscopic concepts, albeit within a completely classical kinetic picture. The first successful application of quantum mechanics to conduction electrons was the semi-classical electron theory developed by Sommerfeld in 1927[21] who applied the new quantum statistics to the old Drude theory. However, as the quote by Bethe at the beginning of this section shows, Sommerfeld did not discuss why the electrons were free, i.e. why the system was metallic. In that same year however, P. Bridgman considered

* Much of this section was taken from references[17],[14], and [19].

† Interview with Bethe, as recorded by T.H. Kuhn in *Archive for the History of Quantum Physics* (New York, Copenhagen, Berkeley and Minneapolis) and referenced in[17].

the question of high density in a paper entitled “The Breakdown of Atoms at High Pressures”[22]. Stimulated by his discovery of the change of certain properties of potassium under high pressure, he postulated that not only high temperature, but also high pressure (i.e. high density) could cause the breakdown of atoms to an electrical gas of electrons and protons. The next year, F. Bloch[23] proposed this theory of the quantum state of independent electrons in a crystalline potential, and soon thereafter A.H. Wilson proposed his theory of why crystals were metals or insulators based on band structure[24]. However, as he himself later wrote[25]: “Bloch’s theory had in fact proven too much. Before his paper appeared it was difficult to understand the existence of metals. Afterwards it was the existence of insulators that required explanation. This problem had been by-passed because it was taken for granted that insulators were merely bad conductors rather than non-conductors, the difference between metals and insulators being a quantitative and not a qualitative one. This concept I now challenged.”

The considerations above are all based in some way on a picture of independent non-interacting electrons. That view was first seriously challenged at a 1937 conference in Bristol, where de Boer and Verwey presented data that convincingly showed that the Wilson theory of metals and insulators gave incorrect results when applied to NiO[26]. Peierls pointed out that this was most likely related to neglect of the electron-electron interactions, and this inspired Mott to consider ideas beyond the simple Bloch-Wilson band-theory of independent electrons and propose his theory of a correlation induced metal-insulator transitions (now called the Mott-transition)[27]. Some years later, Anderson proposed that sufficiently perturbing crystalline symmetry by disorder could also lead to localization within a model of non-interacting electrons and a MIT as well[28].

These quantum pictures are basically $T = 0$ statements, and the difference between a metal and an insulator is crystal clear, “a metal conducts and a non-metal doesn't”[15]. At finite temperatures the definition of a metal becomes more ambiguous. For systems that are insulating at $T = 0$, but which have small gaps, the raising of the temperature thermally excites more and more electrons into conductive states so that the conductivity becomes temperature dependent. Even more spectacular variations in conductivity occur happen as the temperature is raised high enough provoke a structural change. For example upon melting, Si has a large conductivity jump to a value similar to that of many metals. In fact, the periodic table of melted elements includes more highly conductive materials than the usual periodic table at standard conditions. Thus although the $T = 0$ definitions are clean and well defined, they don't apply well at the finite temperatures usually encountered in nature. An operational definition could be that a metal is a material with a conductivity in the “metallic range”, although this would also include plasmas where the electrons are thermally stripped from their parent atoms. To differentiate between non-degenerate plasmas and degenerate systems, a useful definition would be that metals are materials (solid or liquid) with a reasonably well-defined Fermi-surface[‡]. For this chapter, we shall hold to a combination of the last two definitions: namely we shall call our material (hydrogen) metallic when it has a conductivity in a “typical” metallic range, but is still at conditions where the electrons are expected to be mostly degenerate[§]

[‡] which is strictly defined at $T = 0$ only, but still measurable at finite temperatures far below the Fermi temperature

[§] That is, we assume a Fermi-surface, even if it cannot be directly measured (yet).

3.2 Description of the Livermore Experiment

... I experienced retrospective fear and at the same time a kind of foolish pride, at having confirmed a hypothesis and having unleashed a force of nature. It was indeed hydrogen, therefore: the same element that burns in the sun and stars, and for whose condensation the universes are formed in eternal silence.

–Primo Levi¶–

The Livermore experiments[10] were carried out with a two-stage gas-gun which accelerates an impactor plate up to $\sim 7km/s$[29]! Needless to say, the plate impact on a cryostat containing liquid hydrogen produces extremely high transient pressures, in fact pressure and temperature conditions extreme enough for the metallization of hydrogen. In contrast to the diamond-anvil cell techniques which produce static pressures and remain at low temperatures[2, 3, 4], this dynamic shock technique simultaneously raises the pressure and temperature. The novel aspect of the Livermore experiments is their use of a reverberating multiple shock technique which keeps the final temperature much lower than traditional single shock techniques do[30]. Important also in this is an initial state at low temperatures – hence the cryostat. The result is megabar pressures but at temperatures where the electrons are still degenerate. (see [10, 31] and figure 3.1 for more details).

The compressed state of hydrogen only exist for about 200 ns, short on chemical and phase-transition timescales, but long enough on molecular time-scales to achieve thermodynamic equilibrium in a single phase, and also very long on the time scale of present day modern electronics. An important point to keep in mind is that the system may not have reached its equilibrium phase should it happen that the system has just crossed a phase boundary. On the other hand, because of its high chemical reactivity and large mass-diffusion coefficient it is essential to have a temperature

¶ Primo Levi in *The Periodic Table*, Schocken Books, New York, (1984), p 28.

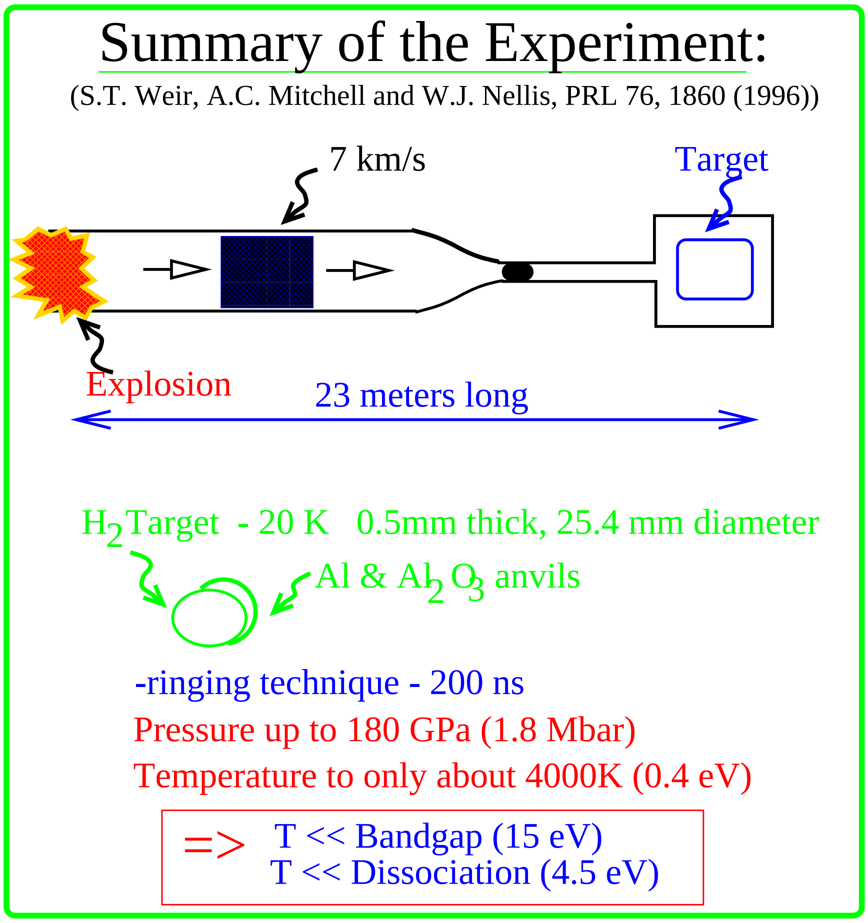

Figure 3.1: **Schematic of the Livermore Experiment**

A two-stage light-gas gun was used to accelerate the impactor plate up to $\sim 7 km/s$[29]. The initial energy source which drives the impactor is caused by gunpowder (although the initial thrust is not quite as spectacular as the explosion shown in the figure above). The cryogenic hydrogen sample is 0.5 mm thick and 25 mm in diameter, at an initial temperature of 20 degrees K, and contained between two sapphire anvils, which are in turn contained between two aluminum disks. The density mismatch between the sapphire and the hydrogen causes the multiple shocks. This arrangement can lead to pressures of over 180 GPa, and concomitant temperatures around $3000K$. These conditions are maintained for about 200 ns, after which the whole cryogenic and measuring apparatus disintegrates under the extreme pressure. Within this short time window (but still long on molecular timescales), fast electronics coupled with a four-probe measurement scheme is used[10] to directly measure the resistivity.

pulse. In fact, this temperature pulse should be short on the chemical time-scales, but long enough to achieve thermodynamic equilibrium, precisely the conditions achieved by the shock compression technique!

Pressures, which are directly available through shock impedance matching, and resistances, which are directly measured, are the only directly assessible quantities, densities, temperatures etc... must all be calculated. Nellis et al[10] used two equations of state, one was developed by Kerley[32] before recent shock data were available; it neglects molecular dissociation, and another is due to Ross and was based on earlier shock experiments. It explicitly includes molecular dissociation[33]. Based on these calculations, they claim systematic uncertainties in calculated density and temperature of 5% and 20%, respectively, and they plot the experimental resistivity data as $\log(\rho)$ versus pressure. The change in slope at 140 GPa is indicative of the transition to the metallic state (see figure 3 of [31]). When these results were plotted in the semiconducting range, 93-135 GPa, and fit to the conductivity of a a thermally activated semiconductor:

$$\sigma = \sigma_0 \exp(-E_g(D)/2k_BT), \tag{3.1}$$

where σ is electrical conductivity, σ_0 depends on density D and relatively weakly on T (typically as $T^{3/2}$), $E_g(D)$ is the density-dependent mobility gap in the electronic density of states of the fluid, k_B is Boltzmann's constant, and T is temperature, the seven data points with error bars of 20 to 50% were fit to Eq. (1), the results being: $E_g(D) = 1.12 - (54.7)(D - 0.30)$. $E_g(D)$ is in eV, D is in mol/cm^3 ($0.29 - 0.32$ mol/cm^3), and $\sigma_0 = 66$ $(\Omega cm)^{-1}$. Similar results are obtained using densities and temperatures calculated with Kerley's model[10]. σ_0 =200-300 $(\Omega cm)^{-1}$ is typical of liquid semiconductors[34]. Full GW calculations predict a theoretical rate of $40eV/(mol/cm^3)$[35] for bandgap closure near metallization at 0

K in a molecularly disordered hcp hydrogen. This is comparable to the fluid value of $\sim 60eV/(mol/cm^3)$ obtained by fitting to equation 3.1, so that $E_g(D)$ and $k_B T$ are equal at a density of 0.32 mol/cm^3 and a temperature of $\sim 2600K$ $(0.22eV)$. In this region the energy gap is smeared out thermally, activation of electron carriers is complete, disorder is saturated in the fluid, and conductivity is expected to be weakly sensitive to further increases in pressure and temperature, provided the fluid does not change significantly. Interestingly, the measured resistivity flattens out (rather like Iodine), at pressures of 140 to 180 Gpa to a value around $500\mu\Omega cm$, equivalent to a conductivity of $2000(\Omega cm)^{-1}$, which is typical of the fluid (monatomic) alkali metals Cs and Rb at 2000 K undergoing the same transition[36].

3.3 General Theoretical Considerations

In hydrogen, at the conditions of the experiment, the confluence of thermal and quantum effects link the physics of dissociation and metallization, electronic and atomic ordering, ionization and chemical (cluster) formation. Together these lead to a remarkably rich phase diagram, most of which remains experimentally unexplored. The metallization experiment[10] reveals a new section of this phase diagram, and hints to its further structure, as shown in Fig. (3.2).

Traditional theoretical interest has focussed on the change from a diatomic to a monatomic liquid or plasma, as well as the change from a metal to an insulator. In the new experimental regime now opened up, translational energies appear to match the vibron energies, and as such the metallization experiment may be probing both types of changes. With these confluences in mind we comment in turn on some interesting theoretical questions raised by the experiment, namely: **(a)** Why does the resistivity, the primary measured quantity, take the value it does?, **(b)** Why does the metal-insulator transition occur at a considerably lower pressure in the liquid than is predicted in the solid?, **(c)** What is the detailed mechanism of the metal-insulator transition?, and **(d)** What further experimental probes might clarify the situation?

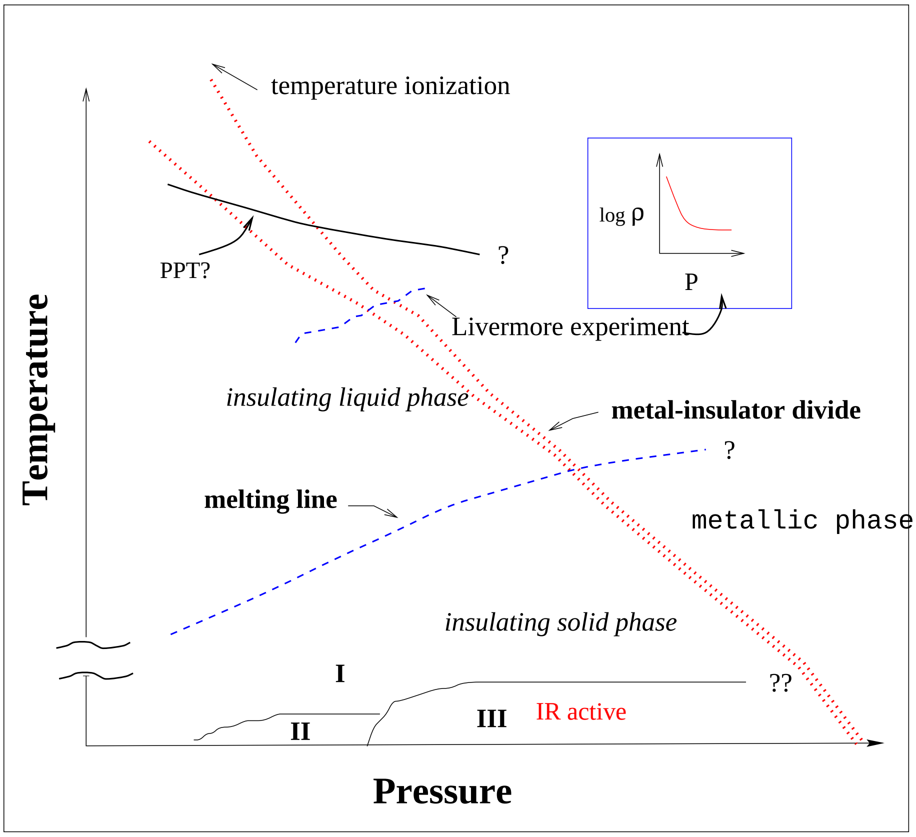

Figure 3.2: **Schematic Phase Diagram of Hydrogen**

The MIT in the liquid occurs at considerably lower pressure than is predicted for the transition in the solid. We suggest a metal-insulator band (not necessarily a sharp transition) starting from the zero-temperature solid, and increasing in temperature with decreasing density as depicted above. At very low temperatures it will be sharp with the character of a thermodynamic phase transition. At the other extreme of low density and very high temperatures, the metallization will be by gradual transformation to a temperature ionized plasma. At zero temperature the metal-insulator transition is predicted to occur before (at lower density than) the diatomic-atomic transition. What happens at higher temperatures remains to be established. Possibilities include the crossing or merging of the lines, as well as their termination in one or two critical points. Recent theoretical predictions of a Plasma Phase Transition (PPT)[37, 38, 39] are schematically depicted as well. Also depicted in the figure is the Simon equation for the melting line, and the orientationally disordered (I) and ordered phases (II) and (III) found in the solid[2]. We emphasize that this phase diagram is merely schematic; it is just a plausible guide and much still needs to be filled in.

3.4 The Scale of Resistivity in Liquid Metallic Hydrogen

The fundamental approach to the transport properties of liquid metals is via the Kubo-Peierls-Greenwood theory, based on linear response of the system to a weak external field $E(t)$. The static conductivity $\sigma(\omega = 0)$ is then given by:

$$\sigma(0) \sim \int_0^\infty < j(0)j(t) > dt \tag{3.2}$$

where $<< j(0)j(t) >>$ is a current-current correlation function for the many-electron system, and $<<>>$ is an average over electron states and atomic configurations. If the self-energy of the electron system is sufficiently small (from all sources of interaction) then an expansion in the self-energy leads to an inversion of σ for the resistivity, and at lowest order this is equivalent to first-Born approximation within the Boltzmann semi-classical approach to transport. In the high temperature limit it leads to the well known Ziman formalism [40, 41, 42] for degenerate electron systems, and this has been remarkably successful at predicting the resistivity of liquid metals to within about a factor of two, as well as trends seen in alloys, thermopower and the temperature dependence of the resistivity[43]. It requires as input the static structure factor $S(q)$ of the scattering system, an electron-ion-interaction, and the assumption of an appropriate high temperature limit.

To assess the applicability of this approach to the present problem, we may consider the case of liquid Si and Ge which prior to melting are not metals, though conduction by thermally excited carriers is evident. As fluids they are significantly under-coordinated (5 to 6 fold) which reflects persistent covalent effects and hence interactions going beyond the pair model. In applications of the Ziman formalism to this problem, the tangible effects of remnant covalency are included only through the static structure factor $S(q)$; 4 electrons per ion are usually assigned to the conduction process [but see below].

In some ways, the situation for hydrogen can be considered physically similar to Si or Ge, only more extreme. It is, again, a fundamentally covalent (but not necessarily a network) system, and structurally it cannot be described just in terms of pairwise proton-proton interactions. The viewpoint taken from liquid Si (a metal) can be taken here if the state possesses a plausible Fermi surface: in the application of the weak scattering formalisms covalency manifests itself primarily through $S(q)$ and in the specification of the fundamental excitations associated with the structure. As a first approximation (compare with the case for Si), two electrons per "molecule" could be taken to participate in conduction, but with a significant density of states correction to be applied later. Given this fundamental picture essentially tied to the pairing picture of the solid, we proceed to investigate the resistivity of liquid metallic *molecular* H_2 (in the experimental metallization regime) starting with the Ziman expression [40, 41, 42]. We express the resistivity ρ_L originating with a given type of carrier as:

$$\rho_L = \frac{m}{n_c e^2 \tau}, \tag{3.3}$$

where m is the carrier mass, n_c is the carrier density, and τ is a measure of the relaxation time. In its simplest high temperature‖ form the Ziman formalism gives:

$$\rho_L = \left(\frac{a_0 \hbar}{e^2}\right) \frac{6\pi}{(n_s)(k_F)^2} \int_0^1 S(y)|v(y)|^2 (y)^3 d(y), \tag{3.4}$$

where $y = q/2k_F$ is the wave vector scaled by twice the Fermi wave-vector, n_s the number density of scatterers, $v(y)$ the screened coulomb potential, $S(y)$ the

‖ In this case the temperature is high compared to acoustic phonon type modes that determine inter-pair motion, but less than the optic intra-pair vibron type modes so that we are dealing with a diatomic structure factor $S(q)$.

structure factor describing the proton-proton density fluctuations which scatter the carriers, and $(a_0\hbar/e^2)$ can be viewed as the atomic unit of resistivity (it has the value of $21.7\mu\Omega cm$).

The structural average required in the static structure factor appearing in (3.4) is not simple given the conditions of the experiment. In the first place translational energies appear well matched to rotational energies, and also to vibron energies. The kinematic transfer of energy from translational to vibrational degrees of freedom will be competitive with transference of translational energy to rotational energies. Accordingly, for this system the temperature and the density conspire in such a way that a standard averaging over rotational degrees of freedom prior to translational averaging is not secure. Secondly, orientational and translational entanglement leads to considerable self-averaging in the determination of the static structure factor. Thirdly, it has to be emphasized that so far as the vibron excitations are concerned, the system is not at high temperatures‖, which affects both structural[44] and scattering[45] physics.

In a naive approach using the usual free-electron density of states, and with the approximations introduced above for the structure factor $S(q)$, a resistivity of about 50 $\mu\Omega cm$ is found from (3.4), a significantly larger figure than obtained in previous calculations of monatomic H[46], but still considerably lower than the 500 $\mu\Omega cm$ measured experimentally[10]. However, this is to be expected since in the one-electron picture we also anticipate a significant decline in the density of states at the Fermi energy[47].

If the band-gap has only just closed we expect a lowering of the density of states as compared with the full free-electron case which in turn can be linked to a significantly reduced effective carrier density. Equation (3.3) shows that a reduced number of carriers raises the resistivity[48]; we also expect related multiple-scattering and other strong-coupling effects[49] to be relatively important in this regime, and these effects also lead to higher resistivities. Thus by taking into account physics beyond the usual one-band picture our result of $\sim 50\mu\Omega cm$ can only be seen as something of a lower bound. Since the overlap and related electron density is expected to increase with increasing density, this modified Ziman picture predicts that the resistivity at fixed temperature should continue to fall with increasing pressure so long as the liquid maintains its pairing correlations. We emphasize, however, that the pairs are in no sense permanent (again an analogy to fast exchange in liquid Si can be made) although they are long-lived on *electronic* timescales and as such influence the electronic structure.

At present the experimental results have large error bars (20% in the metallic state) and are in too small a pressure range to confirm or falsify any predicted pressure dependence of the resistivity, but the actual value of the resistivity near metallization seems consistent with this picture, though this is not the only possible interpretation (see below).

3.5 The Onset of the Metal Insulator Transition

At first sight the lower pressure and density of the metal-insulator transition in the liquid compared to the solid may seem surprising. One would expect the greater disorder (as compared with the solid) to delay the closing of the gap and the subsequent onset of metallization as is for example the case in Hg, another divalent pressure-induced metal-insulator transition[50]. However, a closer look at the origin of the bandgap in the solid phase reveals a more complex possibility which can be illustrated in the Pa3 structure, an isotropic solid which best mimics the high coordination and orientational averaging characteristics of the "paired" liquid. The lower bands in such a structure can be represented by an equivalent face-centered cubic description[51] where the principal Fourier components of the electron interaction with pairs are given by

$$V_{111} = (3/4\pi r_s^3 a_0^3) S_0(111) v(111) \tag{3.5}$$

and

$$V_{200} = (3/4\pi r_s^3 a_0^3) S_0(200) v(200). \tag{3.6}$$

Here S_0 is the structure factor per proton, and is given by

$$\begin{aligned} S_0(l,m,n) = \frac{1}{4}\{\cos 2\pi\alpha(l+m+n) &+ (-1)^{m+n}\cos 2\pi\alpha(l-m+n) \\ &+ (-1)^{l+m}\cos 2\pi\alpha(-l+m+n) \\ &+ (-1)^{n+l}\cos 2\pi\alpha(l+m-n)\} \end{aligned} \tag{3.7}$$

with $\alpha = d(r_s)/\sqrt{3a}$ ($2a$ being the separation, on average, between protons), and $v(K)$ is the Fourier transform for the screened potential of a single proton.

Increase of the temperature to ($k_BT \sim \hbar\omega_{vib}$) significantly excites the pairs into higher anharmonic vibrational states resulting in large amplitude spatial fluctuations. These in turn will lower the gap by a corresponding Debye-Waller factor, and given that the excursions are appreciable, the lowering can be significant. This can be demonstrated most easily by extending one of the 4 pairs in the Pa3 structure to a separation of $2d'$ ($2d' > 2d$) while the other basis pairs are kept fixed. From (3.7) the structure factor per proton for such a separation becomes

$$S(l,m,n) = S_0(l,m,n) - \frac{1}{2}\sin[\pi(\alpha' - \alpha)(l+m+n)]\sin[\pi(\alpha+\alpha')(l+m+n)], \quad (3.8)$$

which shows immediately that the gap will be reduced when the pair extends. This gives a strong hint of the likely effect of temperature, primarily to reduce the gap, and to promote an earlier transition from insulator (or semi-conductor) to metal. Note that a displacement arising with acoustic phonons can also contribute to this effect.

3.6 The Physical Characteristics of the Metal-Insulator Transition

At the one-body level the general closing of the gap with increasing pressure and density appears well established, but what exactly happens upon close approach to the metal-insulator transition in hydrogen? Some possibilities now follow:

3.6.1 Scenario 1: Metal-insulator transition induced by one-body physics

In a continuous single particle approach, the gap closes and progressively more and more carriers are excited into the conduction band; structurally this implies strong pairing correlations. Depending on the decline of this gap, the emerging conductivity can be significant. Experiments and theory converge on a consistent picture for hydrogen where the band-gap decreases with increasing pressure, both in the solid[35, 2] and liquid[52] phases. In the solid, the concept of an indirect gap closing with increase of density in the paired phase is robust when calculated in various crystal structures and it also obtains under orientational disorder[7, 53, 35]; if generalized to the separation between mobility edges[54], we expect it to carry through for the liquid phase as well[55]. Accordingly, under the assumption that the liquid remains largely paired, this view leads to a picture where the one-electron physics of the liquid may be similar to that of the solid; under pressure mobility edges are gradually approaching, and if this continues hydrogen will be transformed from a liquid semi-conductor to a liquid semi-metal. As pressure increases further the "bands" overlap (mobility edges cross), and the effective carrier density continues to increase, eventually becoming degenerate[56].

The vibrational dynamics of the H_2 molecules imply an interesting possibility for the scale of conductivity in the semi-metallic regime (i.e. $k_B T \sim E_g$). If we assume that the electrons hop from pair to pair when close approach sufficiently increases orbital overlap, then their time-scale will be set by those translational excursions which bring molecules into sufficient proximity that wave-function overlap is especially effective (i.e. $\tau \sim 10^{-14}$ s). Together with a standard semi-conductor picture invoked to estimate the carrier density (see e.g. p 575 of [57]), this quickly leads to resistivities as low as $\sim 700\mu\Omega cm$ for $E_g \sim 2k_B T$! (recall that the experimental value is $\sim 500\mu\Omega cm$.)

Note, however, that the liquid phase corresponds to proton arrangements that are strongly disordered. If viewed at low temperatures, disorder can lead to states that lack diffusion, via Anderson-localization. The role of temperature is then to excite electrons from such states. The condition for Anderson localization is similar to the condition for the Mott transition; namely:

$$D_m^{1/3} a^* \sim C, \tag{3.9}$$

where a^* is a measure of the localized orbital size, and C is typically about 0.3[54]. Under the assumption that the Bohr radius for diatomic hydrogen is roughly the same as the Bohr radius of monatomic hydrogen, $D_m^{1/3} a^* \sim 0.3$ at experimental metallization conditions. However, as emphasized by T.V. Ramakrishnan: "The main conclusion from the above discussion of criteria [eq (3.9)] for the metal-nonmetal transition is that it is not possible to decide on a particular mechanism from the agreement of the parameters for the transition with the value predicted. Only the detailed physical behavior of the system can help distinguish between various possibilities"**

** T.V. Ramakrishanan in [18], p42.

3.6.2 Scenario 2: Metal-insulator transition and the role of many-body physics

Mott[54] argued that a gap will never close continuously because upon restoration of residual many-body interactions, the formation of excitons which subsequently unbind upon further closing of the gap lead to a jump in the conductivity. We expect in this case that the temperature of $\sim$ 0.3 eV will be too high for the formation of excitons[58] but this does not rule out some other type of correlation driven transition near band-gap closure. For example, the Hubbard U for monatomic hydrogen is about 17 eV[54] while the free-electron band-width at experimental conditions is around 20 eV, which is probably an upper bound. Since the effects of disorder and correlation are expected to reinforce each other[59] the possibility of conductivity by thermal excitation across a declining Mott-Hubbard gap emerges. If we are in the regime where electron-electron interactions play an important role, the effect of spin becomes non-trivial. The twin effects of strong correlation and disorder as they influence the metal-insulator transition are not completely understood; they combine with some force in the hydrogen problem.

The highly successful semi-empirical Herzfeld polarization catastrophe criterion predicts that H_2 will become metallic only upon about $\sim$ 11 fold compression[60] (generally for ordered phases). However, we note that there is some ambiguity in the definition of the various quantities entering these criteria (for instance the meaning of local polarizability in the present environment), a problem that becomes even more acute for hydrogen where the fluid phase is involved.

3.6.3 Scenario 3: Metal-insulator transition induced by structural change

If simple pressure induced band-gap closure in the paired state is preceded by significant structural change, metallization can likewise precede complete closure of this gap. Perhaps the best known case of a metal-insulator transition driven by structural change is the metallic behavior seen when melting the elemental semiconductors such as Si and Ge (as discussed above). The change in band-structure is driven by the change in local atomic structure, in this case a relatively small increase in coordination. In the case of hydrogen, structural change associated with, for example the rapid decline of pairing correlation, is a likely candidate. In the liquid phase, we have a direct parallel of the crystalline case discussed in section VIII. above.

In fact, the Wigner-Huntington proposal[1] itself falls into the class of MI transitions induced by structural changes. Here it was predicted that increasing pressure (at T=0) could lead to dissociation in hydrogen, resulting in a structure with one electron per unit cell and concomitant metallic behavior for paramagnetic states[61]. Even at relatively low densities, increasing the temperature to regimes comparable with the dissociation energy will also rupture the H-H bond, possibly leading to metallic (conducting) behavior. The case at hand is clearly much more subtle. At the extreme pressures of the shock experiment, the H-H bond is significantly weakened, but even at $r_s = 1.5$ (~ 9 fold compression) the corresponding well depth continues to have a magnitude significantly larger than the temperatures achieved[65]. To date no evidence of static pressure induced dissociation in the solid has been observed, even at the significantly higher pressures of $350GPa$ achieved by ultra pressure diamond anvil-cell techniques[4]. Although the evidence above refers to zero-temperature solids in particular structures, increasing the temperature is not likely to change the well depth significantly.

At these extremely high densities and temperatures, the very concept of *dissociation* is nebulous. High temperatures will excite large amplitude stretching motion, leading for example to exchange of atoms from neighboring pairs, or to the transient formation new localized species ("H_3" etc...) and so standard chemical definitions are not unique. Perhaps it is better to speak of local coordination in a completely statistical sense, for example as the integral of the pair correlation function carried out to a certain distance. These changes in local coordination certainly lead to corresponding changes in the global electronic structure as pointed out in an interesting recent tight-binding (TB) molecular dynamics study by Lenosky et al.[66]. Here "dissociation" is defined by asserting that two atoms constitute a dimer if each forms the nearest neighbor atom of the other. Atoms not identified as belonging to a dimer are then termed dissociated "monomers". Interestingly, they find that states near the chemical potential have a large projection onto these "monomers", and so by virtue of the Mott formula, for which resistivity scales as the inverse square of the density of states at the Fermi energy, the resistivity in their simulation scales inversely with the square of the average number of "monomers". The mechanism they propose (similar to that suggested by Ross[67]) in which the "dissociation" plays a crucial role is a possible candidate for what might happen in liquid metallic hydrogen. However the large Hubbard U, included only indirectly through the effective parameters in TB, suggests that dissociation does not necessarily imply a conducting state. This may help explain why the TB conductivities found at low density and pressure are much higher than the experimental ones[66].

Recently Pfaffenzeller and Hohl[68] carried out Car-Parrinello ab-initio molecular dynamics (AIMD) simulations on the metallic side of the M-I transition and find an even higher "dissociation fraction". Because of the extremely short life-time of the pairs they term the metallic liquid "monatomic", even though it retains significant pairing correlations. Their lowest density is slightly higher than the metallization density calculated for the experiments ($D_m = 0.4 mol/cm^3$ vs. $0.32 mol/cm^3$) and they find a resistivity about a factor 6 smaller than the experiments. Simulating the metal-insulator transition with AIMD is difficult because the local density approximation (LDA) underestimates the gap, and the sensitivity on k-point sampling[69] (the AIMD calculations above use only one k-point) makes accurate large-scale simulations computationally intensive. Once again, the large Hubbard U implies that spin correlations may be important, necessitating AIMD simulations based on spin density functional theory instead of the usual paramagnetic ansatz.

But whether any of these these mechanisms describe the shock experiments[10] fully has yet to be established. The gap closes with increasing density even in an entirely diatomic phase, and if the TB or AIMD even slightly over-estimate the "dissociation", the metallization in the simulations will occur through the "dissociation mechanism" instead of through a pure band-overlap scenario. In fact, as evidenced from comparison of pair correlation functions, the TB and AIMD results give a larger "dissociation" fraction than the path-integral monte-carlo (PIMC) results of Magro *et al.*[39]. While PIMC includes the substantial zero-point motion of the protons which the TB and AIMD neglect, PIMC is usually carried out in a much smaller cell. Presently it is not clear which method is best suited to the experimental regime and the sensitive interdependence of dissociation and metallization physics coupled with a possible role for strong correlations will render an unambiguous interpretation of the simulations difficult.

Early predictions of finite-temperature pressure-induced metallization fall under the general rubric of *Plasma Phase Transitions* (PPT)[37]. Most theories take a chemical approach, that is the species (bound states) are well defined, and this is at variance with the extremely short life-times predicted by simulations. Besides ignoring the possibility of band-overlap metallization, the chemical models are typically based on pair-potentials and a free-rotation approximation, both of which are ill-defined at these densities as we have noted. The most comprehensive chemical model calculations were carried out by Saumon and Chabrier[38] who predict for the PPT a critical point at $T = 15310$ K and a density of $D_m = 0.18\ mol/cm^3 (rs \sim 2)$, and at higher densities and lower temperatures an increasingly discontinuous transition between a diatomic insulating state and an ionized (conducting) monatomic phase (see also Fig. (3.2)). In support of these chemical models, the physically based PIMC calculations[39] also give rather similar results. On the other hand the TB simulations give a gradual transition to a more "monatomic" phase. The metallization experiments appear just out of the range of the PPT predictions. To establish the existence of a PPT by shock experiments will also require a range of temperature and density data.

Clearly the experiments are in a very interesting regime; the interplay of thermal and electronic effects brings the system close to both the closing of the gap *and* the onset of pair fragmentation, the two being interconnected. Which occurs first will depend sensitively on the actual temperature and pressure and one could imagine different behaviors at different state points. For example at densities just below the proposed diatomic metal-insulator transition at 0 K one would expect a I-M transition of the band-overlap type while at higher temperature and lower densities structural change, if it exists, becomes more important. A definitive electronic interpretation of the Livermore shock experiments is still lacking, and could prove to be quite unlike the conventional explanations of transport properties of ordinary liquid metals.

3.7 Future Experimental Probes

Considerations based both on a simple band-overlap scenario within the Ziman formulation, and the "dissociation" based mechanism proposed by Ross and Lenosky *et al.*[66, 67], predict that the conductivity is high, but that it should drop with increasing density. Experiments going to higher pressure would therefore be of great interest. However, so also would shock experiments at about the same compression but lower temperatures. If the arguments given above are valid, then as depicted in Fig. (3.2), a boundary should be crossed (at fixed P) locating the I-M transition. One could also envisage that at even higher pressures, the I-M transition would be at low enough temperature to be within reach of static pressure techniques such as diamond anvil cells[70].

3.8 Conclusions

Depending on temperature, the transition to a conducting state in hydrogen may be quite unusual. The tenacity with which H retains its pairing, an effect driven largely by exchange, can be manifested even in a metallic environment and at quite high temperatures. Though covalent, this ensuing state is not of a network character as in molten Si (or Ge), but a rapid exchange of pairs (akin to the fast exchange proceeding in Si and Ge) may be proceeding. It is an interesting and perhaps novel state of matter, which now merits considerable further study.

Bibliography

[1] E. Wigner and H.B. Huntington, J. Chem Phys. **3**, 764 (1935).

[2] H-K. Mao and R.J. Hemley, Rev. Mod. Phys. **66**, 671 (1994).

[3] H. N. Chen, E. Sterer, and I. F. Silvera, Phys. Rev. Lett. **76**, 1663 (1996).

[4] A. L. Ruoff, in *High Pressure Science and Technology*, edited by W. Trzeciakowski (World Scientific, Singapore, 1996), pp. 511-516; C. Narayana, H. Luo, J. Orloff and A. L. Ruoff, *Solid Hydrogen at 351 GPa: Still the Reluctant Alkali*, Cornell preprint (1997).

[5] N. W. Ashcroft, Physics World **8**, 43 (1995).

[6] D.E. Ramaker, L. Kumar, and F.E. Harris, Phys. Rev. Lett. **34**, 812 (1975) (note that this reference has no bands in it).

[7] C. Friedli and N.W. Ashcroft, Phys. Rev. B **16**, 662 (1977).

[8] A.S. Balchan and H.G. Drickamer, J. Chem. Phys. **34**, 1948 (1961), B.M Riggelman and H.G. Drickamer, J. Chem. Phys. **38**, 2721 (1963)

[9] D. J. Stevenson, Rep. Prog. Phys. **46**, 555 (1983).

[10] S.T. Weir, A.C. Mitchell and W.J. Nellis, Phys. Rev Lett. **76**, 1860 (1996), S.T. Weir and W.J. Nellis, *ibid* ..., and .S.T. Weir, A.C. Mitchell and W.J. Nellis, manuscript submitted to Phys. Rev. B.

[11] W. J. Nellis, M. Ross, and N. C. Holmes,Science **269**, 1249 (1995); W. J. Nellis, S. T. Weir, and A. C. Mitchell, Science **273**, 936 (1996).

[12] R. P. Butler and G. W. Marcy, Astrophys. J. **464**, L153 (1996); R. P. Butler and G. W. Marcy, Astrophys. J. **474**, L115 (1996); M. Mayor and D. Queloz, Nature **378**, 355 (1995).

[13] V. N. Zharkov and T. V. Gudkova, in *High-Pressure Research: Application to Earth and Planetary Sciences*, Y. Syono and M. H. Manghnani, Eds., (Terra Scientific Publishing Co., Tokyo, 1992), pp.393-401.

[14] P.P. Edwards and M.J. Sienko, Intern. Rev. Phys. Chem **3**, 83 (1983).

[15] As late as 1996, the late Sir Nevill Mott wrote: "I've thought a lot about 'What is a metal' [and] I think one can only answer the question at $T = 0$. Thus a metal conducts [and] a non-metal doesn't." (P.P. Edwards, private communication).

[16] *Symposium on The Beginnings of Solid State Physics*. Proc. R. Soc. Lond. A 371, 1-177 (1980).

[17] L.H. Hoddeson and G. Baym in [16].

[18] *Metallic and Non-Metallic States of Matter* (Taylor and Francis, London (1985)), ed. by P.P. Edwards and C.N.R. Rao.

[19] D.E. Logan and P.P. Edwards in [18].

[20] Annalen der Physic, **1**, 566 and **3**, 369 (1900).

[21] The results were announced at the 1927 Volta conference and accepted almost immediately[17].

[22] P.W. Bridgman, Phys. Rev. **29**, 188 (1927).

[23] F. Bloch, Z. Phys **52**, 555 (1928), *ibid* **57**, 545 (1929).

[24] A.H. Wilson, Proc. R. Soc. A **133**, 358 (1931). *ibid* **134**, 277 (1931).

[25] A.H. Wilson in [16], p45.

[26] J.H de Boer, and E.J.W. Verwey, Proc. R. Soc. **49**, 59 (1937).

[27] N.H. Mott in [18].

[28] P.W. Anderson, Phys. Rev **109**, 1492 (1958).

[29] A. H. Jones, W. M. Isbell, and C. J. Maiden, J. Appl. Phys. **37**, 3493 (1966).

[30] C. S. Yoo, G. E. Duvall, J. Furrer, and R. Granholm, J. Phys. Chem. **93**, 3012 (1989).

[31] W.J. Nellis, A.A. Louis and N.W. Ashcroft, to appear: Phil. Trans. Roy. Soc. A. (1997)

[32] G. I. Kerley, in *Molecular-Based Study of Fluids*, edited by J. M. Haile and G. A. Mansoori (American Chemical Society, Washington, 1983), pp. 107-138.

[33] N. C. Holmes, M. Ross, and W. J. Nellis, Phys. Rev. B **52**, 15835 (1995).

[34] N. F. Mott, Phil. Mag. **24**, 2 (1971).

[35] H. Chacham, X. Zhu, and S.G. Louie, Phys. Rev. B **46**, 6688 (1992).

[36] F. Hensel and P. P. Edwards, Phys. World, April, **43** (1996).

[37] The PPT was first proposed by L. Landau and G. Zeldovich, Acta. Phys. Chim. USSR, **18**, 194 (1943) for a somewhat different system. Since then the term PPT has been applied to a multitude of different transitions of the insulating-conducting type.

[38] D. Saumon and G. Chabrier, Phys. Rev. A **46**, 2084 (1992).

[39] W.R. Magro, D.M. Ceperley, C. Pierleoni and B. Bernu, Phys. Rev. Lett. **76**, 1860 (1995), W.R. Magro, PhD thesis, University of Illinois (1995).

[40] J. M. Ziman, Phil. Mag. **6**, 1013 (1961).

[41] T.E. Faber *Introduction to the Theory of Liquid Metals* (Cambridge University Press, Cambridge 1972).

[42] M. Shimoji, *Liquid Metals* (Academic Press, London 1977).

[43] The resistivity of the liquid metallic state is often easier to calculate than that of the solid metallic state because in the former the scattering is dominated by density fluctuations while in the latter the scattering may come from a multitude of different sources such as defects, impurities etc...

[44] In the usual application of the Ziman formalism, it is assumed that the temperature scale is such that $k_BT >> \hbar\omega$ for all excitations of interest in the system. While these conditions hold for translational and rotational energy scales, this is not true for vibrons. In fact, the temperature is quite closely matched to the vibron energies; a confluence that leads to the possibility of near resonant scattering processes. By taking fixed diatomic molecules we ignore the effect of vibrational excitation on the structure factor $S(k)$. We use an expression for the diatomic structure factor that includes the bond-length of $1.4a_0$ and a Percus-Yevick structure factor for the hard sphere system with $\sigma = 0.29$ and $\eta = 0.29$ for the center-of-mass-center-of-mass part and as a first approximation neglects contributions from anisotropy (i.e. the free-rotation approximation (see e.g. J-P. Hansen and I. R. McDonald, *Theory of Simple Liquids*, (Academic Press, London 1986))). The rotational and translational time-scales are about equal at this density, making the free-rotation approximation suspect. But even though simulations[66, 68] give extremely short life-times for the "molecules", a structure factor based on the static pair and free-rotation approximations does reasonably well (see for example A. Bunker, S. Nagel, R. Redmer and G. Röpke, Phys. Rev. E (1997), to appear).

[45] The neglected vibrations lead to inelastic scattering effects. Baym (G. Baym Phys. Rev **135**, A1691 (1964)) showed that in this case the crucial quantitity is $S(\vec{k},\omega)$, the dynamic structure factor for the protons defined by:

$S(\vec{k},\omega) = \int_{-\infty}^{\infty} dte^{-i\omega t} < \hat{\rho}(\vec{k},t)\hat{\rho}^{\dagger}(\vec{k},0) >$

where $\hat{\rho}(k)$ is the one-particle density operator for protons) the resistivity is then given by: $\rho \sim \int_0^{2k_f} q^3 dq|v(q)|^2 \int_{-\infty}^{\infty} \frac{d\omega}{2\pi} S(\vec{k},\omega)\frac{\beta\hbar\omega}{(\exp(\beta\hbar\omega)-1)}$ which reduces to the usual Ziman formula for $k_B T >> \hbar\omega$. The effect of the vibrations can be calculated and gives a correction to the static structure factor $S(q)$ proportional to q^2, but with a small enough prefactor (the same order as the correction for finite ion mass) to be ignored at this level of approximation.

[46] D. J. Stevenson and N. W. Ashcroft, Phys. Rev. A **9**, 782 (1974).

[47] One reason for the success of the Ziman formalism is the so-called Edwards cancellation theorem which states that the d.o.s. corrections (as manifested in the effective mass) cancel out to first order (see for example[41, 42]). However, in this case the Edwards cancellation theorem probably doesn't hold (see e.g. M. Itoh and M. Watabe, J. Phys. F **14**, L9 1984), and instead Mott's g^2 factor, where g is the ratio of the actual density of states to the free-electron value, must be included[54]. The minimum value of g is typically about 0.3, raising the resistivity by a maximum of about $1/g^2 \sim 10$.

[48] The mean-free path is roughly given by: $l = [174a.u.] \times [(rs/a_0)^2/\rho_\mu]$[57], which implies a mean free path of about $9a.u.$ for a calculated resistivity of $\sim 50\mu\Omega cm$. Thus the Ziman formalism is self-consistent in that sense. A lower effective carrier density raises rs, so that in this approach the mean free path is still greater than the inter-molecular spacing for the larger (experimental) resistivities.

[49] See for example H. Kitamura and S. Ichimaru, Phys. Rev. E, **51**, 5006 (1995).

[50] G. Kresse and J. Hafner, Phys. Rev. B, **55**, 7539 (1997).

[51] N.W. Ashcroft in *Elementary Processes in Dense Plasmas,* ed by S. Ichimaru and S. Ogata, (Addison Wesley, 1995).

[52] W. J. Nellis, A. C. Mitchell, P. C. McCandless, D. J. Erskine, and S. T. Weir, Phys. Rev. Lett. **68**, 2937 (1992).

[53] E. Kaxiras, J. Broughton and R.J. Hemley, Phys. Rev. Lett. **67**, 1138 (1991).

[54] N. Mott, *Metal Insulator Transitions* (Taylor & Francis, London 1990).

[55] This in contrast to some narrow gap semi-conductors, or semi-metals like Bi, which would become a good metal upon a very slight distortion of the structure (see e.g. [57]).

[56] The reader might wonder why we use language inspired by bands in this manifestly disordered system where the wave vector **k** is not at all a good quantum number. Although the concept of energy bands is not entirely correct here, it is well known that for many liquid metals the band structure of a solid with similar local coordination gives a good approximation of the electron physics of the liquid[41], and so this is the sense in which we use the concept of bands here.

[57] N.W. Ashcroft and N.D. Mermin, *Solid State Physics* (Holt, Rinehart and Winston, New York 1976).

[58] See e.g. B.I. Halperin and T.M. Rice, Solid State Physics **21**, 116 (1968).

[59] D. J. Thouless in *Ill-Condensed Matter* edited by R. Balian, R. Maynard and G. Toulouse (North Holland, Amsterdam 1979).

[60] P.P. Edwards and M. Sienko, Chemistry in Britain **19**, 39 (1983), M. Ross, J. Chem. Phys **56**, 4651 (1972).

[61] Its interesting that at their original predicted density, the monatomic solid would be close to a Mott-Hubbard insulator!

[62] N.W. Ashcroft, Phys. Rev. Lett. **21**, 1748 (1968).

[63] C. F. Richardson and N. W. Ashcroft, Phys. Rev. Lett. **78**, 118 (1997).

[64] R. J. Hemley, H. K. Mao, A. F. Goncharov, M. Hanfland, and V. Struzhkin, Phys. Rev. Lett. **76**, 1667 (1996).

[65] Full ab initio LDA calculations of the pair potential in the solid phase at the liquid metallization densities give a well depth of about 3 eV, and also the correct vibron frequency of about 0.5 eV. These calculations also show very strong many-body effects making pair-potentials suspect (see for example, B. Edwards and N.W. Ashcroft, unpublished). Even free H_2^+ is strongly paired with a dissociation energy of about 2.8eV, a fact which helped motivate an earlier prediction of metallization in the molecular liquid[62]. In the solid, vibron overtones have been measured up to pressures of 170 GPa[3, 64].

[66] T.J. Lenosky J.D. Kress, L.A. Collins, I Kwon, Phys. Rev. B **55**, 11907 (1997). T.J. Lenosky J.D. Kress, L.A. Collins, I Kwon J. Quant. Spect. Radiat. Trans (1997), to appear.

[67] M. Ross, Phys. Rev. B **54**, R9589 (1996).

[68] O. Pfaffenzeller and D. Hohl, Preprint 1997.

[69] See for example B. Edwards, N.W. Ashcroft and T.J. Lenosky, Euro. Phys. Lett. **34**, 519 (1996) and J. Kohanoff *et al.* Phys. Rev. Lett. **78**, 2783 (1997).

[70] Heating of hydrogen can cause diamond anvils to fail, but at high enough pressures the the metal-insulator transition should occur at temperatures that may be low enough to avoid this failure.

Chapter 4

A Single Atom in an Electron Gas

4.1 Introduction to the Problem: Reducing the Atom to a Pseudo-Potential in Jellium

Immerse a single point charge Q into an electron gas*. The first Z_A electrons will get sucked into bound states†, localized near the center of charge Q , practically oblivious to the electron gas from which they originated. Following standard usage, we shall call this new object, the potential plus Z_A bound electrons, an *ion* of valence $Z = (Q - Z_A)$. At a one-electron level, the exclusion principle requires the wave-functions of the remaining scattering state electrons to be orthogonal to the Z_A bound states, a constraint that can only be satisfied by introducing multiple nodes in the scattering state wave-functions near the ion center, implying a higher kinetic energy. Thus the scattering state electrons are effectively repelled by the

* With a suitable rigid charged background to insure electro-neutrality of the entire electron gas plus charge Q system

† This depends on the density, for high enough electron density there will be no bound states.

bound core region and the overall effect of the attractive potential is weakened. We model this by a much weaker *pseudo-potential*, that is, an electron-ion potential with ideally the same scattering properties as the full ion, but with the bound core electrons now safely tucked away into its definition and subsequently ignored[1]. In this chapter we use a simple local form which doesn't have the exact scattering properties as the full ion plus core electrons, but has only one parameter which greatly facilitates our investigations. Since where we are mainly interested in the response of an electron-gas to an atom and not details of the atoms themselves this slight loss of accuracy is not important. The most popular of these local pseudo-potentials is the the Ashcroft or empty-core pseudo-potential (APP)[3]:

$$v^{ps}(r) = \begin{cases} 0 & r < R_c \\ -2Z/r & r \geq R_c, \end{cases} \tag{4.1}$$

which in Fourier space is given by:

$$v^{ps}(k) = \int d\vec{r} v^{ps}(r) e^{i\vec{k}\cdot\vec{r}} = -\frac{8\pi}{q^2} cos(kR_c). \tag{4.2}$$

(We use atomic units throughout). The repulsive effect of the core electrons is modeled simply by setting the inner part of the Coulomb potential to zero and the single parameter, R_c, is typically fixed either by an atomic property such as the ionization energy or else by some measurable material property of the crystalline state such as the Fermi-surface if the system is metallic. It is an average representation of an ionic dimension. An important parameter related to R_c is q_0, the first k-space zero of the pseudo-potential:

$$q_0 = \frac{\pi}{2R_c}. \tag{4.3}$$

In spite of its simplicity, the APP works remarkably well, especially for simple metals, and has been the well tested work-horse of many analytical and semi-analytical theories. Other local and non-local pseudo-potentials have also been widely used, but we chose the APP primarily because of its simplicity.

Having suitably reduced the atom in an electron gas problem to an ion of valence Z, now represented by a pseudo-potential $v^{ps}(r)$, we turn to the question: "What is the total response of an electron gas to such a pseudo-potential perturbation?". Even though the bound core-states are accounted for, the pseudo-potential still attracts the scattering state electrons, resulting in a local inhomogeneity surrounding the potential an induced density $\rho(r)$ with the property:

$$\int_V \rho(r) d\vec{r} = Z, \tag{4.4}$$

i.e. the induced density has a charge equal to the ionic valence; the ion is "perfectly screened" at long range (note that the total electron density is $\rho_0 + \rho(r)$). The rest of this chapter will concern itself with ways of calculating this induced density $\rho(r)$.

4.2 Infinite Order Response within the Local Density Approximation (LDA)

The advent of the Hohenberg-Kohn theorem[5] and the associated Kohn-Sham equations[6, 7] (see also appendix C) introduced many new simplifying concepts to electronic structure theory. In particular the Kohn-Sham equations, which follow from an energy minimization principle[7], reduce the many-body interacting electron-gas problem to a one-body Schroedinger equation moving in a (self-consistent) external potential of the form:

$$v_{eff}(\vec{r}) = v^{ext}(\vec{r}) + \int \frac{2\rho(r')}{|\vec{r}-\vec{r'}|} d\vec{r'} + \mu_{xc}(\vec{r};[\rho]). \tag{4.5}$$

The first term is the external potential $v^{ext}(\vec{r})$, the second is the screened (Hartree) term due to the induced charge $\rho(r)$, and the last term is the so-called exchange correlation potential $\mu_{xc}(\vec{r};[\rho])$, which contains all the effects of correlation and exchange and into which are lumped all the complexities of the full interacting many-body problem. However, for the ground state, the Hohenberg-Kohn theorem[5] states that the exchange-correlation potential is a unique albeit unknown *functional* of the one-body density $\rho(r)$ and in fact several approximations based on this idea exist, the best known of which is the so-called local density approximation (LDA)[6, 7] which we adopt for this chapter. For a single atom modeled by a spherically symmetric pseudo-potential, the Kohn-Sham Schroedinger equation reduces to a single differential equation in the variable r, which can then be solved numerically‡, provided special care is taken to enforce the perfect-screening sum-

‡ For the case of two hydrogen atoms in an electron gas, this problem becomes considerably more complex, and various approximations must be invoked to extract a problem numerically tractable in real space; k-space methods must be used instead[11].

rule of equation (4.4). Many groups have already acquired considerable expertise in this problem[13], which forms an important input for effective medium theories of metallic bonding[12]. We adapted one version of this code by G. Eliasson and K. Jacobsen to calculate the total LDA response of an electron gas to a pseudo-potential of the form given by equation 4.1. Its output is the "exact" or infinite order response.

4.3 Linear and Non-linear Response Theory

4.3.1 The general formulation of response theory

The output of the self-consistent Kohn-Sham formalism can formally be expanded in powers of the perturbing (pseudo)potential:

$$\rho(k) = \chi_1(k)v^{ps}(k) + \sum_{\vec{k}_1}\sum_{\vec{k}_2}\chi_2(k,k_1,k_2)v^{ps}(k_1)v^{ps}(k_2) + ..., \tag{4.6}$$

where the interacting response functions $\chi_n(k_1...)$ are properties of the *homogeneous* electron gas. The first two are given by:

$$\chi_1(k) = \frac{\chi_1^0(k)}{\epsilon(k)} \tag{4.7}$$

and

$$\chi_2(k1,k2,k3) = \frac{\chi_2^0(k1,k2,k3) + \frac{1}{2}\mu_2(k1,k2,k3)\chi_1^0(k1)\chi_1^0(k2)\chi_1^0(k3)}{\epsilon(k1)\epsilon(k2)\epsilon(k3)}, \tag{4.8}$$

where the $\chi_n^0(k_1..)$ are the response functions for the non-interacting case, the $\mu_n(k_1...)$ are the homogeneous limit of functional derivatives of the exchange correlation potential w.r.t. the density, and $\epsilon(k)$ is the dielectric function given by:

$$\epsilon(k) = 1 - \left(\frac{8\pi}{k^2} + \mu_1(k)\right)\chi_0^1(k). \tag{4.9}$$

More details on these response functions and their definitions can be found in Appendix D. The induced density of equation 4.6 can also be written, order by order as:

$$\rho(k) = \rho_1(k) + \rho_2(k) + \rho_3(k) + ..., \tag{4.10}$$

where each ρ_n is identified with the contributions stemming from nth order of response and obeys the perfect screening sum-rule:

$$\int \rho_n(r)d\vec{r} = \begin{cases} Z, & n = 1, \\ 0, & n > 1. \end{cases} \tag{4.11}$$

This is most easily proven in k-space. At first order, for small q, the potential scales as $\sim Z/q^2$, while the response function $\chi^1(q)$scales as $\sim q^2$. Thus the sum-rule is completely saturated at linear order in the response series. The question naturally arises: do the higher order terms *collectively* sum to zero for small q, or do they do so *individually*? If the potential is multiplied by an arbitrary factor λ, the nth term in the series (4.6) scales as λ^n. Since the sum of higher order terms must equal zero for arbitrary λ each term must *individually* be zero for $q \to 0$.

4.3.2 Linear response theory

The first term in the expansion (4.6) is the familiar linear response term:

$$\rho_1(k) = \chi_1(k) v^{ps}(k) \tag{4.12}$$

which already saturates the perfect screening sum-rule of equation 4.11 :

$$\rho_1(k=0) = Z. \tag{4.13}$$

Note that given a choice for Z, this sum-rule sets the overall scale of linear response for all rs and R_c. In general linear response is expected to work better for small rs (high density) and large R_c (small perturbations). For large enough rs bound states set in and linear response theory breaks down [more on this later]. As demonstrated in figure 4.1 linear response works remarkably well and captures the dominant response of the electron gas, something which is not at all a-priori obvious since an atom is not generally considered a weak perturbation. It needs to be understood.

4.3.3 2nd order and full non-linear induced density

The full second order response function $\chi_2^0(q1, q2, q3)$ for non-interacting electrons was first calculated by Lloyd and Sholl[8]; their forms are used in what follows. Later

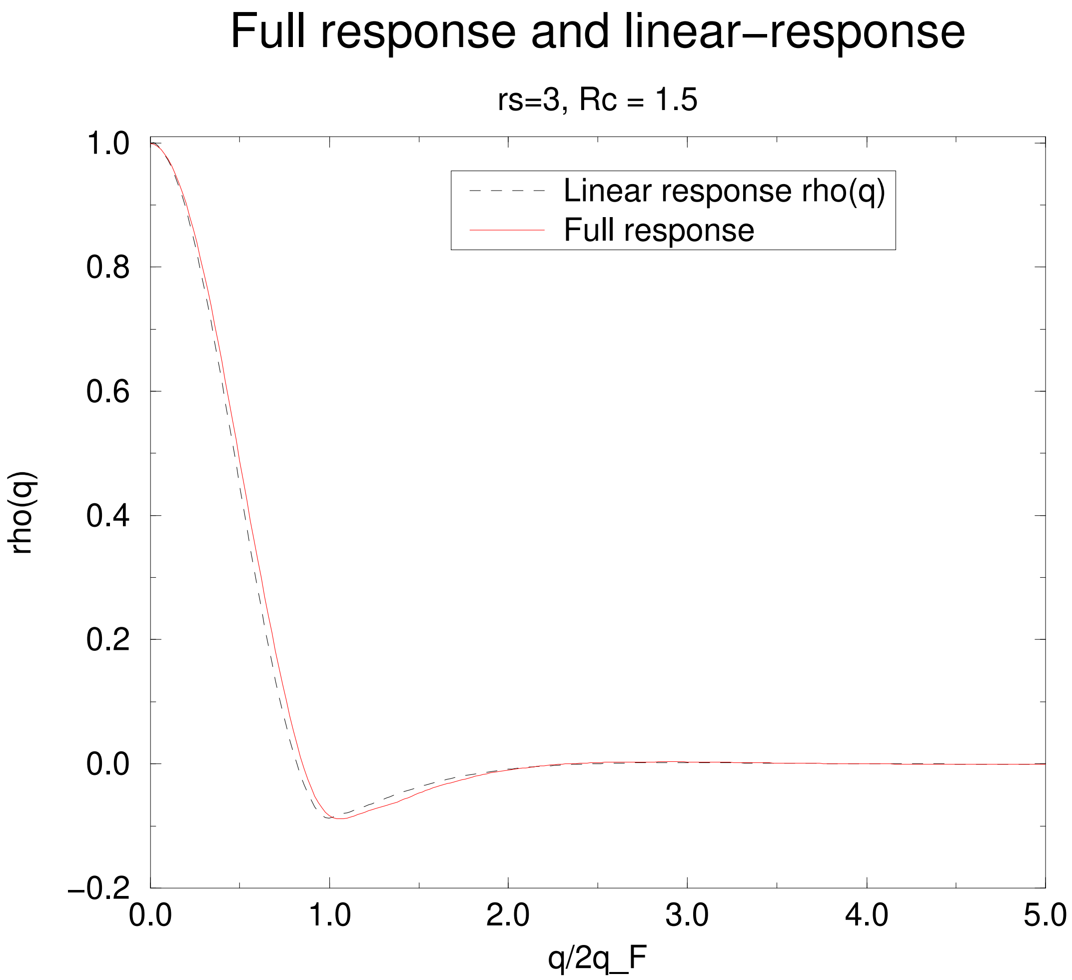

Figure 4.1: **density in k-space for an LDA embedded APP and a linear response APP**
For the density parameter $rs = 3$ and atomic APP parameter $R_c = 1.5$ are plotted the full LDA embedded APP response and the linear response. Note how well the linear response captures the full response already.

approximate forms for the 3rd and 4th order expressions were given by Hammerberg and Ashcroft[9], and also by Kagan *et. al*[10]. From equation 4.6, the second order induced density is given by:

$$\rho_2(k) = \sum_{\vec{k}_1} \sum_{\vec{k}_2} \chi_2(k, k_1, k_2) v^{ps}(k_1) v^{ps}(k_2) \tag{4.14}$$

Where $\chi_2(k, k_1, k_2)$ is the full interacting response function defined in Appendix D. Translational invariance of the unperturbed electron gas imposes on the sum a delta-function constraint of the form:

$$\vec{k} + \vec{k}_1 + \vec{k}_2 = 0, \tag{4.15}$$

so that the double sum (4.14) reduces to an integral of the form:

$$\begin{aligned} \rho_2(k) \quad = \quad & \frac{1}{(2\pi)^2} \frac{1}{k\epsilon(k)} \int_0^\infty dk_1 k_1 \frac{v^{ps}(k_1)}{\epsilon(k_1)} \int_{|k1-k|}^{|k1+k|} dk_2 k_2 \frac{v^{ps}(k_2)}{\epsilon(k_2)} \cdot \\ & \left[\chi_2^0(k_1, k_2, k_3) + \frac{1}{2} \mu_2(k1, k2, k3) \chi_1^0(k1) \chi_1^0(k2) \chi_1^0(k3) \right] \end{aligned} \tag{4.16}$$

The integrand is a product of the 2nd order density response function defined in Appendix D, and the oscillatory potential defined in equation 4.2; it is depicted in figure 4.2.

The question naturally arises: How accurate is this 2nd order response theory? Does it actually capture the most of the higher order response?

In fact, as shown in figure 4.3 and figure 4.4, the second order response result performs remarkably well, far beyond our initial expectations. When compared to the full response the maximum error is on the order of 0.5% for these conditions[§]. This calls for a more thorough exploration within the space of the atomic variable q_0 (related to R_c through equation 4.3) and the electron-gas variable $2k_F$ (twice the Fermi-wave vector k_F, related to the density parameter rs by: $k_F = 1.919/rs$).

[§] And that error may very well be due to numerical errors in truncating the Friedel oscillations

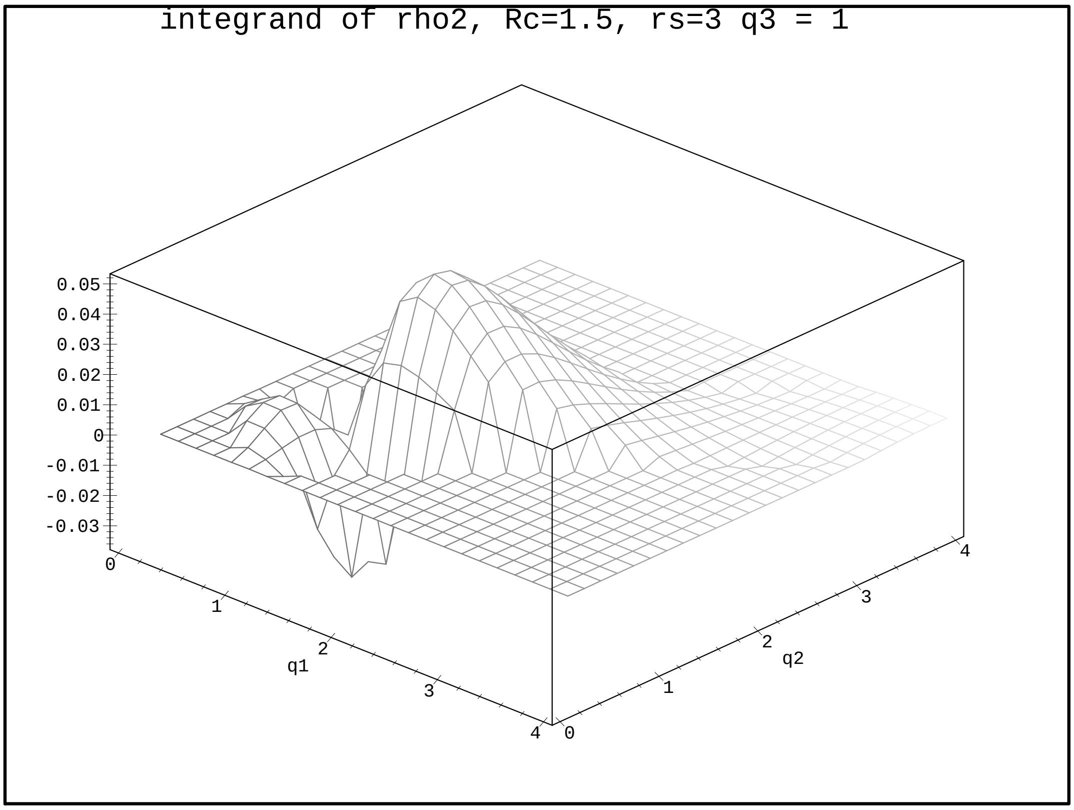

Figure 4.2: **Integrand of equation 4.16 for $k = 1, rs = 3, R_c = 1.5$.**
Note that the dominant contribution comes from wave-vector moduli near $2k_F$ and that the integration volume is restricted by the limits $(k < k_1 + k_2)$ $(k_1 < k + k_2)$ and $(k_2 < k + k_1)$ which stem from the delta-function constraint 4.15 and must be simultaneously satisfied. $2k_f = 1.28$ a.u. and $q_0 = 1.05$, and both lengthscales are visible in the integrand. Note that there is some cancellation due to the oscillation of the pseudo-potentials.

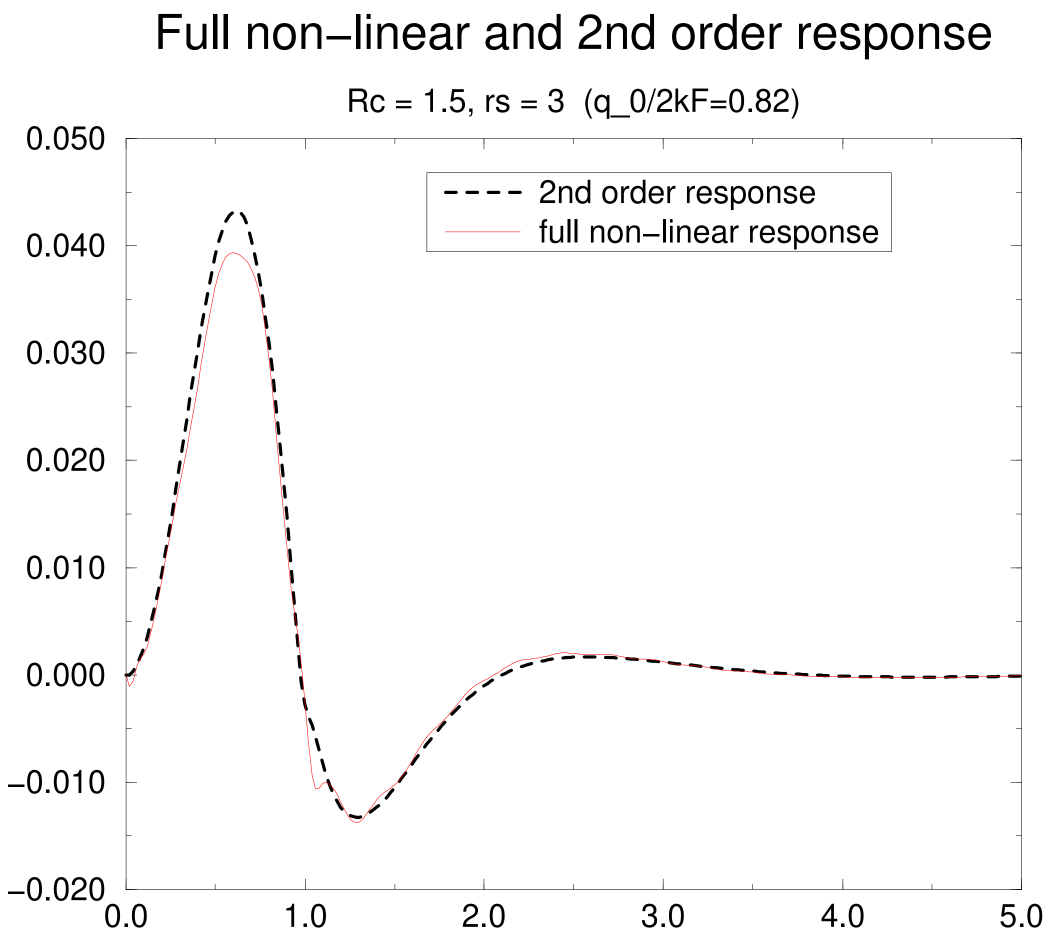

Figure 4.3: **Full non-linear LDA response** $:\rho(k) - \rho_1(k)$ **compared to the second order response** $\rho_2(k)$ **for** $rs = 3$ $R_c = 1.5$**,** $Z = 1$**.**
Compared in the figure above are the full non-linear LDA response (i.e. the infinite order summation of equation 4.6, and also the 2nd order response of equation 4.16. For the scale, compare this to the full response, which goes to $rho(q = 0) = Z$, or to the linear response depicted in figure 4.4. The LDA result has some slight numerical errors because the real-space calculations are cut-off for a certain radius and Friedel oscillations are then ignored.

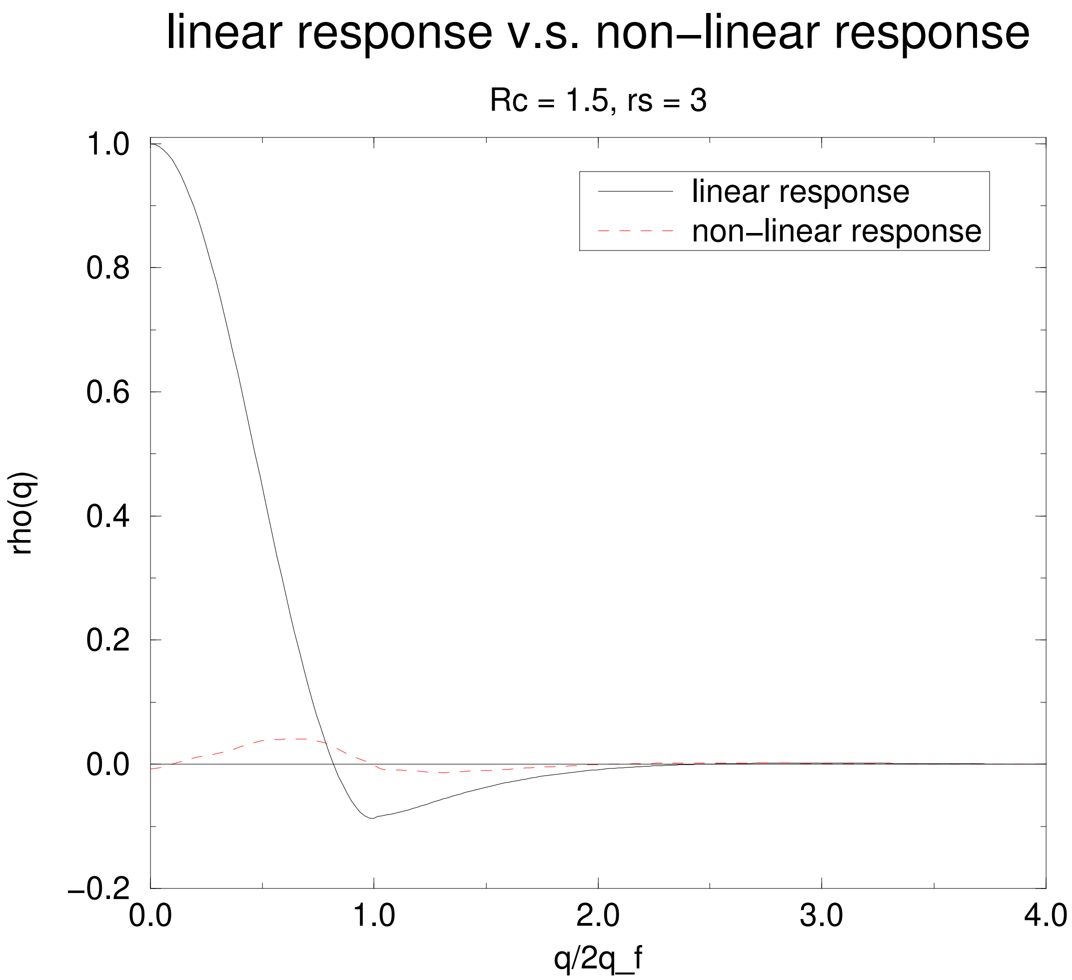

Figure 4.4: **Linear response compared to 2nd order response for $rs = 3$, $R_c = 1.5$, $Z = 1$.**
By plotting the linear response (which empirically captures the bulk of the full response) and the second-order response (which captures the bulk of what's left over) we obtain a sense of the scale of the first two orders in the expansion of equation 4.6.

Table 4.1: **Summary of the figures for fixing rs and varying R_c**

Figure	*electron density rs*	*APP cutoff parameter R_c*
figure (4.5)	$rs = 2$	$R_c = 0.0 \rightarrow 2.0$
figure (4.6)	$rs = 3$	$R_c = 0.0 \rightarrow 2.0$
figure (4.7)	$rs = 5$	$R_c = 0.0 \rightarrow 2.0$

2nd order response for q_0 v.s. $2k_F$

The first variation we investigate is the influence of R_c for a fixed rs; the parameters are listed in table 4.3.3. The degree of non-linear response increases as rs increases (and the density goes down). This can be understood at the level of Thomas-Fermi¶ theory; the second order Thomas-Fermi response is given by:

$$\chi_2^{TF}(k_1, k_2, k_3) = \frac{1}{6\pi^2 k_F} \tag{4.17}$$

which is independent of the arguments k_i and scales with rs, becoming more important at lower densities (higher rs). We expect that as R_c *increases* and the APP potential becomes weaker, the non-linear response *decreases*‖ A more careful look at figures 4.5 - 4.7 shows that things aren't quite so simple: Increasing R_c does not always imply decreasing response. Also, the functional form of the non-linear response varies depending on R_c. A look at the length-scales hints at a more illuminating way to plot the effect of the response: namely, first fixing $q_0/2k_F$ and then varying the electron density parameter rs. The parameters in the figures are summarized in table (4.3.3). The total response for a given $q_0/2k_F$ does always increase with increasing rs. Note how similar the functional forms are for a given

¶ Or Fermi-Thomas

‖ Keep in mind that the scale of the linear response is set by the perfect-screening sum-rule: $\rho_1(k = 0) = 1$ for all R_c and rs in this case.

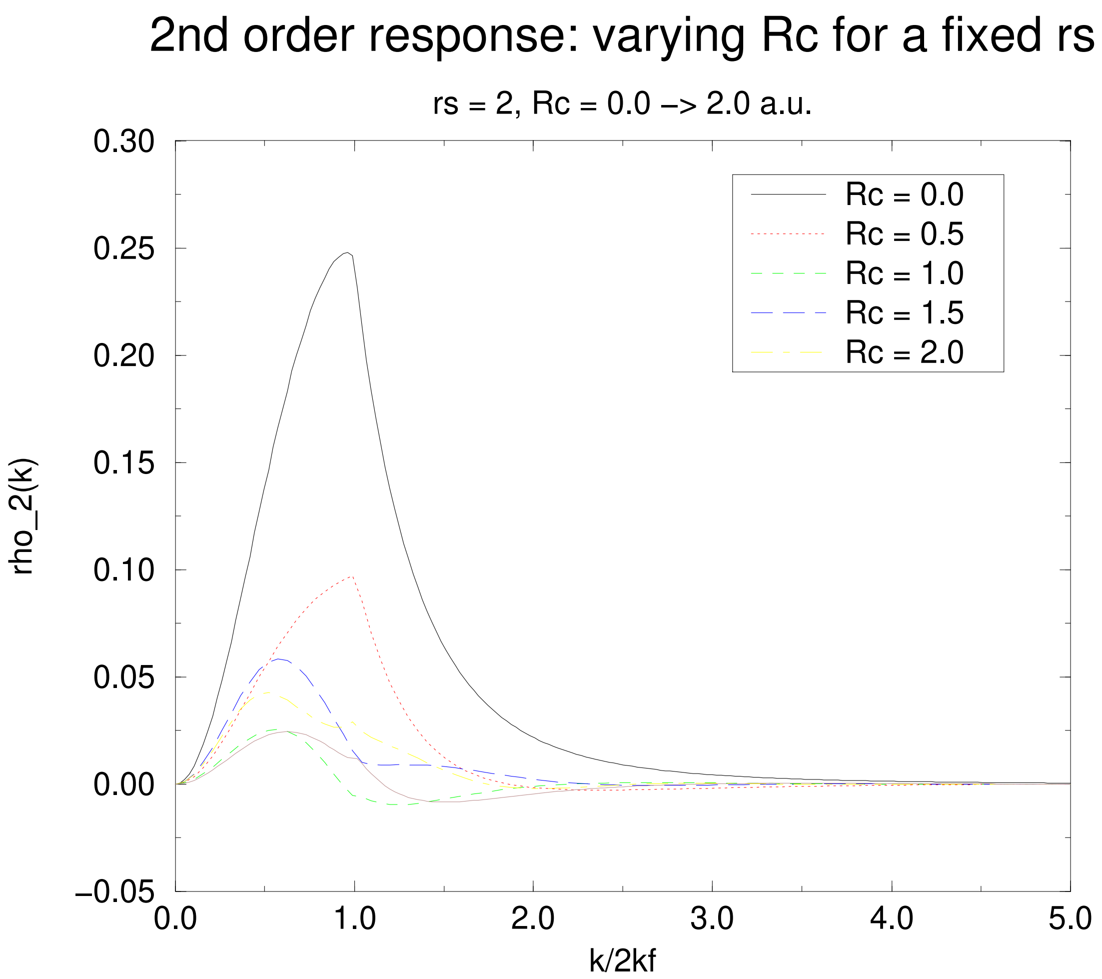

Figure 4.5: **2nd order response: varying R_c for a fixed $rs = 2$**
For a fixed rs, we vary R_c from 0.0 a.u. (Hydrogen) to 2.0 a.u. (equivalent to an ionization energy of about 0.36 Ry). In this case, $rs = 2$ is equivalent to a very high density (about that of aluminum)

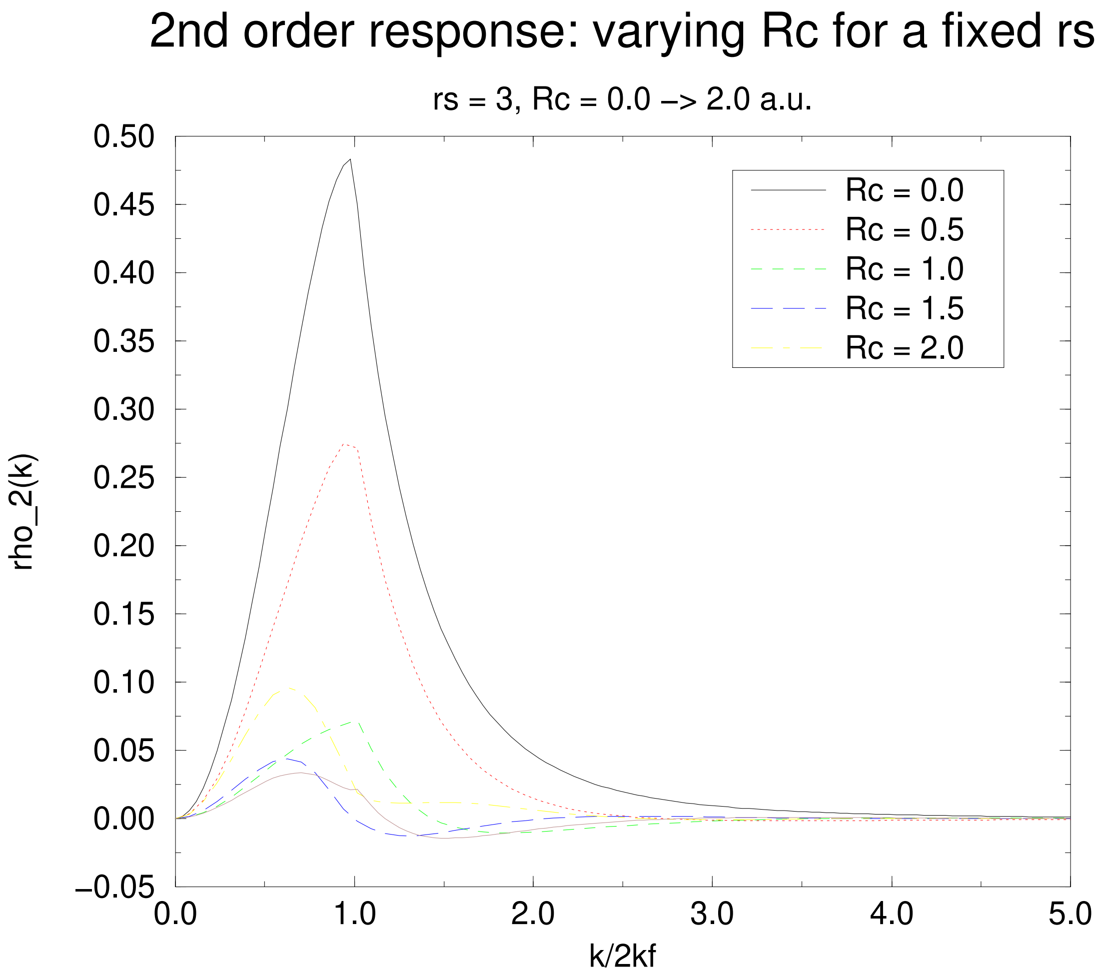

Figure 4.6: **2nd order response: varying R_c for a fixed $rs = 3$**
For a fixed rs, we vary R_c from 0.0 a.u. (Hydrogen) to 2.0 a.u. (equivalent to an ionization energy of about 0.36 Ry). In this case, $rs = 3$ is equivalent to a moderately high density (about that of silver or gold (materials that include d-electrons))

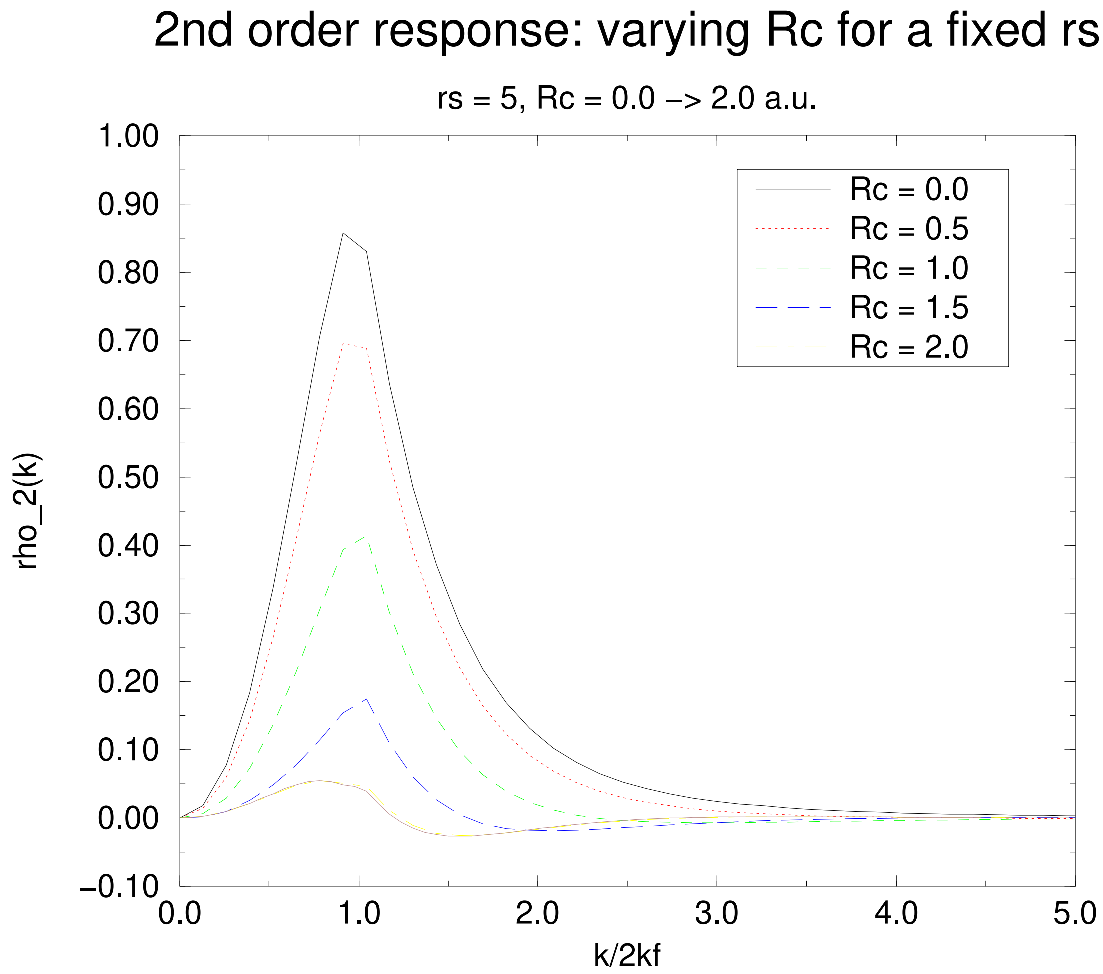

Figure 4.7: **2nd order response: varying R_c for a fixed $rs = 5$**
For a fixed rs, we vary R_c from 0.0 a.u. (Hydrogen) to 2.0 a.u. (equivalent to an ionization energy of about 0.36 Ry). In this case, $rs = 5$ is equivalent to a relatively low density (about that of potassium)

Table 4.2: **Summary of the figures for fixing $q_0/2k_F$ and varying rs**

Figure	*length-scale ratio* $q_0/2k_F$	*electron density* r_s
figure (4.8)	$q_0/2k_F = 0.5$	$rs = 1 \rightarrow 5$
figure (4.9)	$q_0/2k_F = 0.75$	$rs = 1 \rightarrow 5$
figure (4.10)	$q_0/2k_F = 0.9$	$rs = 1 \rightarrow 5$
figure (4.11)	$q_0/2k_F = 1$	$rs = 1 \rightarrow 5$
figure (4.12)	$q_0/2k_F = 1.25$	$rs = 1 \rightarrow 5$
figure (4.13)	$q_0/2k_F = 1.5$	$rs = 1 \rightarrow 5$
figure (4.14)	$q_0/2k_F = 2$	$rs = 1 \rightarrow 5$
figure (4.15)	$q_0/2k_F = \infty$ (hydrogen)	$rs = 1 \rightarrow 5$

$q_0/2k_F$. Among other things, the dielectric function $\epsilon(k)$ and the correlation parts of the local field corrections spoil the almost perfect scaling with rs.

Higher order response for hydrogen: $q_0 = \infty$

Hydrogen is an extreme limiting case of the Ashcroft empty-core pseudo-potential. There are no core-electrons and therefore no softening of the potential into a pseudo-potential. In fact, the lack of a core region produces qualitatively different behavior. For example the so-called "cusp-theorem"[14, 15, 16] implies that the induced density drops off as $\rho(k) \sim 1/k^4$ for large k[17]. Thus hydrogen is a worst-case scenario; the non-linear response is particularly strong. In fact, for a single proton potential in an electron gas, bound states set in for $rs > 1.7274$ and the linear response formalism is ill-defined [For more on this see the section on bound states].

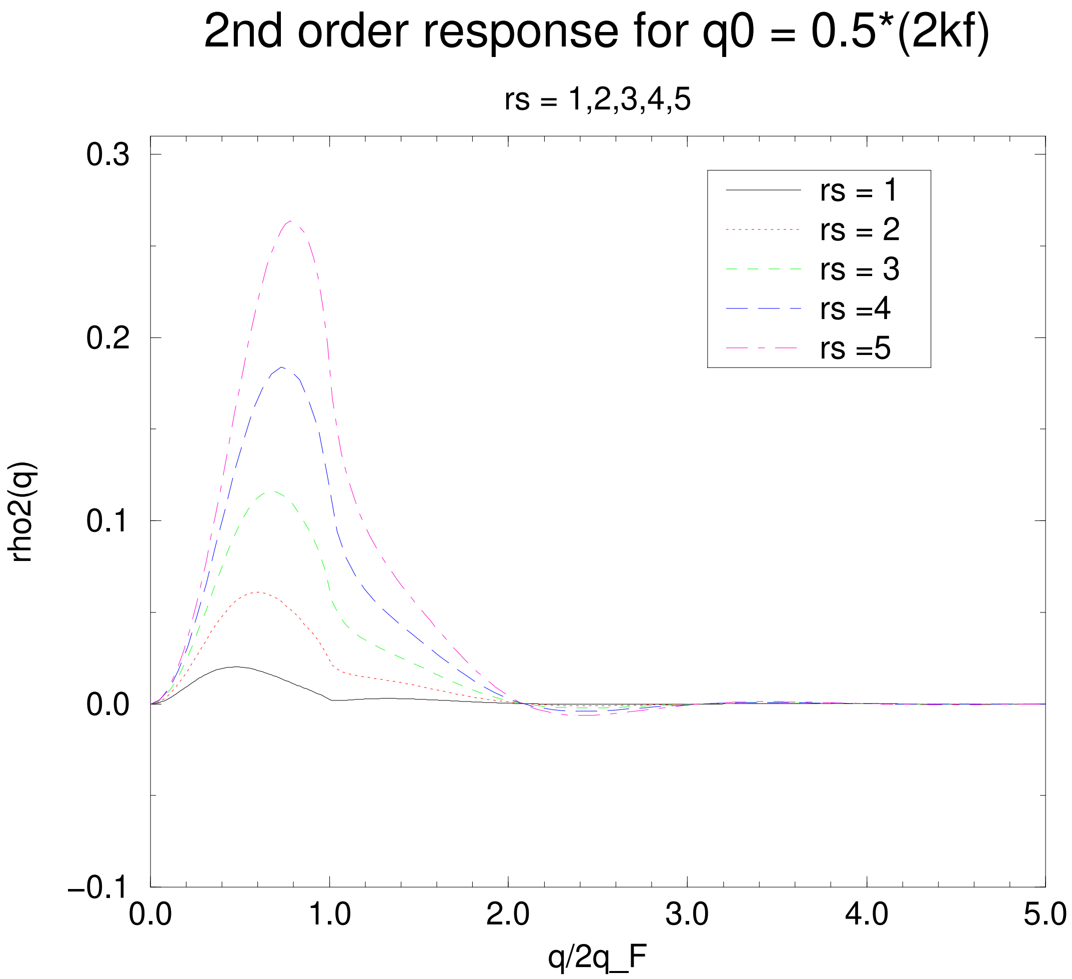

Figure 4.8: **2nd order response for** $q_0/2k_F = 0.5$; $rs = 1..5$
For $rs = 1..5$ we plot the second order response for $q_0/2k_F = 0.5$. Note how the functional form appears nearly the same, just scaled in the y-direction by a factor which increases with increasing rs

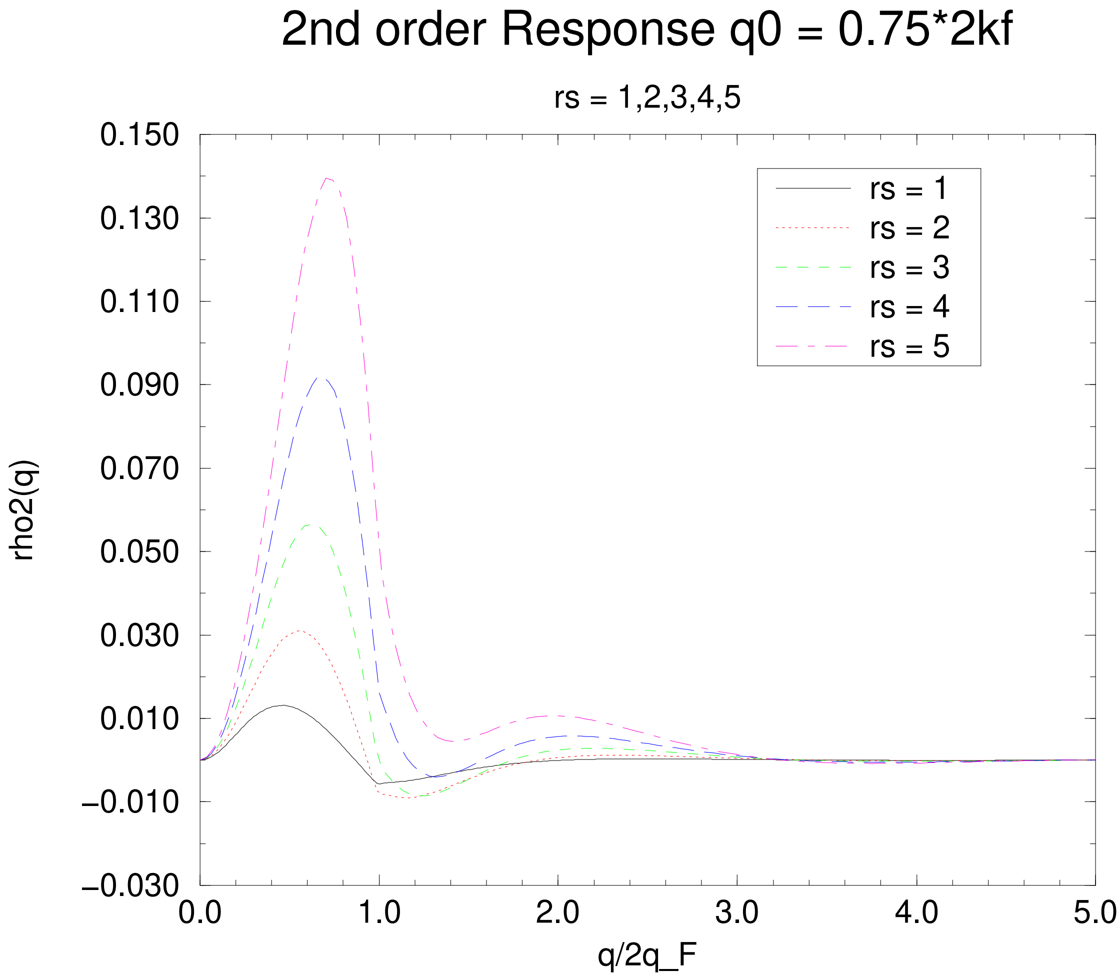

Figure 4.9: **2nd order response for** $q_0/2k_F = 0.75$; $rs = 1..5$
Same as figure 4.8, but with $q_0/2k_F = 0.75$

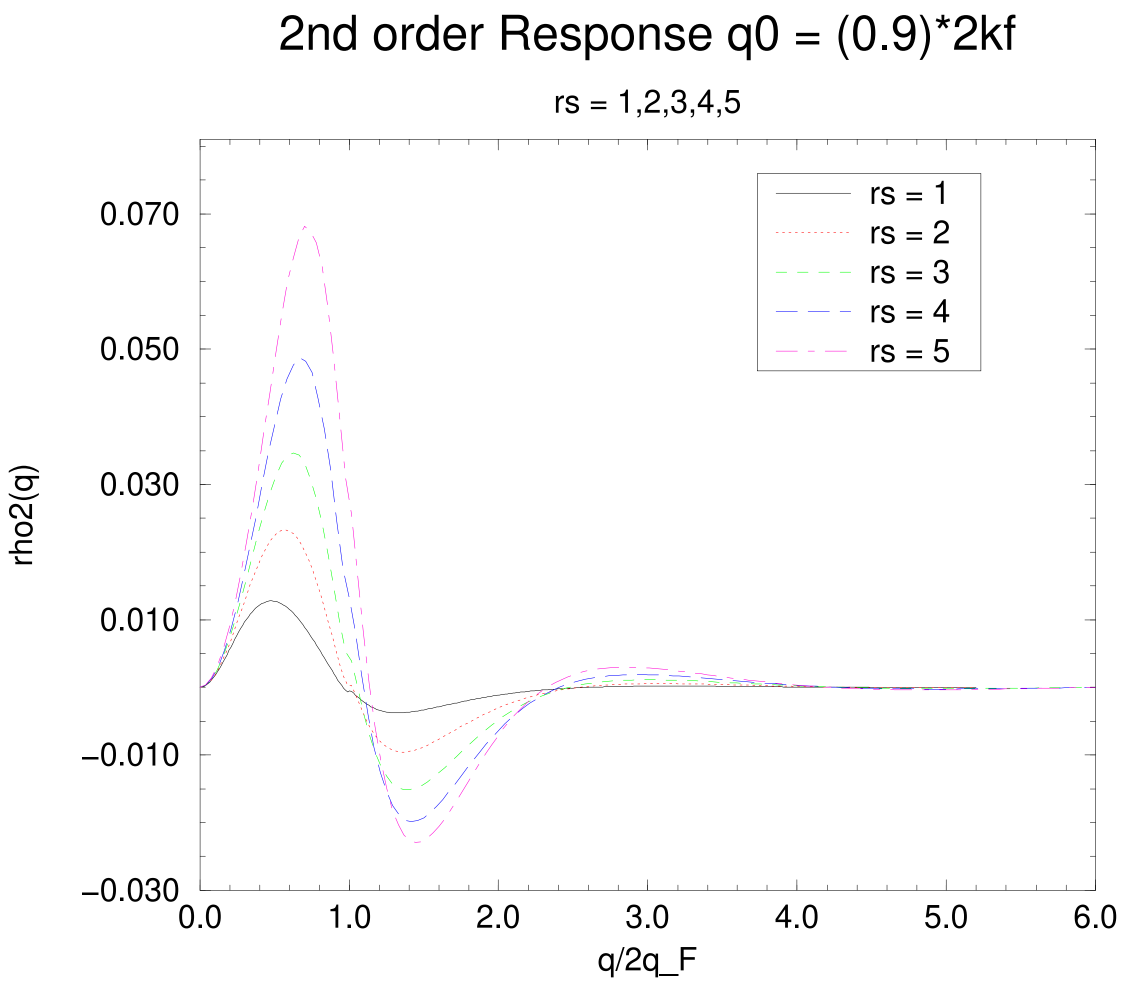

Figure 4.10: **2nd order response for $q_0/2k_F = 0.9$; $rs = 1..5$**
Same as figure 4.8, but with $q_0/2k_F = 0.9$

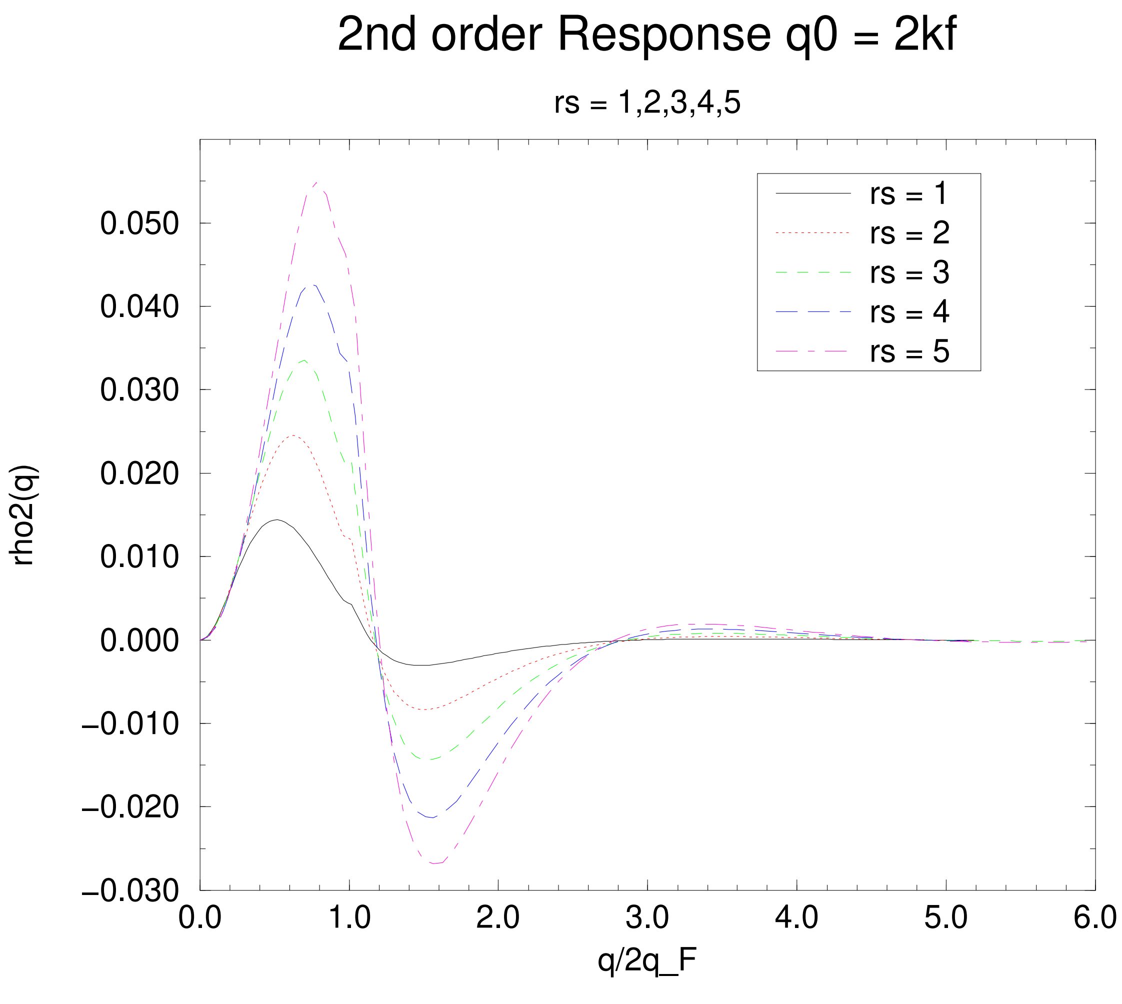

Figure 4.11: **2nd order response for $q_0 = 2k_F$; $rs = 1..5$**
Same as figure 4.8, but with $q_0/2k_F = 1$ Note how small the response has become.

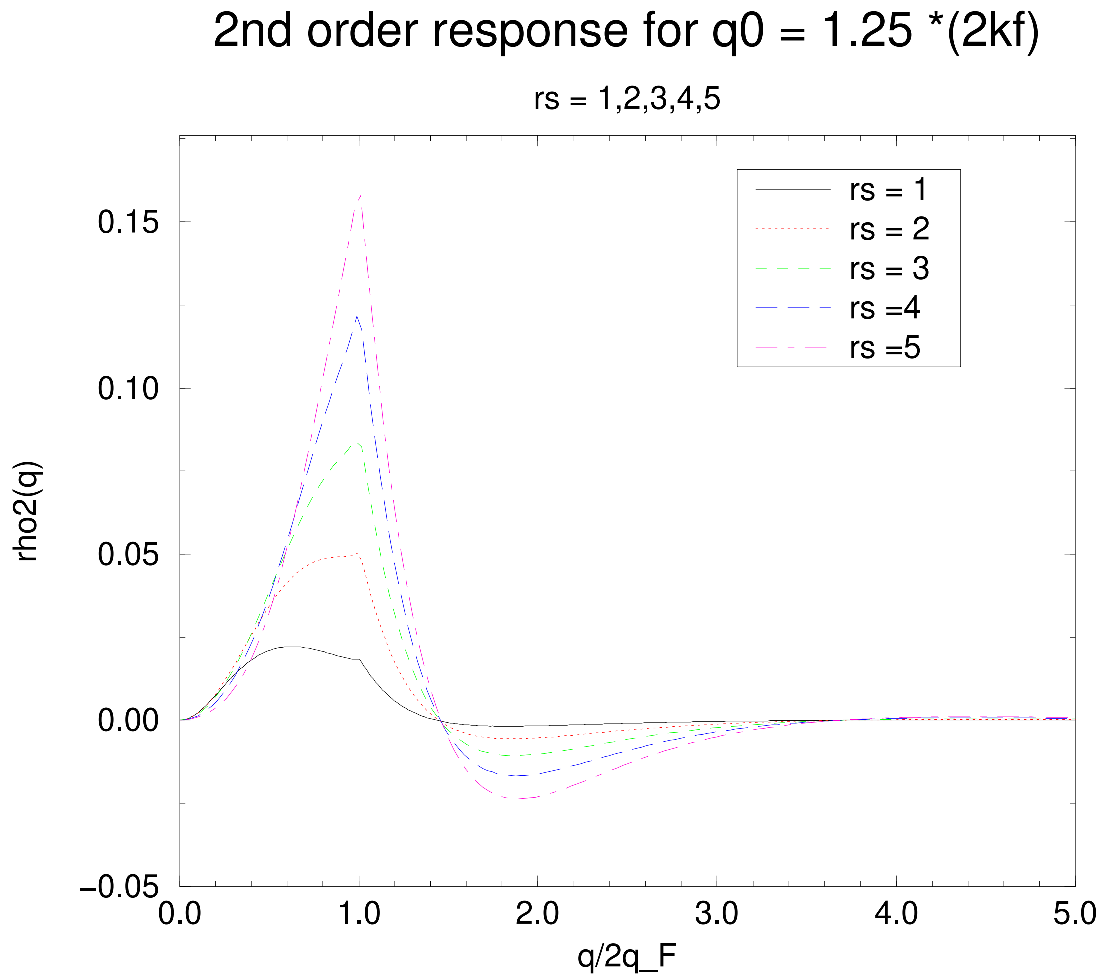

Figure 4.12: **2nd order response for** $q_0/2k_F = 1.25$; $rs = 1..5$
Same as figure 4.8, but with $q_0/2k_F = 1.25$ Note the similarity in scale (but difference in shape) with $q_0/2k_F = 0.75$.

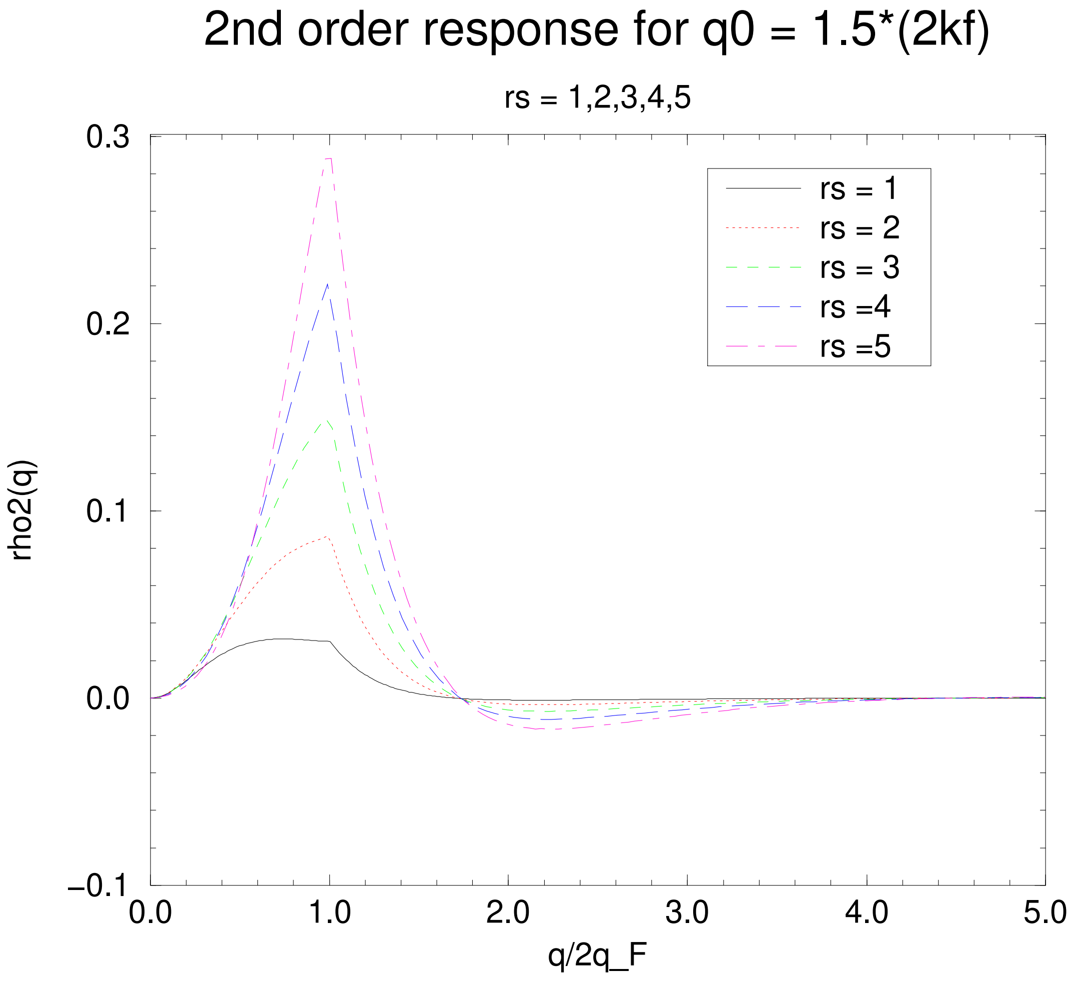

Figure 4.13: **2nd order response for $q_0/2k_F = 1.5$; $rs = 1..5$**
Same as figure 4.8, but with $q_0/2k_F = 1.5$

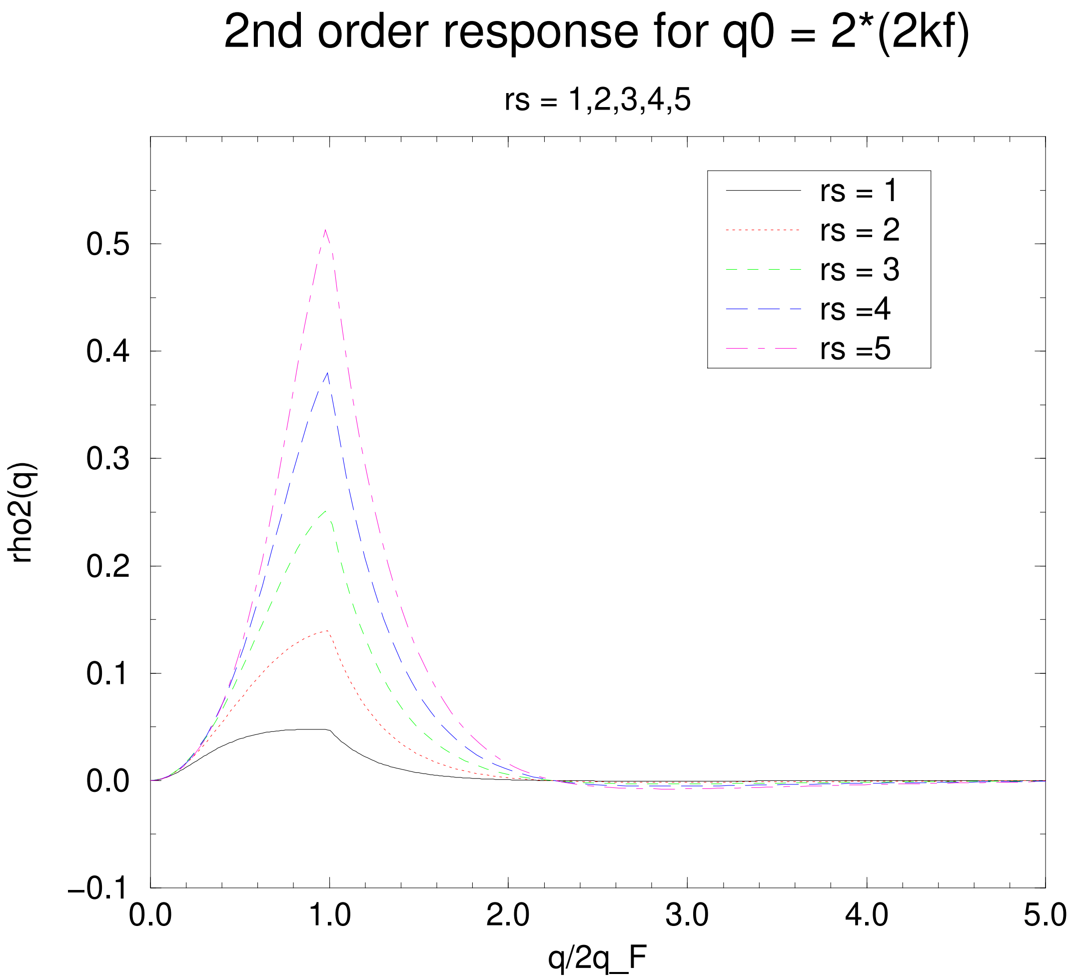

Figure 4.14: **2nd order response for $q_0/2k_F = 2.0$; $rs = 1..5$**
Same as figure 4.8, but with $q_0/2k_F = 0.75$ Larger q_0 implies smaller R_c and concomitant larger 2nd order response.

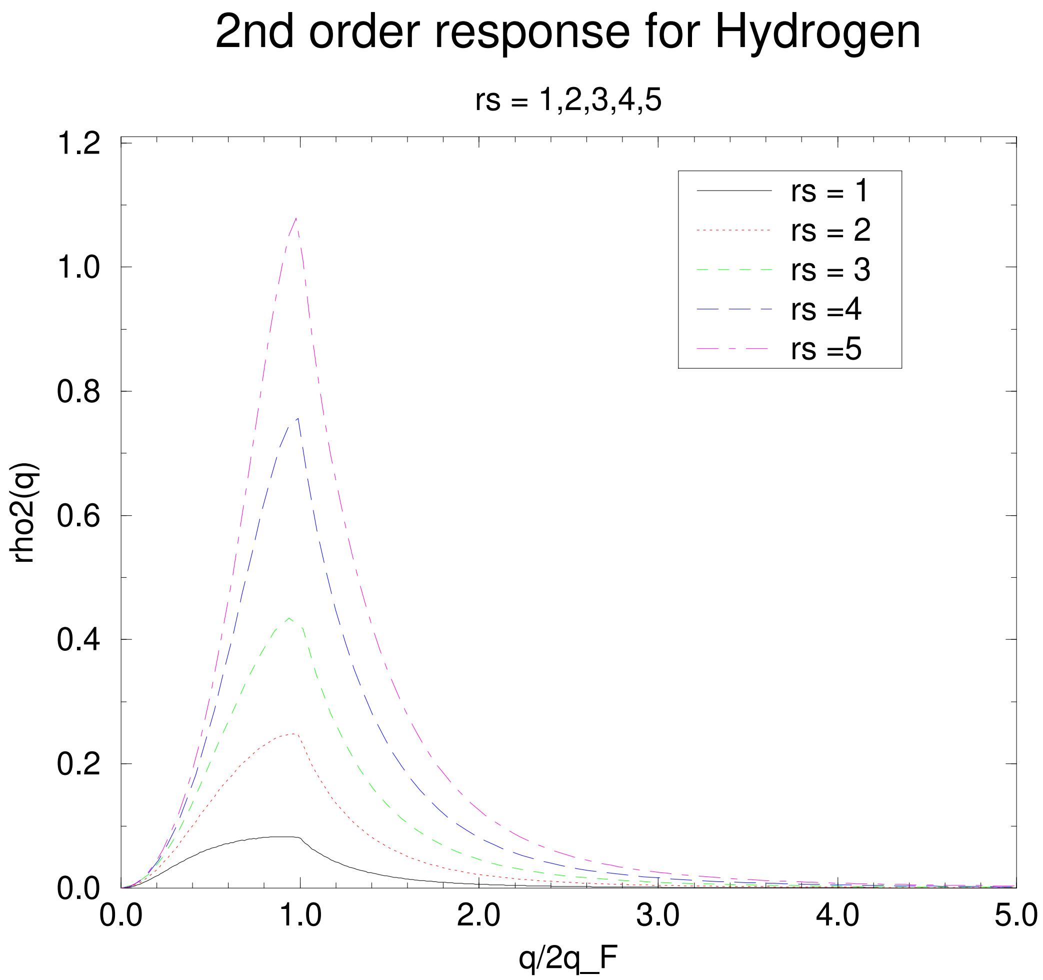

Figure 4.15: **2nd order response for $q_0/2k_F = \infty$ (i.e. hydrogen) ; $rs = 1..5$** For hydrogen we plot the second order response for $rs = 1..5$ Note how the functional form appears nearly the same, just scaled in the y-direction by a factor which increases with increasing rs. Note also how large the 2nd order response is compared to the APP of the previous figures.

The second minimum at $q_0 = 2k_F$

A look at the preceding figures shows a remarkable decrease in the 2nd order response, with a minimum at $q_0 = 2k_F$. This is depicted in figure 4.16 where the maximum of the second order response is used as a measure of the total second order response for $rs = 3$ (the same picture holds for other rs as can easily be seen by comparing figures 4.8 - 4.14). Apparently, when $q_0 \sim 2k_F$, there is a local minimum in the scale of second order response. We attribute this minimum to the following physical effect: The second order response function $\chi_2(k, k_1, k_2)$, peaks when the summed arguments in (4.14) are near $2k_F$. If the pseudo-potential zero-crossing q_0 is at the response peaks at $2k_F$, a maximum cancellation or *destructive interference of the atomic and electronic lengthscales* occurs, leading to a minimum in second order response. We postulate that a similar interference effect occurs for higher order terms in the series (4.14). At normal equilibrium conditions, most metals have an atomic R_c parameter and an electron density rs parameter such that the ratio $q_0/2k_F$ varies between about 0.75 and 1, very near the minimum in non-linear response. At present we know of no physical reason why this should be linked to a minimum of the second order response. The ratio of the atomic and electronic length scales is set by simply assembling N empty-core pseudo-potentials with a given R_c together with the requisite number of electrons and letting the system come to equilibrium with its surroundings. Girifalco[18] has even taken the experimental rs parameters together with a simple formulation of the energy (neglecting pair and higher order terms which only contribute a few % to the energy anyway) and by setting the pressure ($p = -(\partial E/\partial V)$) to zero, he obtained a very reasonable set of R_c parameters, demonstrating that the ratio is set almost completely by volume energy terms and is almost independent of structure and 1st or 2nd order response[20]. Thus at present it appears that the minimum in higher order response may be a fortuitous situation. but in retrospect the presence of this minimum may help explain why the ever popular linear response formulations of materials have been so successful. We note that historically, the NFE approximation has often been justified in a more general context than linear response alone by appealing to the fact that for a crystalline solid, the reciprocal lattice vectors are typically near the pseudo-potential zero-crossing q_0 so that the scattering is small[2].

4.3.4 The effect of local field factors

For comparison with the LDA infinite order response we needed the LDA local field factors, easily derivable as derivatives of the known LDA exchange correlation potential. The question immediately arises: What are the effects of exchange and correlation on this induced density? To answer this we plot the second order density without μ_1 or without μ_2 or without both (the latter is equivalent to the random phase approximation (RPA)[2]). The figures are summarized in table (4.3.4)**. Note how the two orders of exchange correlation effects cancel each other out at second order.

4.3.5 The role of bound-states

In Mott's seminal 1949 paper[21] he demonstrated how the screening of a Coulomb potential in an electron gas would, with increasing electron density, lead to the disappearance of the bound state and thus eventually to metallic behavior for an array of such potentials. If the Thomas-Fermi screening is applied the potential

** Note the slight change in notation, in the the exchange correlation factors μ_i are denoted by $G_i(..) = (8\pi/q^2)\mu_i$.

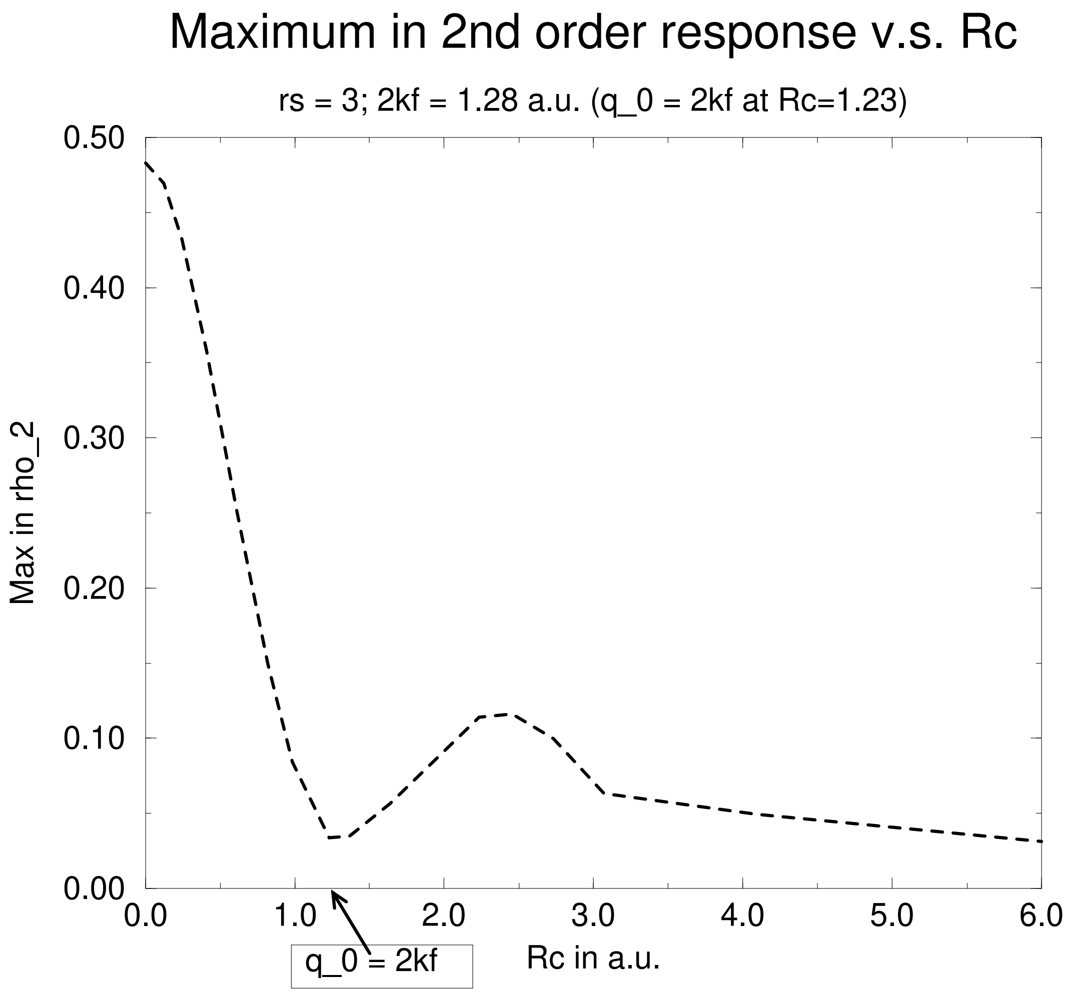

Figure 4.16: **Maximum in 2nd order response for $rs = 3$ as a function of R_c** We plot the maximum in second order response as a function of R_c for $rs = 3$. As expected, the response is largest for $R_c = 0$, or hydrogen, but note the secondary minimum at $q_0 = 2k_F$. It is about a factor 3 smaller than the secondary maximum at $\sim q_0/2k_F = 0.5$. This minimum in the higher-order response occurs near the normal equilibrium conditions of most metals; the exception being hydrogen.

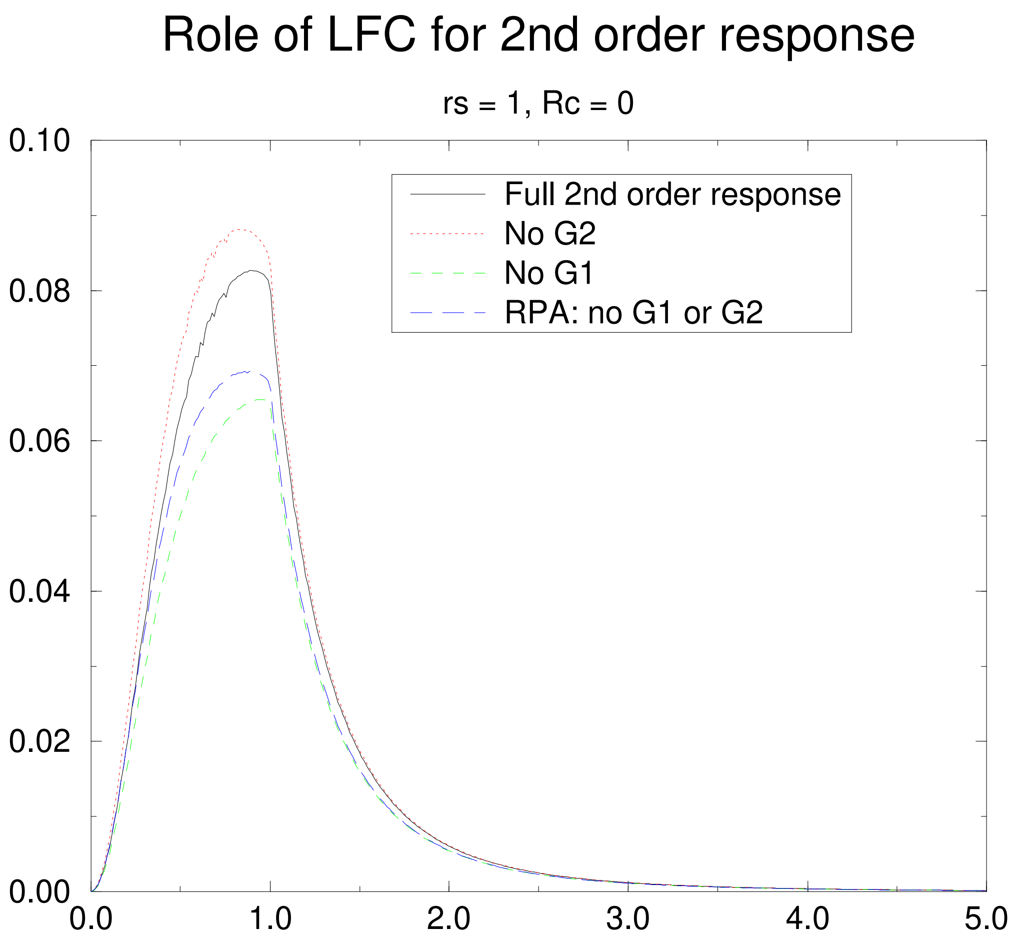

Figure 4.17: **Effect of local field corrections on response:** $rs = 1$, $R_c = 0$ **(hydrogen)**
Note how the effects of the 1st and 2nd order local field factors (called G1 and G2 here) partially cancel each other out.

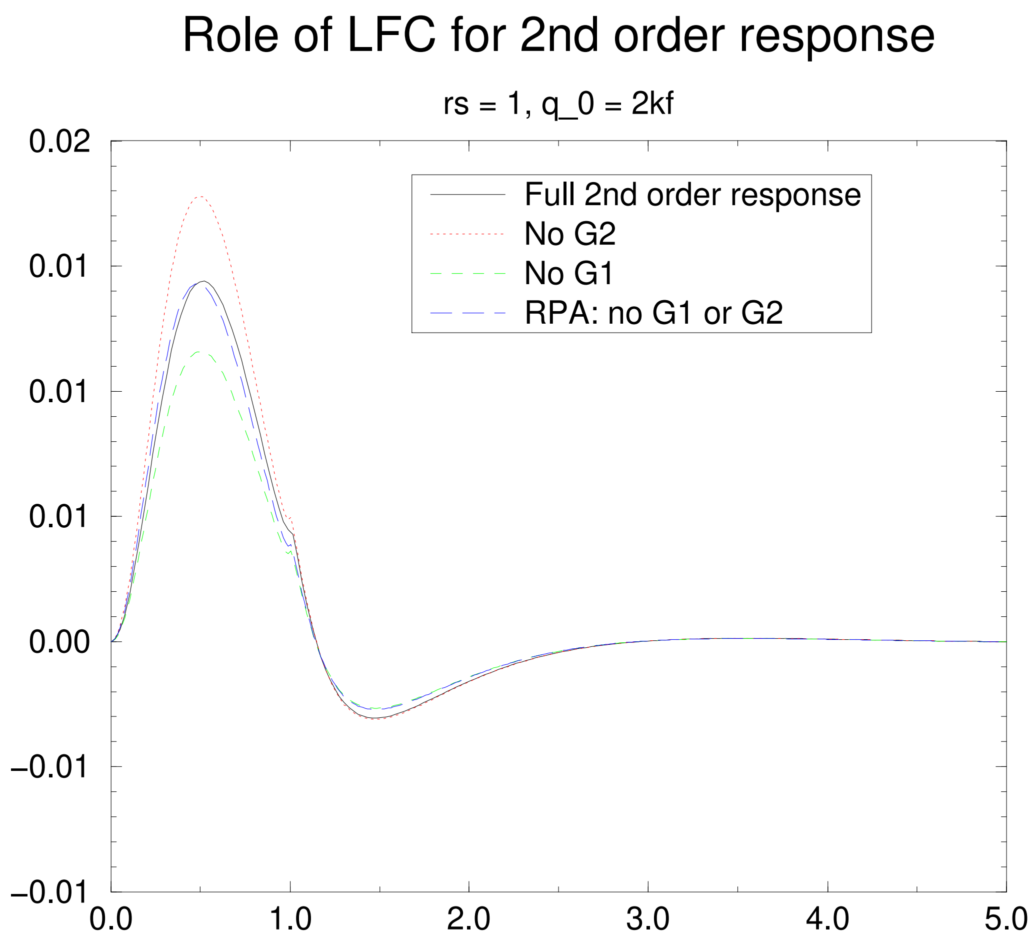

Figure 4.18: **Effect of local field corrections on response:** $rs = 1$, $q_0 = 2kf$ Here the effects of the 1st and 2nd order local field factors (called G1 and G2 here) almost exactly cancel each other out.

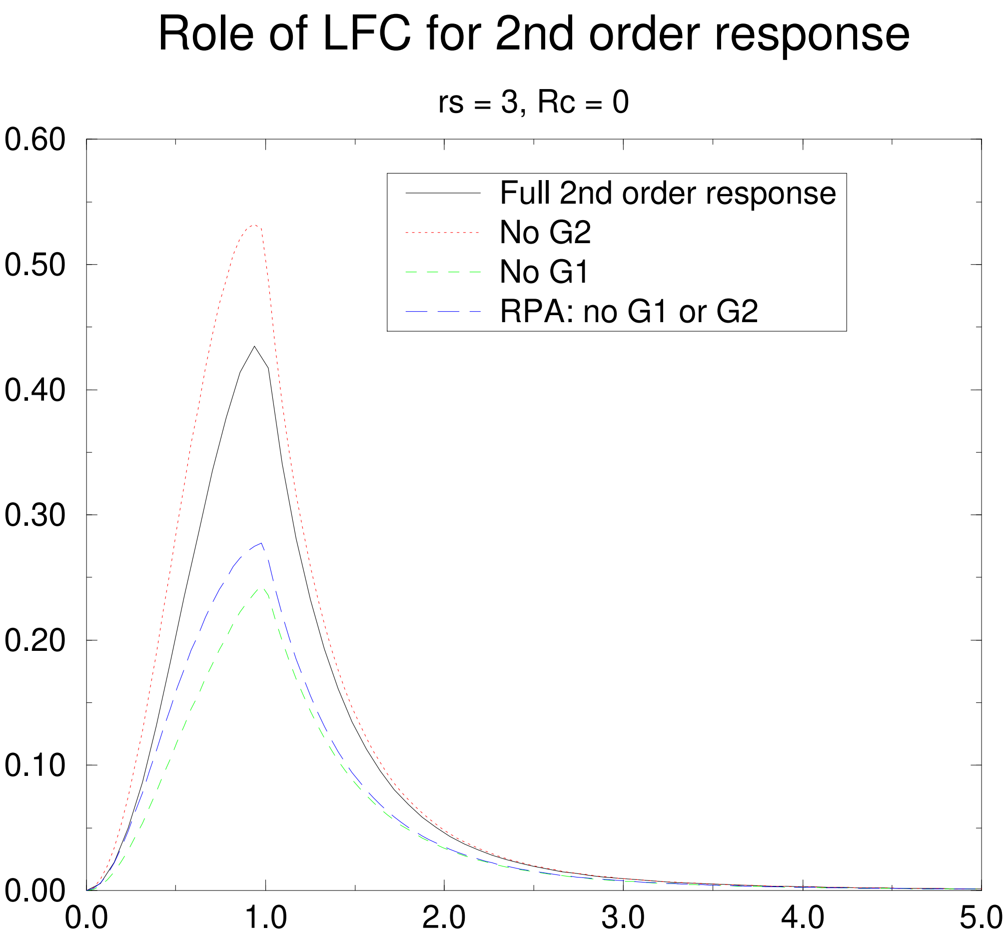

Figure 4.19: **Effect of local field corrections on response:** $rs = 3$, $R_c = 0$ **(hydrogen)**
Note that technically we are in the bound-state regime here; the response formalism is ill-defined.

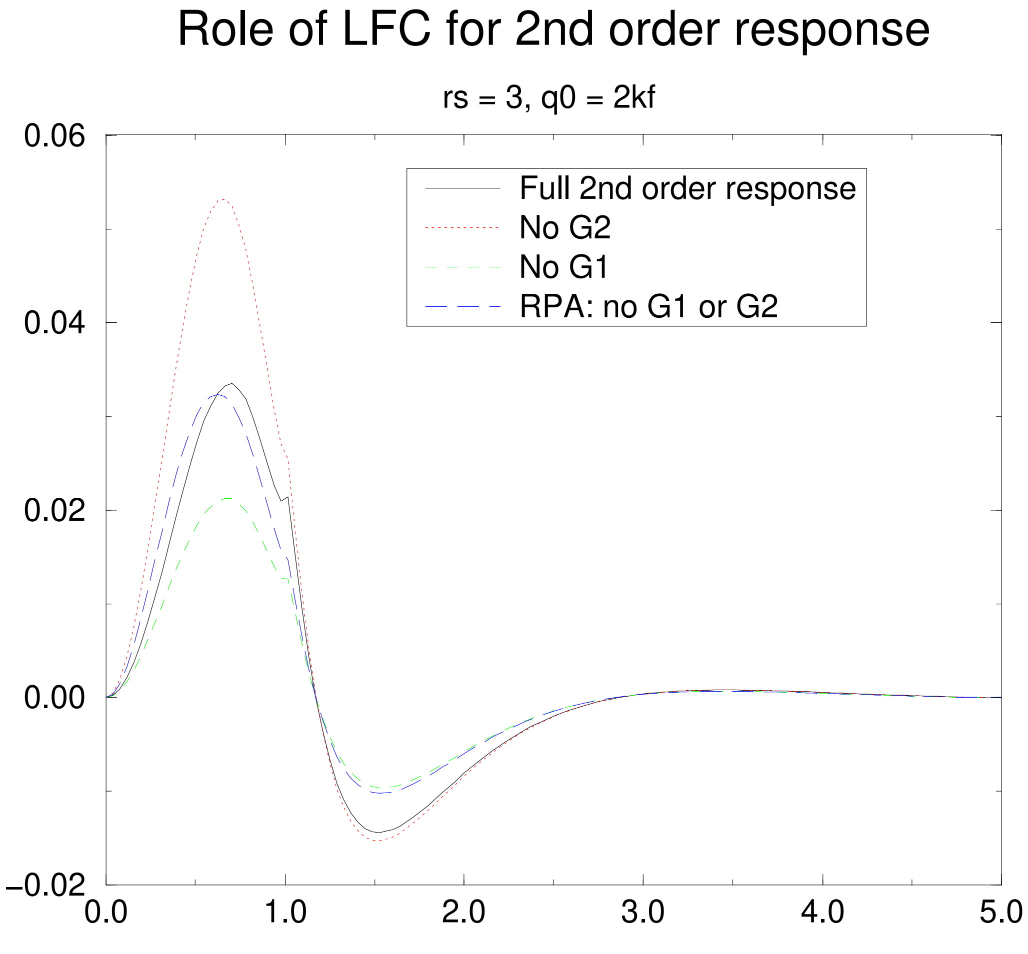

Figure 4.20: **Effect of local field corrections on response:** $rs = 3$, $q_0 = 2k_F$

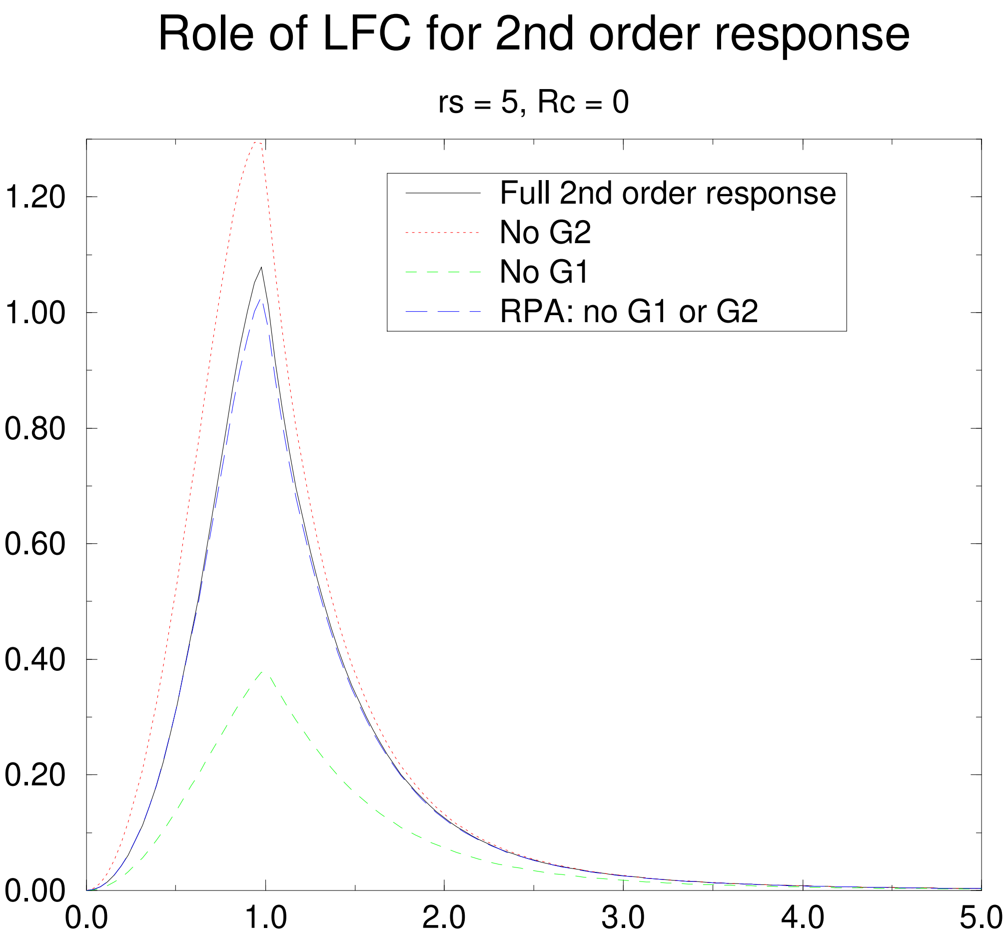

Figure 4.21: **Effect of local field corrections on response:** $rs = 5$, $R_c = 0$ **(hydrogen)**
Again, note that technically we are in the bound-state regime here; the response formalism is ill-defined.

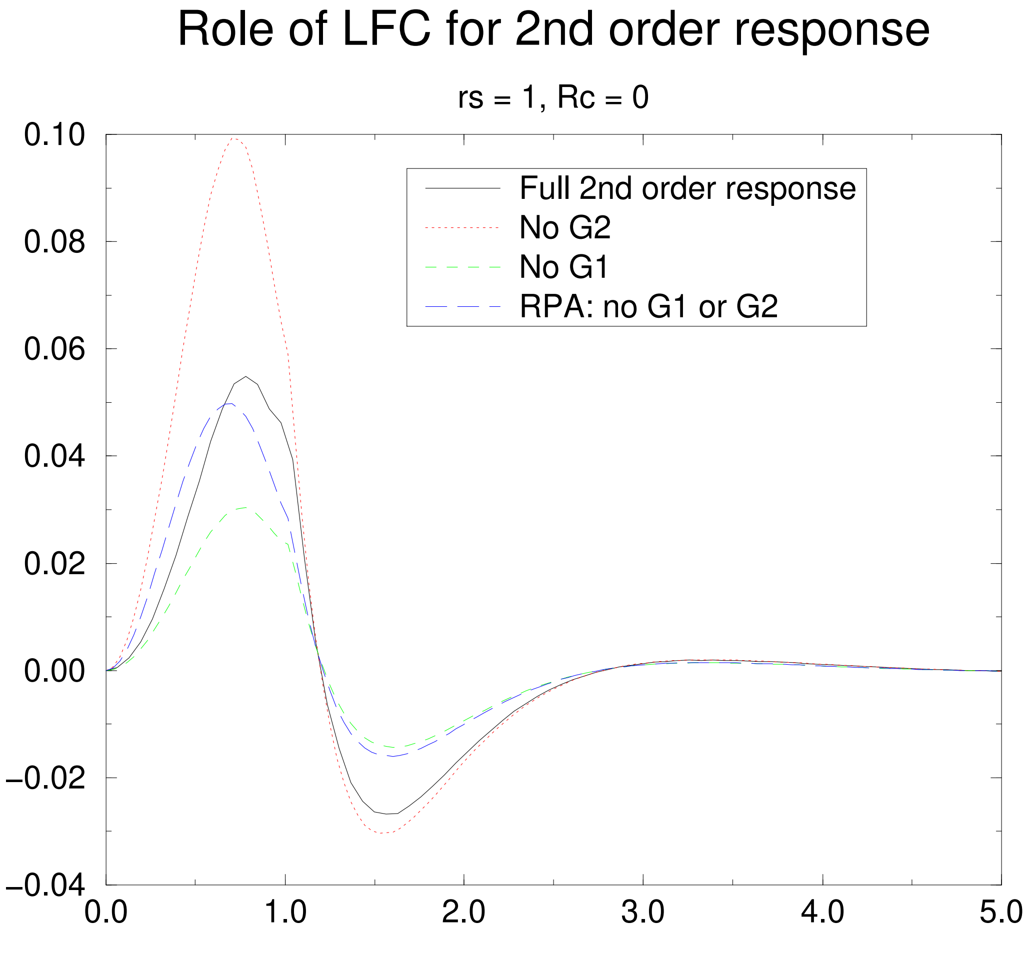

Figure 4.22: **Effect of local field corrections on response:** $rs = 5$, $q_0 = 2k_F$

Table 4.3: **Summary of the figures for fixing $q_0/2k_F$ and varying the local field factors G_i.**

Figure	*length-scale ratio* $q_0/2k_F$	*electron density* r_s
figure (4.17)	$q_0/2k_F = \infty$ (hydrogen)	$rs = 1$
figure (4.18)	$q_0/2k_F = 1$	$rs = 1$
figure (4.19)	$q_0/2k_F = \infty$ (hydrogen)	$rs = 3$
figure (4.20)	$q_0/2k_F = 1$	$rs = 3$
figure (4.21)	$q_0/2k_F = \infty$ (hydrogen)	$rs = 5$
figure (4.22)	$q_0/2k_F = 1$	$rs = 5$

becomes:

$$v(r) = \frac{-2Z}{r} e^{-q_{TF} r}, \tag{4.18}$$

where q_{TF} is the inverse screening length given by[22]:

$$q_{TF} = 0.815 k_F \left(rs\right)^{1/2} \tag{4.19}$$

in atomic units. According to Mott, the bound-state disappears roughly when;

$$q_{TF} a_H^* \sim 1, \tag{4.20}$$

where a_H^* is the effective Bohr radius (which we'll take to be a_0 (=1 in atomic units)). From this he derived his famous scaling law for doped semi-conductor metal-insulator transitions[23]. Later more accurate analytical and numerical calculations[24, 25] gave a critical q_{TF} of:

$$q_{TF}^* = \left(\frac{0.83991}{Z}\right)^{-1}, \tag{4.21}$$

so that the critical electron density parameter rs^* at which bound-states disappear for a Coulombic potential with Thomas-Fermi screening is:

$$rs^* = \frac{1.7274}{Z^2}. \tag{4.22}$$

For an APP screened in the same manner, the critical rs^* still scales in roughly the same with Z and is an increasing function of R_c. For example when $Z = 1$, the $rs^*(R_c = 1) \sim 3.7$ and $rs^*(R_c = 1.5) \sim 4.4$. The response formulation is derived from a plane-wave basis set and breaks down when bound-states are involved[26], while the LDA program we use takes the bound states into account. Thus direct comparisons between the two approaches are strictly correct only for rs less than the critical rs^*. However, in a real physical system, the ions are not isolated. Instead multiple ions combine to form an electron band, lowering the ionization threshold, and increasing considerably the rs^* for a given R_c. Response theory without bound states may be physically valid to higher values of rs than one would naively expect based on the criterion above. In fact, the atom-in-jellium calculations form an important input for effective medium theories[12] of metallic bonding, and some care as to the effect of these (physically spurious) bound states should probably be taken into consideration. As an example of their effect, we show in figure 4.23 the full response minus linear response that was so well approximated by the 2nd order response for the case of no bound states (see for example figure 4.3). Note how the bound-state gives an opposite sign for LDA non-linear response from the 2nd order response[††]

As a caveat to the arguments above, we add that although for systems like

[††] This difference is not due to the the potential being too strong for a convergent response summation. At small q the non-linear response goes as q^2 with an easily calculable positive pre-factor.

aluminum, the single pseudo-potential has bound-states while the physical system, with many potentials together, is metallic (i.e. no bound states), the opposite is true of hydrogen. At the critical density of $rs^* = 1.7274$ the physical system with many potentials together is still well within the (diatomic) insulating regime.

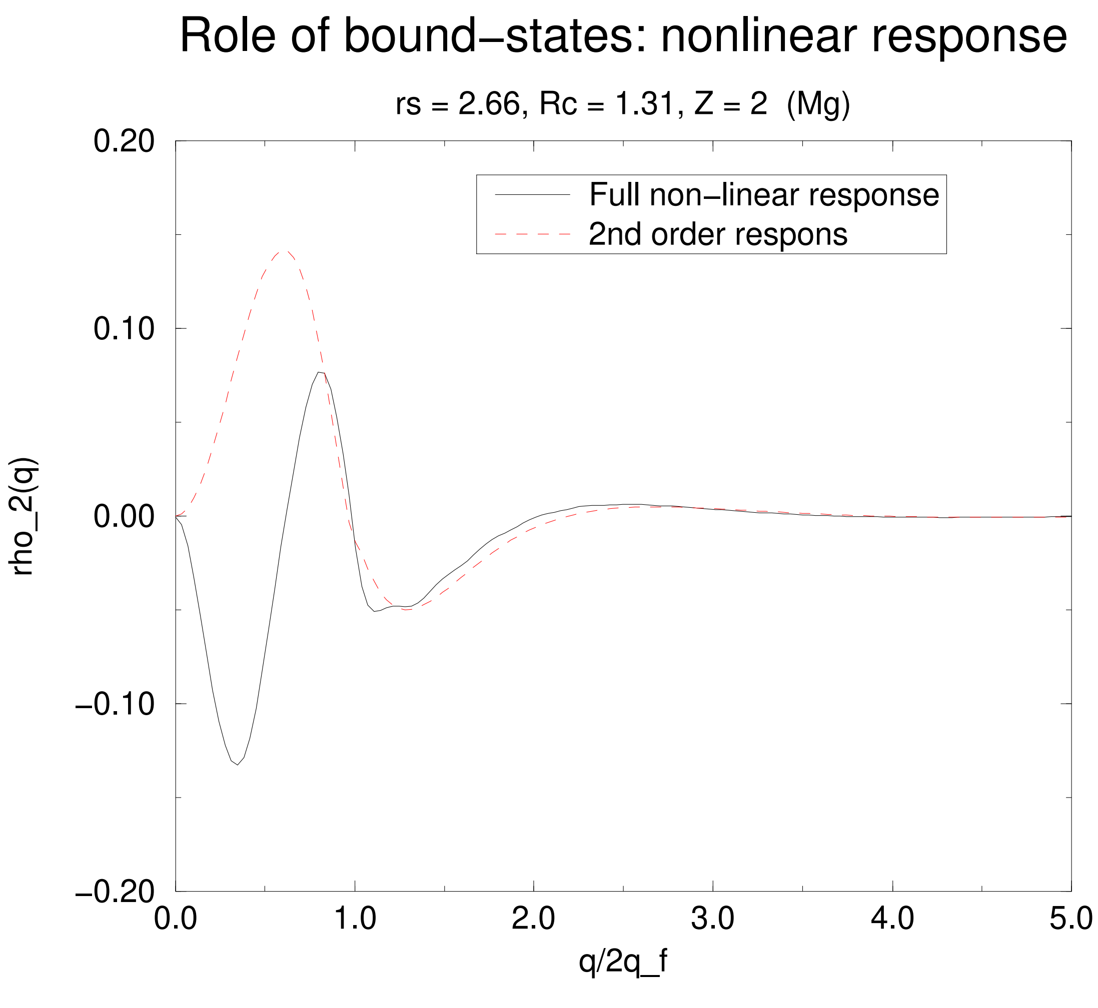

Figure 4.23: **Non-linear response with a bound state compared to 2nd order response theory.**
The single $Z = 2$ potential with parameters for Magnesium has a bound-state and as a consequence, response theory breaks down.

4.4 Final Discussion and Conclusions

In conclusion we have shown why linear response works remarkably well and captures the dominant structure of the density induced by an external pseudo-potential. One could imagine that this stems from higher terms that vary in sign and thus cancel between different orders, but, as depicted in figure 4.3, the second order term actually dominates the non-linear response and is itself small. Thus instead, it appears that each higher order term in the series is small (self cancellation within each term); the series converges very rapidly. This stems in part from an interference effect between the atomic length scale q_0 and the electronic length-scale $2k_F$. The glaring exception to all this is hydrogen. Because it has no core region and thus no interference effect to lower the higher order terms in the response series, the higher order terms are not small, the series may not even converge.

The ability of the second order term to capture the dominant part of the non-linear response allows us to explore the effects of exchange and correlation on non-linear response. One interesting result is that the exchange-correlation effects cancel each other between first and second order which implies that theories based on a linear response approximation only may over-estimate the effect of exchange and correlation. An important example of this would be effective ion-ion potentials derived from a linear response approximation. Hydrogen may be an important exception.

Bibliography

[1] A great body of work on pseudo-potentials already exists. Currently the most popular are the so-called "Ab-Initio" pseudo-potentials used in plane-wave numerical techniques[2, 4] which require the density outside a given core radius to be identical to that of the full atom. If in addition the inner part is "norm-conserving", then the derivatives of the scattering phase shifts are also correct, so the new "pseudo-atom" can be more easily transferred to different condensed matter environments. Before the emergence of (non-local) Ab-Initio pseudo-potentials, various empirical forms were fit to some know experimental data (e.g. Fermi-surface properties etc...). For an extensive overview of that earlier work see for example M. Cohen and V. Heine in *Solid State Physics* **24** (1970).

[2] J. Hafner, *From Hamiltonians to Phase Diagrams*, (Springer Verlag, Berlin, (1987)).

[3] N.W. Ashcroft, Phys. Lett. **23**, 48 (1966).

[4] M.C. Payne, M.P. Teter, D.C. Allan, T.A. Arias, and J.D. Joannoppoulos, Rev. Mod. Phys. **64**, 1045 (1992).

[5] P. Hohenberg and W. Kohn, Phys. Rev. **136**, B864 (1964).

[6] W. Kohn and L.J. Sham, Phys. Rev. **140**, A1133 (1965).

[7] R.M. Dreizler and E.K.U. Gross, *Density Functional Theory* (Springer Verlag, Berlin (1990)).

[8] P. Lloyd and C. Sholl J. Phys. C **1**, 1620 (1968). see also:E.G. Brovman, Yu. Kagan, A. Holas, Sov. Phys. JETP **34**, 1300 (1972).

[9] J. Hammerberg and N.W. Ashcroft, Phys. Rev. B **9**, 409 (1974).

[10] Yu. Kagan, V.V. Prushkarev, A. Holas Sov. Phys. JETP **46**,511 (1977).

[11] A. Ferraz, N.H. March and F. Flores, J. Phys. Chem. Solids, **45** 627 (1984).

[12] K. W. Jacobsen, J.K Norskov and M.J. Puska, Phys. Rev. B **35**, 7423 (1987).

[13] Z.D. Popovic and M.J. Stott, Phys. Rev. Lett. **33**, 1164 (1974);M.J. Puska, R.M. Nieminen and M. Manninen, Phys. Rev B **24** 3037 (1981).

[14] T. Kato, Commun. Pure Appl. Math. **10**, 151 (1957).

[15] J. C. Kimball, Phys. Rev. A **7** 1648 (1973).

[16] A. E. Carlsson and N.W. Ashcroft, Phys. Rev. B **25**, 3473 (1982).

[17] See for example K. Moulopoulos and N.W. Ashcroft Phys. Rev. B **56**, 4439 (1997).

[18] L. A. Girifalco, Acta Metallurgica **24**, 759 (1976).

[19] D. G. Pettifor, *Bonding and Structure of Molecules and Solids*, (Claredon Press, Oxford (1995)).

[20] For more discussion of metallic cohesion and the role of response see for example [2] chapter 3, or [19] chapter 5.

[21] N.F. Mott, Proc. Phys. Soc. A **62**,416 (1949).

[22] N.W. Ashcroft and N.D. Mermin, *Solid State Physics* (Holt, Rinehart and Winston, New York 1976).

[23] See for example : P.P. Edwards and M.J. Sienko, Intern. Rev. Phys. Chem **3**, 83 (1983) for a discussion.

[24] L. Hulthén and K.V. Laurikainen, Rev. Mod. Phys. **23**, 1 (1951).

[25] F.J. Rogers, H.C. Gaboske, and D.J. Harwood, Phys. Rev. A. **1**, 1577 (1970).

[26] J.A. Moriarthy, Phys. Rev. B **1**, 1363 (1970).

Chapter 5

Electron-Ion Structure Functions

5.1 Introduction

At a near fundamental level, liquid metals are complex binary fluids consisting of ions in a sea of conduction electrons, their physical properties linked to the three corresponding correlation functions $S_{II}(k)$, $S_{eI}(k)$ and $S_{ee}(k)$. We present a simple scheme to calculate these and show in particular that the electron-ion structure factor $S_{ei}(k)$ appears to fall into one of two general classes depending only on the k_0, the position of the first zero of the induced valence density $\rho(k)$, relative to k_p, the first peak of the ion-ion structure factor*.

Liquids are differentiated from gases by non-trivial structure at the level of two-body correlation functions; they are generally close in density to solid phases. For two-component systems these correlation functions are defined in k-space as:

$$S_{\alpha\beta}(k) = \frac{< \hat{n}_\alpha(\vec{k})\hat{n_\beta}(-\vec{k}) >}{(N_\alpha N_\beta)^{1/2}} - (N_\alpha N_\beta)^{1/2}\delta_{k,0}. \tag{5.1}$$

* See the end of section 5.3 for more discussion of the possibility of crossover between the two classes.

The $S_{\alpha\beta}(k)$ are referred to as static structure factors and

$$\hat{n}_\alpha(\vec{k}) = \sum_{i=1}^{N_\alpha} e^{i\vec{k}\cdot\vec{r}_{i\alpha}} \tag{5.2}$$

is the Fourier transform of the one-particle density operator of component α. The indices α and β refer to ions, (I), or electrons, (e). In real space the correlations are described by the pair or radial distribution function $g_{\alpha\beta}(r)$ defined for uniform states by:

$$g_{\alpha\beta}(|\vec{r}_1 - \vec{r}_2|) = \frac{\langle \hat{n}_{\alpha\beta}(\vec{r}_1, \vec{r}_2)\rangle}{n_\alpha n_\beta}, \tag{5.3}$$

where $\langle \hat{n}_{\alpha\beta}(\vec{r}_1, \vec{r}_2)\rangle$ is the two-particle distribution function[3]. The radial-distribution function $g_{\alpha\beta}(r)$ has a simple physical interpretation: "it is directly proportional to the conditional probability of finding a particle of species β at a distance r from the origin, the condition being that there is a particle of species α at the origin"†. The structure factors and radial distribution functions are related by:

$$S_{\alpha\beta}(k) = \delta_{\alpha\beta} + (n_\alpha n_\beta)^{\frac{1}{2}} \int_V d\vec{r} e^{i\vec{k}\cdot\vec{r}} \left(g_{\alpha\beta}(r) - 1\right). \tag{5.4}$$

The determination of the ion-ion structure factor $S_{II}(k)$ and the electron-electron structure factor $S_{ee}(k)$ are interesting problems in their own right (one largely quantum mechanical, the other largely classical), and have been the focus of much research: the $S_{II}(k)$ (for a given ion-ion interaction (with electrons traced out)) because of their experimental accessibility; the $S_{ee}(k)$ (with the ions usually smeared into a rigid neutralizing background) because of the importance of the electron fluid‡. In contrast, the electron-ion structure factor $S_{eI}(k)$ has received considerably less attention, partially because it is hard to measure, partially because its

† As described in the appendix of [1]

‡ Compared to the classical liquid, electron liquids are more weakly correlated[12], which is why it may be more appropriate to refer to them as fluids instead of liquids.

exact physical relevance remains largely unexplored and unknown, and partially because it includes both the physics of the ions *and* the physics of the electrons, each of which is traditionally treated with its own set of theoretical techniques. The present chapter will focus on these electron-ion structure factors, and in particular shows how simple techniques culled from the ion physics of $S_{II}(k)$ and the electron physics of response theory (see chapter 4) can be married to produce fruitful insights into $S_{ei}(k)$.

5.2 A Simple Analytical Theory of $S_{ei}(k)$

The electron-ion structure factor can always be re-written in the following fashion:

$$S_{eI}(k) = \frac{n(k)}{\sqrt{Z}} S_{II}(k), \tag{5.5}$$

which simply defines $n(k)$. By taking the Fourier transform we find for the electron-ion radial-distribution function:

$$n_e^0 g_{eI}(r) = n(r) + n_i^0 \int_V n(r - r') g_{II}(r') d\vec{r}', \tag{5.6}$$

which is proportional to the probability of finding an electron a distance r away from an ion I located at the origin. Thus a natural interpretation of $n(r)$ is as the density of a "pseudo-atom",which, when superimposed according the ion-ion radial-distribution function $g_{II}(r)$ gives the correct value of the valence density.

For simple liquid metals $S_{II}(k)$ is well approximated by the Percus-Yevick analytic form for hard spheres[4] with one parameter, the packing fraction η, which is about $\eta \sim 0.46$ for most metals near their triple points. In fact, this reflects the screening and response of electrons in determining the form of the ion-ion interactions. The effect is hard-sphere like!

A first order approximation to the pseudo-atom would be linear response with a simple pseudo-potential such as the Ashcroft empty core pseudo-potential defined in chapter 4, equations 4.1 and 4.2. The linear response already performs remarkably well for a single atom (ion) in an electron gas (the reasons for this are given in chapter 4; see for example figure 4.1) and we expect it to capture the dominant contributions for the case of many ions together as well. Thus the simple first order approximate to the electron-ion structure factor is given by:

$$S_{eI}^{(1)}(k) = \frac{\rho_1(k)}{\sqrt{Z}} S_{II}^{PY}(k), \tag{5.7}$$

where $\rho_1(k)$, defined chapter 4 equation 4.12 is the linear response plus pseudo-potential form of the pseudo-atom. By virtue of the prefect screening response sum-rule (4.11), $S_{eI}^{(1)}(k)$ satisfies the charge-neutrality sum-rule:

$$S_{eI}(k=0) = \sqrt{Z} S_{II}(k=0), \tag{5.8}$$

which, provided the hard-sphere parameter η is correctly chosen, is now related to the compressibility sum-rule:

$$S_{II}(k=0) = n_I k_B T K_T, \tag{5.9}$$

where K_T is the iso-thermal compressibility of the binary *mixture*[1]. In figures 5.1 and 5.2, we compare this simple approach to the full ab-initio Car-Parrinello[2] calculations of de Wijs *et al*[5]. The correspondence is striking, especially considering that the parameters are already set by other physical properties; no fitting is used.

One way to improve this theory would take us along the liquid theory route where integral equation techniques have been perfected to obtain very accurate ion-ion structure factors $S_{II}(k)$[3, 7]. For a given two-body potential, this problem can be considered solved. However, for liquid metals the exact pair-potentials are not known[8], and triplet and higher-body potentials may be relevant also. Yet another approach to ion-ion structure factors would be to use accurate experimental $S_{II}(k)$[10].

For accurate $S_{eI}(k)$'s, improvements in $S_{II}(k)$ must match improvements in calculating the pseudo-atom $n(k)$, a difficult problem tackled in chapter 6. Even ab-initio techniques are hampered by finite size effects; for simple metals integral equation techniques probably are more accurate for $S_{II}(k)$[8], but of course give no insight into pseudo-atoms.

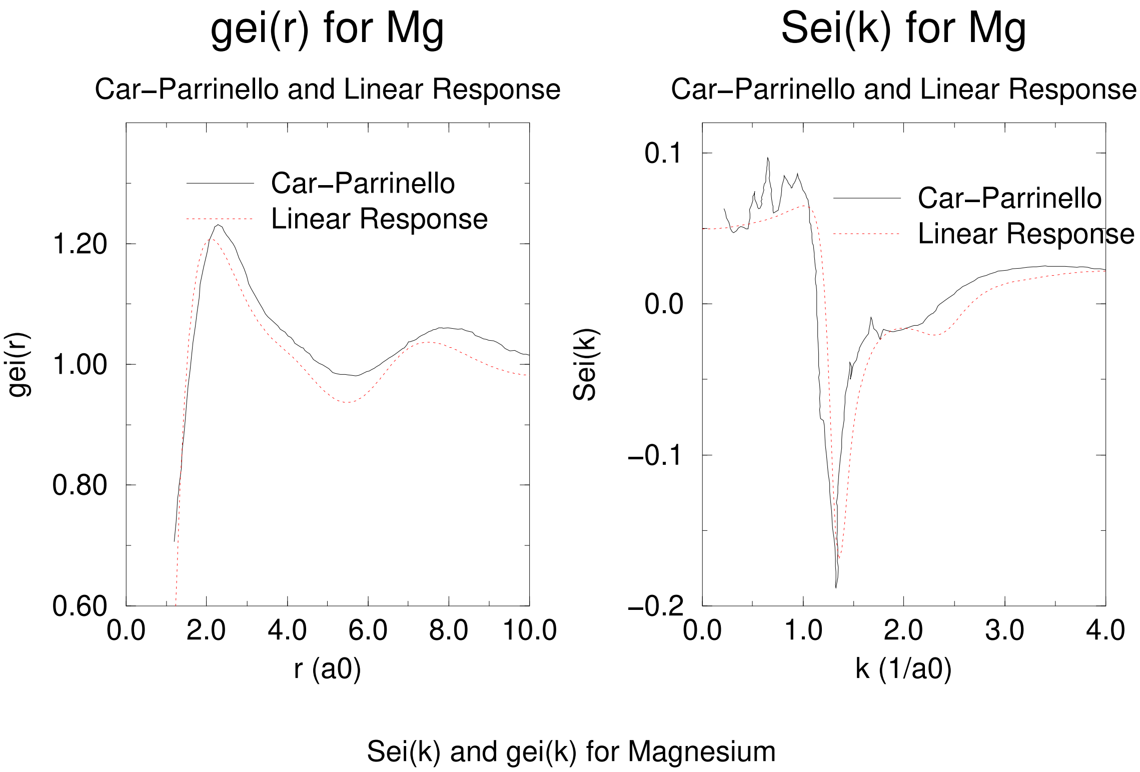

Figure 5.1: $S_{eI}(k)$ **and** $g_{ei}(r)$ **for Mg: Car-Parrinello v.s.** $S^{(1)}_{eI}(k)$
The full Car Parrinello calculations de Wijs *et al* for Mg[5] are compared with the simple approach of equation 5.7 for $R_c = 1.31$, $\eta = 0.47$ and $Z = 2$. Note how well they two approaches coincide. Further adjustment of R_c or η would give an even better fit.

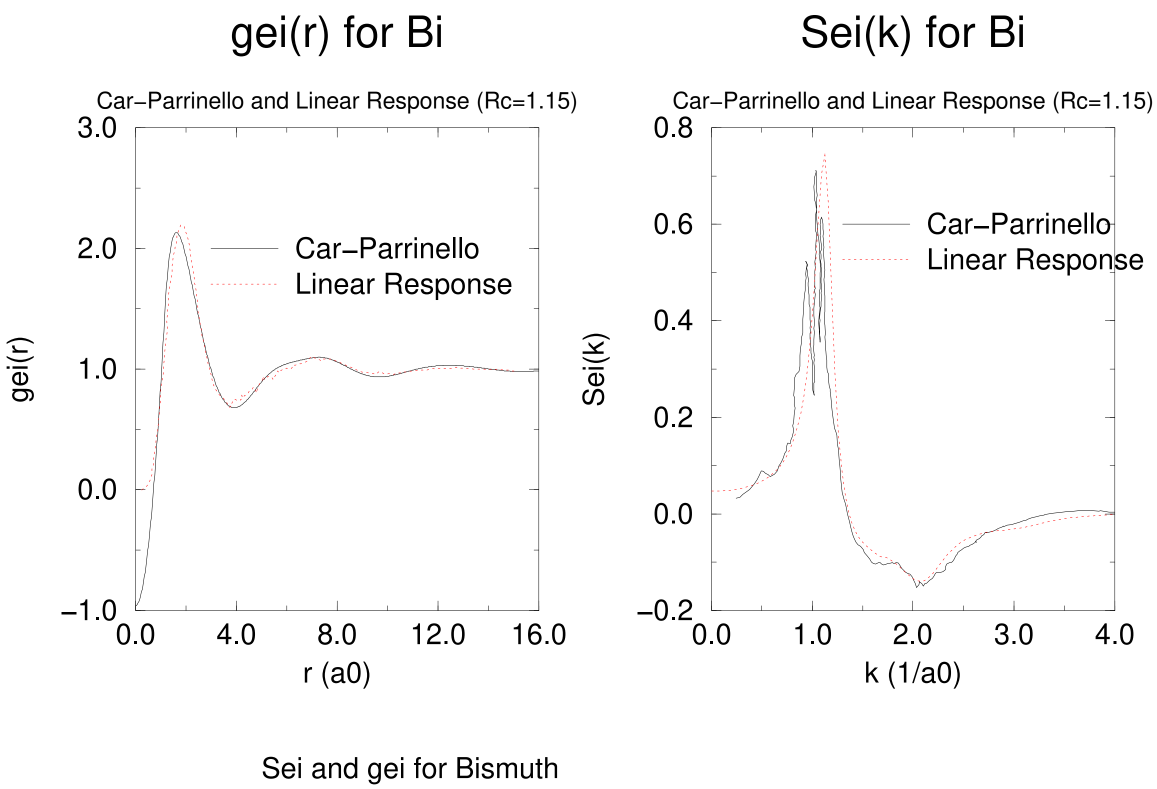

Figure 5.2: $S_{eI}(k)$ **and** $g_{ei}(r)$ **for Bi: Car-Parrinello v.s.** $S_{eI}^{(1)}(k)$
The full Car Parrinello calculations de Wijs *et al* for Bi[5] are compared with the simple approach of equation 5.7 for $R_c = 1.15$, $\eta = 0.46$ and $Z = 5$. Note how well they two approaches coincide. Further adjustment of R_c or η would give an even better fit.

5.3 Two Classes of $S_{ei}(k)$: Low Valence and High Valence

The different forms of $S_{ei}(k)$ for Mg and Bi can be easily explained by looking at the *zero-crossing* k_0 of the pseudo-atom density $n(k)$, which, by virtue of the accuracy of linear response, now understood to be well approximated by the q_0 of equation (4.3). We explore this in figures 5.3 - 5.5 where a comparison with an ab-initio calculation of the pseudo-atom by Chetty, *et al*[9] is made. The linear response $\chi_1(k)$ is positive definite, so oscillations in $\rho_1(k)$ are determined by the pseudo-potential equation 4.2. Because the slope of $n(k)$ is large near the zero-crossing, non-linear corrections have a small effect on k_0. The excellent agreement in q_0 vs k_0 for $R_c = 1.11$ is partially fortuitous as can be seen in figure 5.5 where the real-space pseudo-atom density is plotted. Also, the ab-initio aluminum pseudo-atom density is taken from a crystalline calculation and not a liquid. Nevertheless, because Al is a close-packed structure both in the solid and the liquid, we do not expect the pseudo-atom density to vary much between those two cases. For most metals, q_0 is just a bit less than $2k_F$, and the latter's ratio to k_p, the first maximum in the ion-ion structure factor $S_{II}(k)$, is plotted in figure 5.6: for small valence Z: $2k_F < k_p$; for large valence Z: $2k_F > k_p$.

Thus if the zero-crossing k_0 is at or less than the $S_{II}(k)$ maximum k_p (which will typically happen for low valence Z), the negative part of $\rho(k)$ is selected (filtered) by the ion-ion structure factor since the $S_{ei}(k)$ of equation 5.5 is a product of the two. This results in the forms seen in figures 5.7 and 5.8: the **low valence class** of electron-ion structure factors.

On the other hand, if the zero-crossing k_0 is greater than the $S_{II}(k)$ maximum

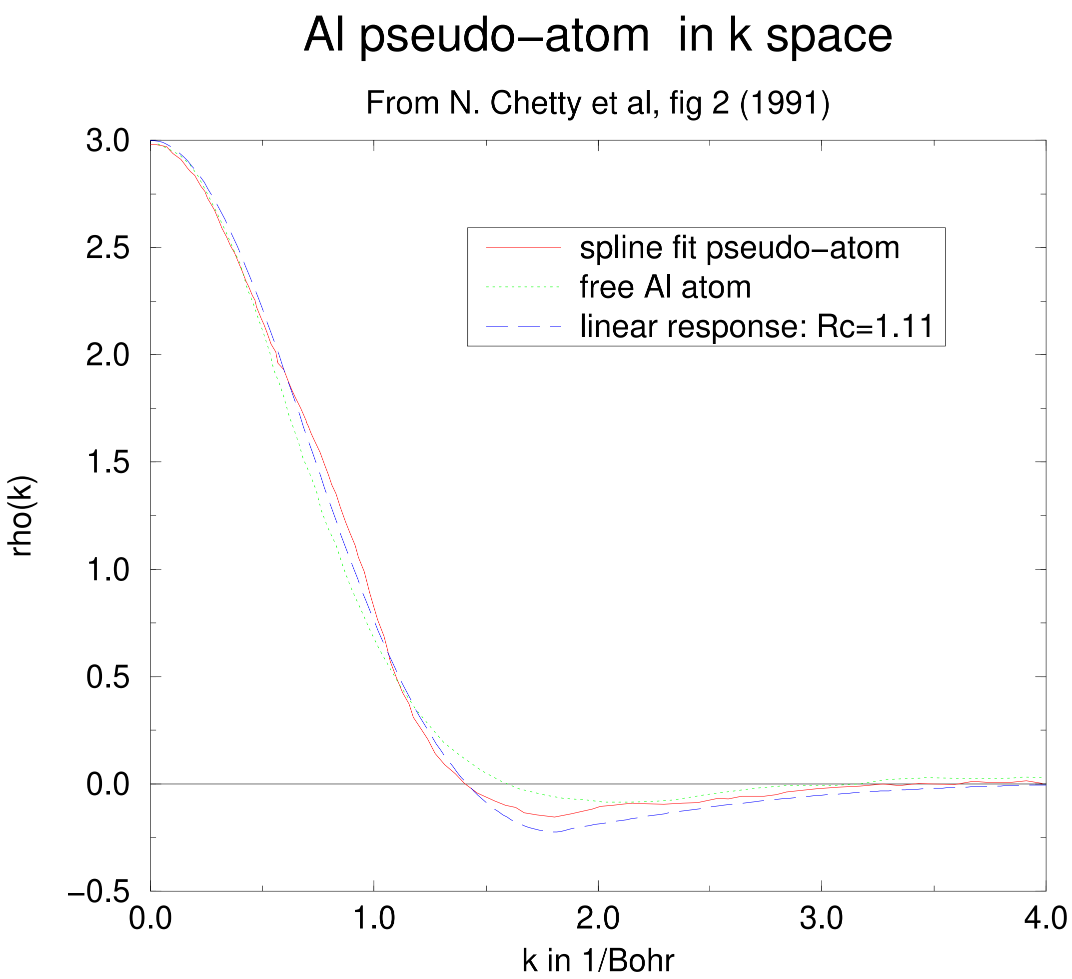

Figure 5.3: **Comparison of full Al pseudo-atom electron density with linear response and a free atom; k-space**
The linear response pseudo-atom $\rho_1(k)$ is compared to the ab-initio results of Chetty *et al.*[9] and also to a free aluminum atom.

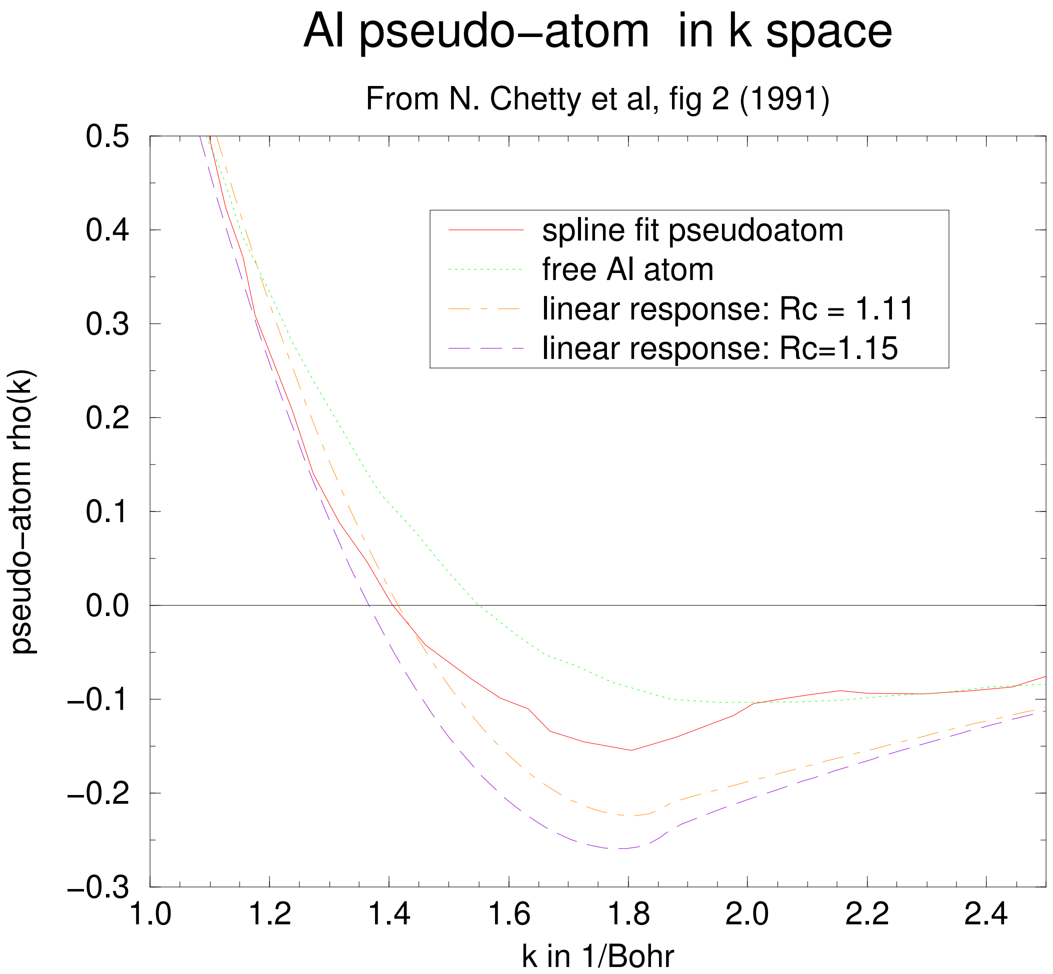

Figure 5.4: **Comparison of full Al pseudo-atom electron density with linear response and a free atom; k-space - emphasis on zero-crossing.**
The same as figure 5.3, but expanded to emphasize the zero crossing. In addition, a linear-response atom for a slightly different R_c is added as well (both are found in the literature) to demonstrate the uncertainty in pseudo-potential parameters.

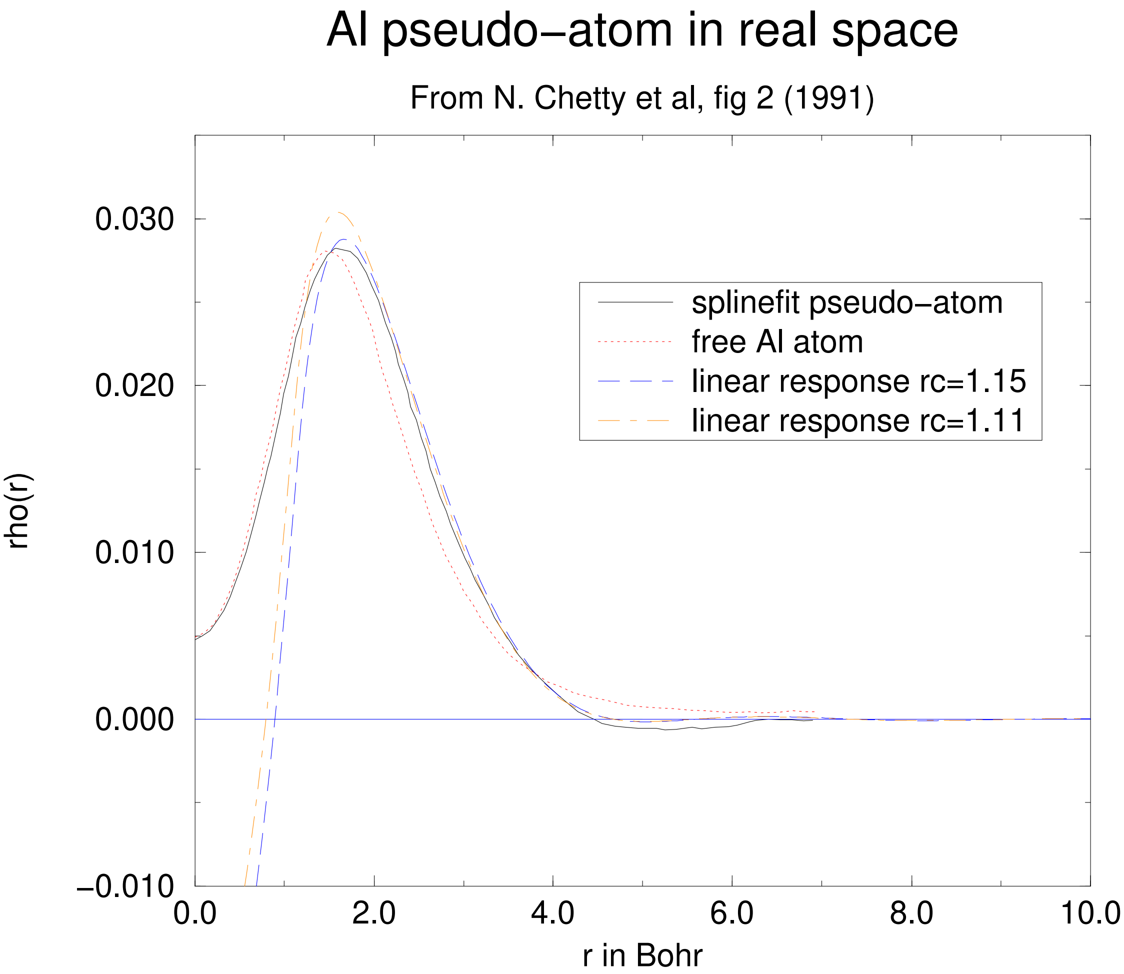

Figure 5.5: **Comparison of full Al pseudo-atom electron density with linear response and a free atom; real-space**
The linear response pseudo-atom $\rho_1(r)$ in real space is compared to the ab-initio results of Chetty *et al.*[9] and to a free aluminum atom.

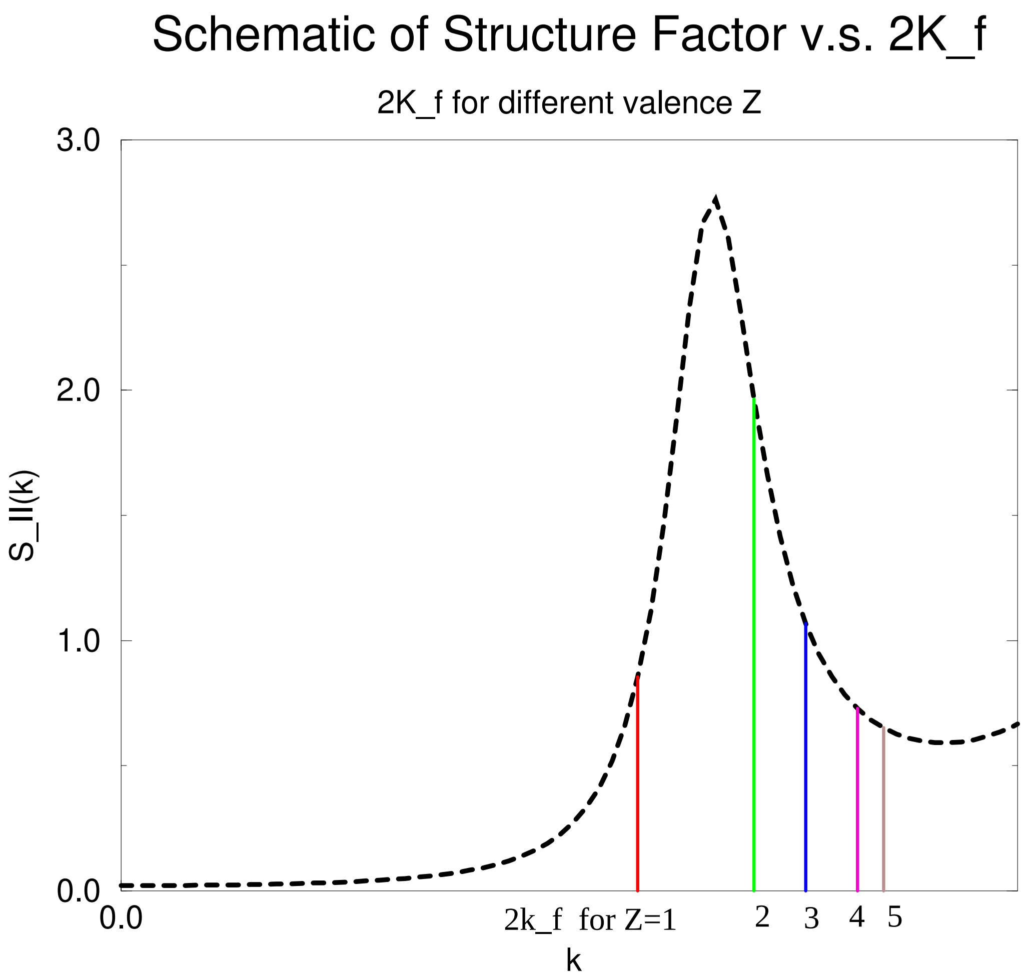

Figure 5.6: **Ratio of $2k_F$ to k_p for a schematic ion-ion structure factor.** As the valence Z increases, so does the $2k_F$ w.r.t. k_p, the first maximum of the ion-ion structure factor $S_{II}(k)$[11].

k_p (which will typically happen for high valence Z), the positive, decreasing part of $n(k)$ is selected (filtered) by the ion-ion structure factor resulting in the form seen in figures 5.9 and 5.10: the **high valence class** of electron-ion structure factors. This then explains the two forms found by de Wijs *et al*[5]: Mg is in the low-valence class, and Bi is in the high valence class[§] Interestingly, Mg has the high valence universal shape if a free-atom $n(k)$ is used. The pseudo-atom density is slightly expanded in real space (see figure 5.5) resulting in a slightly lower zero-crossing in k-space which in turn leads to a dramatic difference in $S_{ei}(k)$. This sensitivity begs the question: at what Z *exactly* does the $S_{eI}(q)$ cross over between the two classes? Clearly the electron-ion structure factors are very sensitive to the exact position of k_0 w.r.t. k_p, but generally for $Z < 3$, we expect the low valence class and for $Z > 3$, the high valence class. However, some care must be taken for the border $Z = 3$. In general we expect $Z = 3$ materials to fall into the high-valence class, but the exception may be aluminum, for which the zero-crossing k_0 may be relatively small w.r.t. $2k_F$ since $q_0/2k_F \sim 0.7$. Thus aluminum could be in a cross-over state between the two classes. This suggests that aluminum is a good potential candidate for experimentally probing the effects of higher order response. Since the ion-ion structure is well known, a measurement of $S_{eI}(k)$ will be very sensitive to the exact location of k_0; small differences in k_0 could lead to large, qualitative differences in $S_{eI}(k)$[¶]. For hydrogen the waters are muddied as usual. The lack of zero-crossing q_0 in the proton potential would imply that its $S_{eI}(k)$ falls into the high-valence class,

[§] de Wijs *et. al.* suggested that the difference was due to the nearly free electron (NFE) bonding of l-Mg v.s. the remnant covalency of l-Bi. However a high valence NFE metal such as l-Pb will have the same $S_{eI}(k)$ form as l-Bi.

[¶] Actually, there is also a $Z = 2$ element for which the exact class may be a bit ambiguous, namely Zn , for which the position of $2k_F$ w.r.t. k_p as well as $q_0/2k_F$ are both expected to be relatively high.

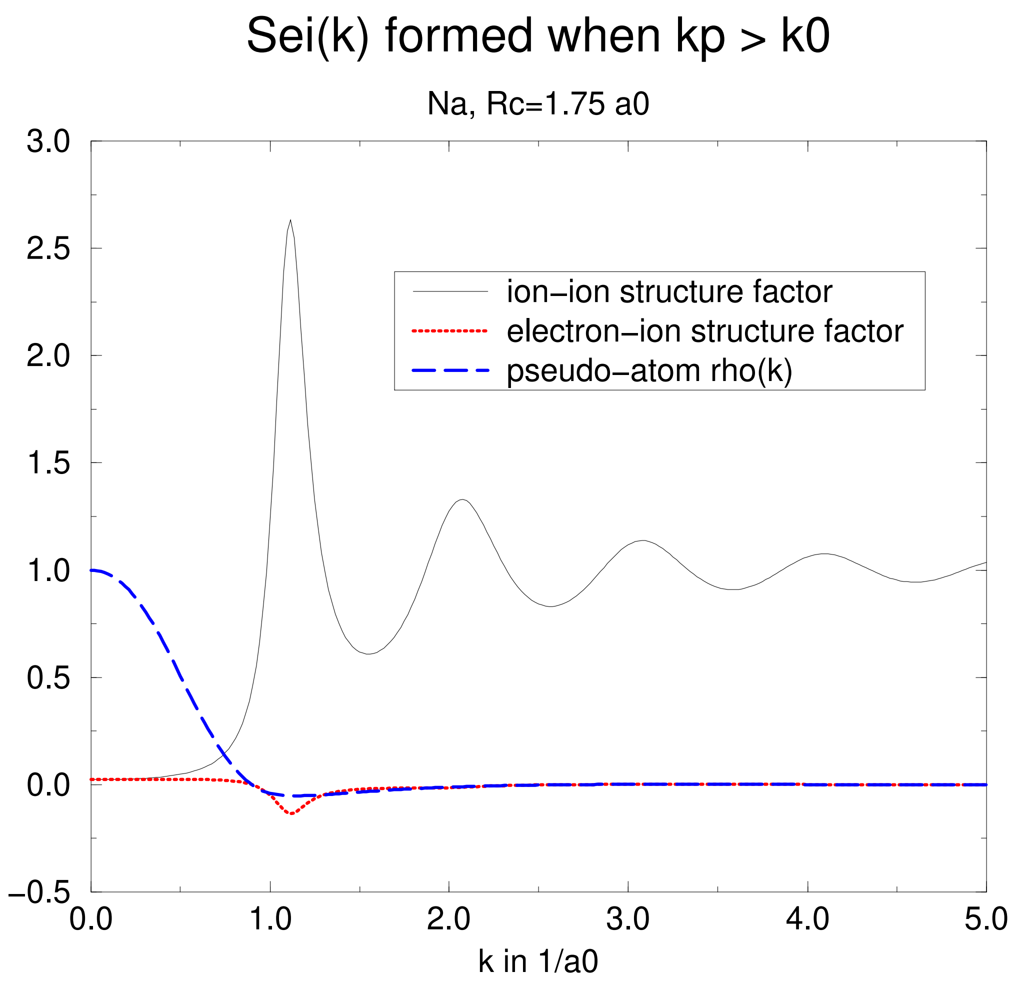

Figure 5.7: **Low valence class of electron-ion structure factors.** $S_{eI}(k)$ is the product of $n(k)$ and $S_{II}(k)$ and its form is dominated by the overlap at the first peak of $S_{II}(k)$. For most metals, q_0 is slightly less than $2k_F$. Since $q_0 \sim k_0$, the pseudo-atom density $n(k)$ has crossed through zero at $k_0 < k_p$, a form leading to the **low valence class** $(Z \leq 2)$ of electron-ion structure factors seen above.

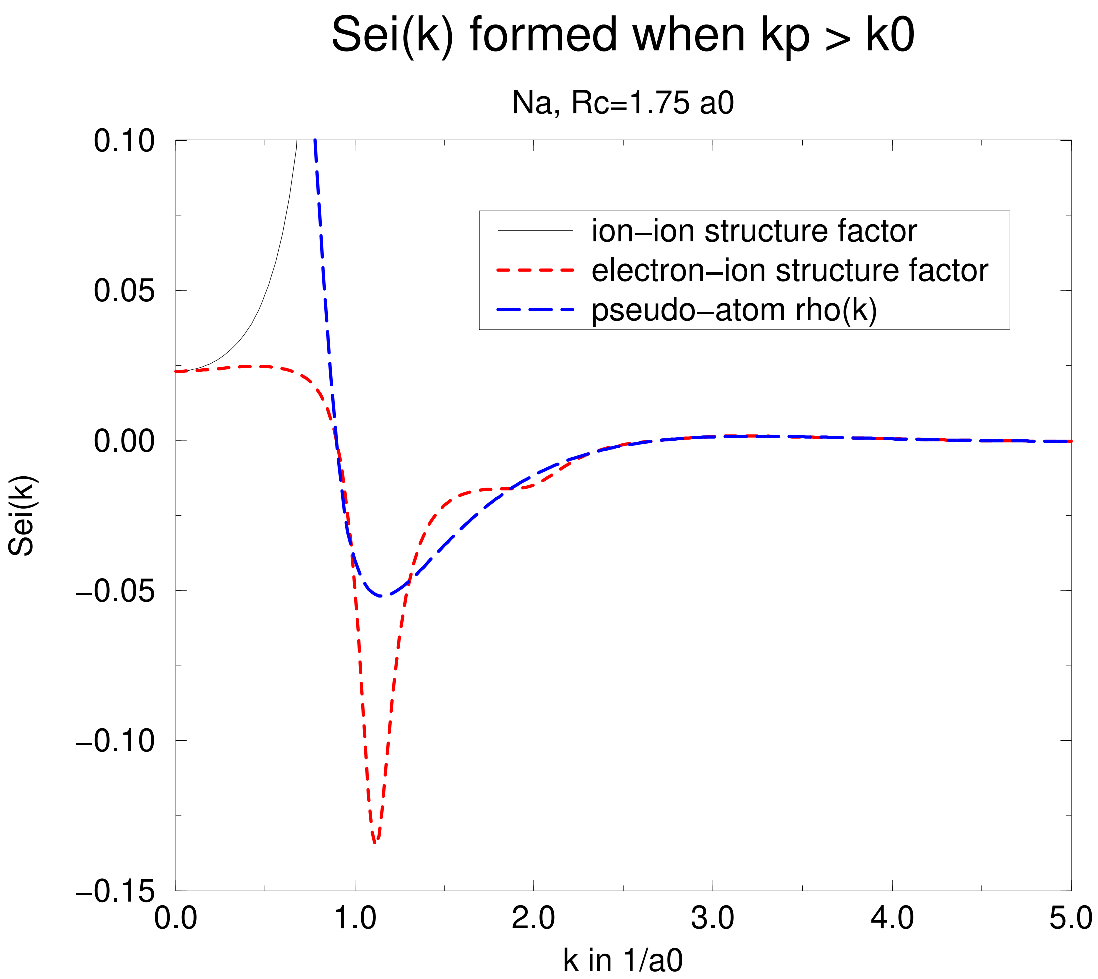

Figure 5.8: **Expansion of fig (5.7): Low valence class of electron-ion structure factors.**
Same as figure 5.7, but on a different scale to accentuate the low-valence form of $S_{eI}(k)$.

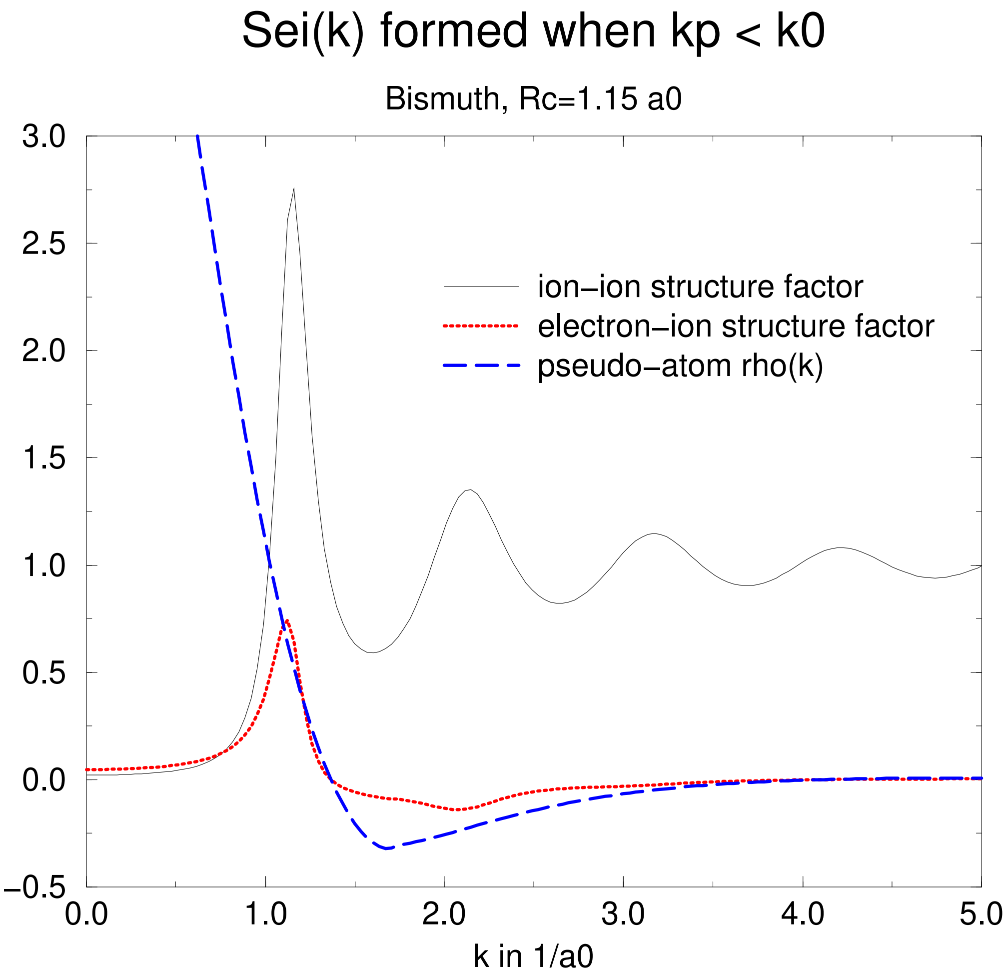

Figure 5.9: **High valence class of electron-ion structure factors.** $S_{eI}(k)$ is the product of $n(k)$ and $S_{II}(k)$ and its form is dominated by the overlap at the first peak of $S_{II}(k)$. For most metals, q_0 is slightly less than $2k_F$. Since $q_0 \sim k_0$, the pseudo-atom density $n(k)$ has crossed through zero at $k_0 > k_p$, a from leading to the the **high valence class** $(Z \geq 3)$ of electron-ion structure factors seen above.

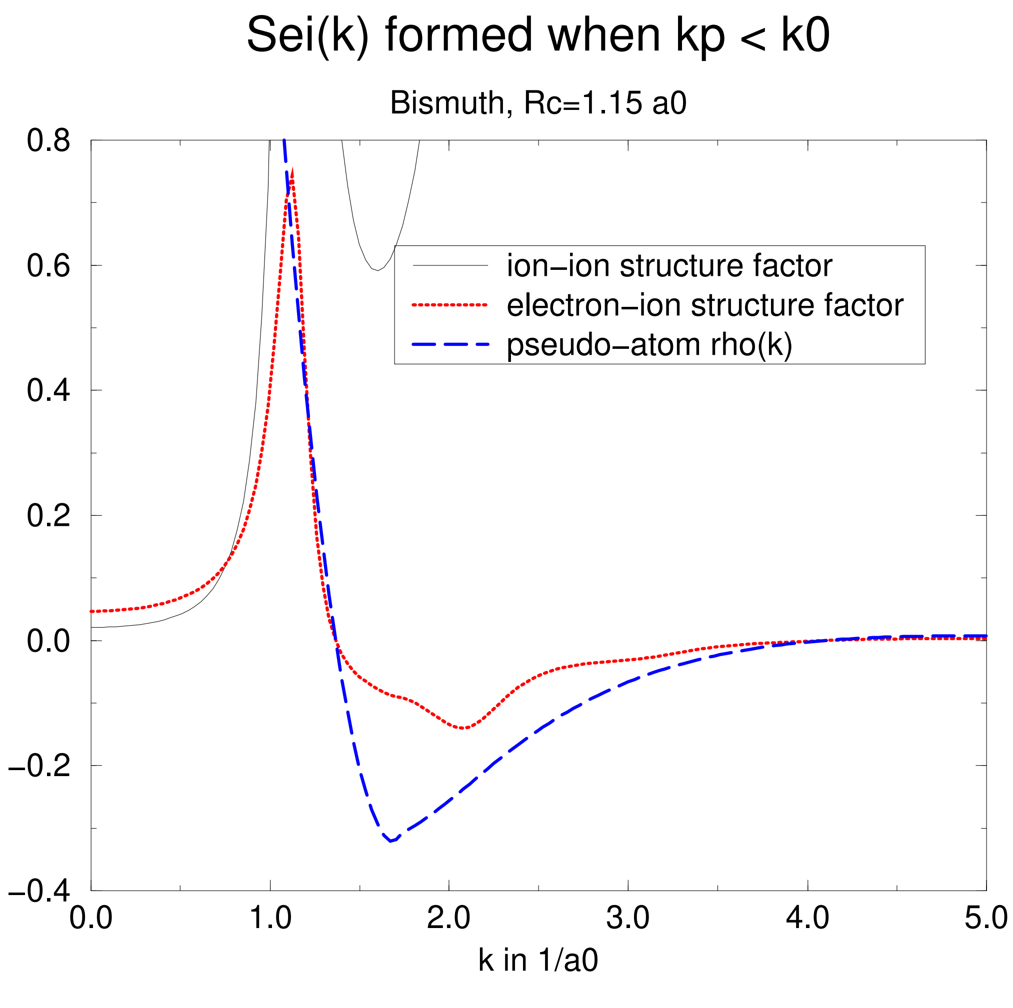

Figure 5.10: **Expansion of fig (5.9): High valence class of electron-ion structure factors.**
Same as figure 5.9, but on a different scale to accentuate the high-valence form of $S_{eI}(k)$.

but the failure of linear response for this system invalidates the analysis above (especially that relating q_0 to k_0). Determining the class to which the $S_{eI}(k)$ of liquid metallic monatomic hydrogen belongs remains to be determined. The class of electron-ion correlations in the experimentally realized possibility of (primarily) molecular metallic hydrogen (see chapter 3) is even more complex.

5.4 Relevance for experiments

Ion-ion liquid structure can be probed by inelastic x-ray scattering from all the electrons, or neutron scattering from the nuclei or electron scattering from both nuclei and electrons. In an important paper, Egelstaff *et al*[13] realized that combining these methods would shed light on electron correlation functions as well. They originally concluded that small differences in X-ray and neutron ion-ion structure factors implied short-range order in the electrons fluid but this was never confirmed. Instead various authors have used these differences to extract electron-ion correlation functions[14], the theory of which was worked out by Chihara[15]. To date the experimental electron-ion structure factors show much more fine structure than the theoretical ones. This deserves further study, and with the advent of more accurate and powerful x-ray and neutron sources currently coming on line, this discrepancy could be resolved. Considering the experimental challenges involved in subtracting from each other two sets of data obtained by different means, each with substantial systematic corrections, and considering the robustness of our simple theoretical approach, we predict that some of the experimental fine structure, especially at high wave vector k, will disappear. The remnant structure unaccounted for by experimental error will shed light on effects going beyond the linear response level. As mentioned above, aluminum is expected to be a particularly interesting candidate to elucidate. Other interesting materials would include Li and Be, both of which have a large valence to core electron ratio, which presumably facilitates the measurement of electron-ion structure factors.

5.5 Electron-Ion Energy

For a two-component mixture of ions and electrons, a portion of the electron-ion energy is given by[‖]:

$$E_{eI} \sim \int d\vec{k} v_{eI}(k) S_{eI}(-k) \tag{5.10}$$

So that for a given pseudo-potential $v_{eI}(k)$, an accurate approximation to $S_{eI}(k)$ implies an accurate electron-ion energy. The fact that the electron-ion structure factor is so well approximated by $S^{(1)}(k)$ implies that using a Percus-Yevick hard-sphere structure factor plus linear response, perhaps the most popular approach to simple theories of liquid metals, is far more satisfactory than one might initially expect. Further insight into the origin of the electron-ion energy is found in figures 5.11 and 5.12 where we schematically depict the energy integrand and integral of equation 5.10. For example, for metals in the low-valence class, the largest contribution comes from wave-vectors slightly greater than q_0.

[‖] See chapter 6 for a further discussion of this point.

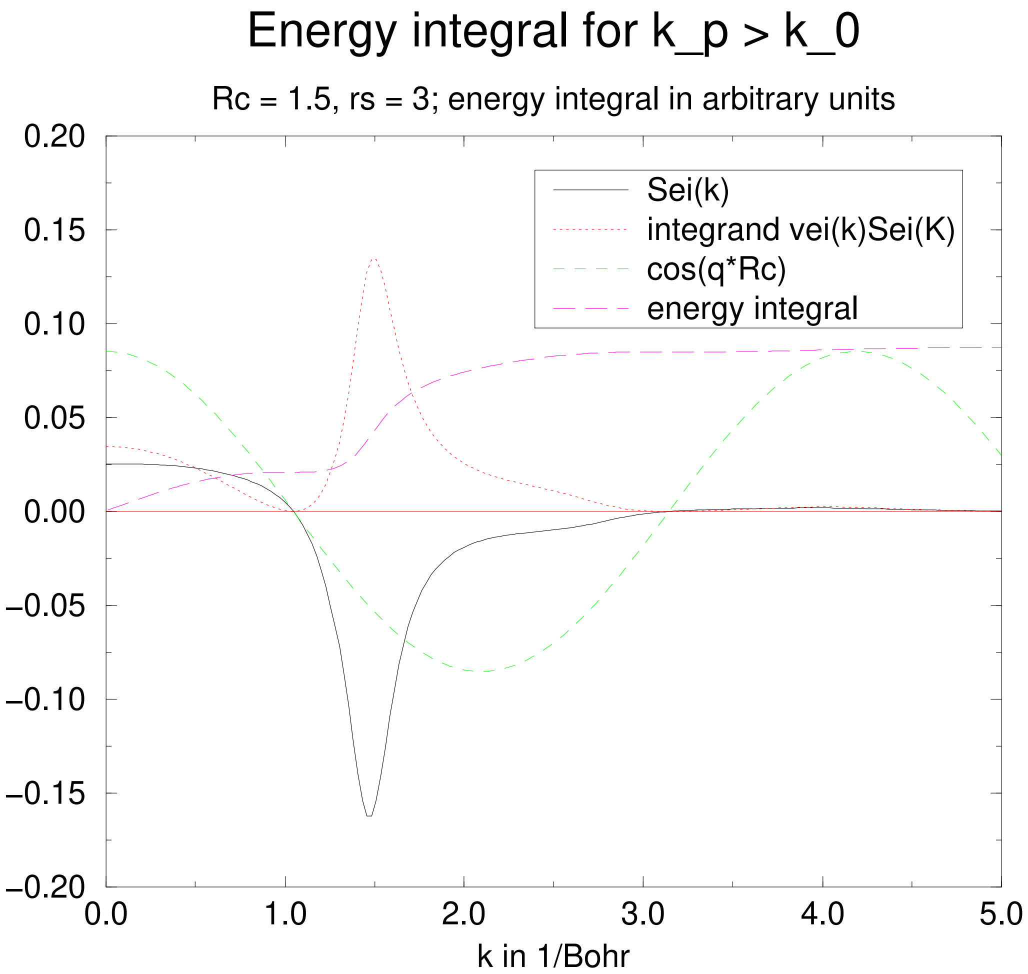

Figure 5.11: **Schematic of the energy integrand for $k_p > k_0$ (low valence class)**
The energy integrand of equation 5.10 v.s. k (this includes the $4\pi k^2$ volume factor). The units are arbitrary. Note how most of the integral is dominated by the area around q_0, the zero-crossing of $\cos(q * R_c)$

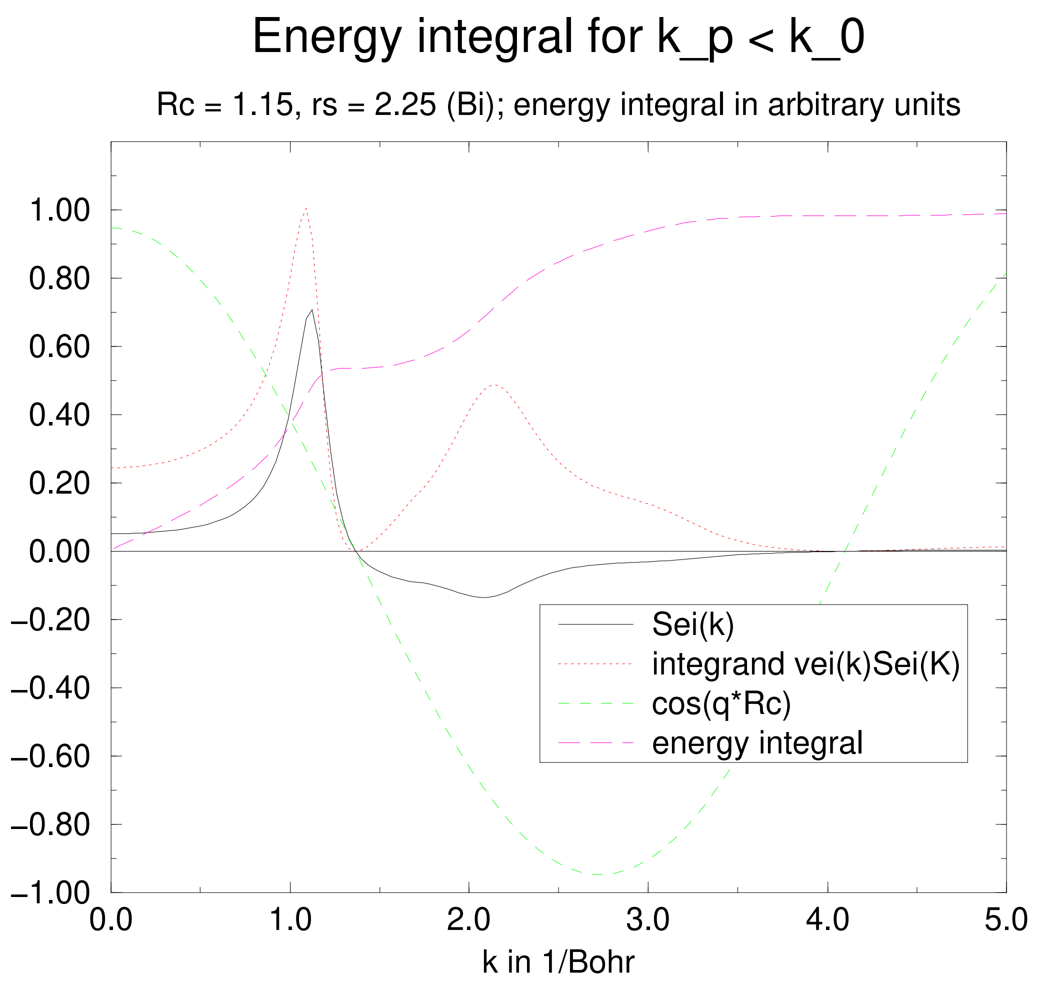

Figure 5.12: **Schematic of the energy integrand for $k_p < k_0$ (high valence class)**
The energy integrand of equation 5.10 v.s. k (This includes the $4\pi k^2$ volume factor). The units are arbitrary. For the high-valence class the energy picks up contributions from a larger volume of k space than is the case for the low valence class.

5.6 Conclusions and Further Work

Just as the ion-ion structure factor $S_{II}(k)$ is well represented by *one class* : that of the hard-sphere liquid, which is in turn well approximated by the analytic Percus-Yevick form and one parameter η, so also the electron-ion structure factor $S_{eI}(k)$ is well represented by *two classes*: that of the *high valence* ($Z \geq 3$) and *low valence* forms ($Z \leq 2$), both of which are well-approximated by an analytic linear-response for electrons augmented by a Percus-Yevick hard-sphere expression for the ions and two parameters. These two classes are best understood by comparing the zero-crossing k_0 of the pseudo-atom density $n(k)$ with the first maximum k_p of the ion-ion structure factor $S_{II}(k)$. We showed that even a simple linear response plus hard-sphere structure factor works very well here, because it gets the zero-crossing k_0 right. We therefore expect these results to be **robust**; more sophisticated calculations are not likely to change the qualitative features for most simple liquid metals (the exceptions being l-H, l-Al, and perhaps l-Zn).

Experiments measure $S_{ei}(k)$ by subtracting x-ray and neutron-scattering data. Up till now there has not been very much agreement between experiments. We claim that a careful consideration of the possible systematic errors incurred in comparing two different techniques as well as new, more powerful x-ray and neutron sources may shed more light on this situation, and that aluminum would be a particularly interesting material to study.

Bibliography

[1] For a review, see N.W. Ashcroft and D. Stroud, Solid State Physics **33**, 1 (1978).

[2] R. Car and M. Parrinello, Phys. Rev. Lett. **55** , 2471 (1985).

[3] J-P. Hansen and I. R. McDonald, *Theory of Simple Liquids*, (Academic Press, London (1986)).

[4] N.W. Ashcroft and J. Lekner, Phys. Rev. **145**, 83 (1966).

[5] G. A. de Wijs B. Pastore, A. Selloni, and W. van der Lugt, Phys. Rev. Lett. **75**, 4480 (1995).

[6] S. Cusack, N.H. March, M. Parrinello and M. P. Tosi, J. Phys F: Met. Phys. **6**, 749 (1976).

[7] K. Hoshino and M. Watabe, J. Phys. Soc. Japan **61**, 1663 (1992).

[8] J. Hafner, *From Hamiltonians to Phase Diagrams*, (Springer Verlag, Berlin, (1987)).

[9] N. Chetty, K. W. Jacobsen and J. K. Norskov, J. Phys: Condens. Matter **3**, 5437 (1991).

[10] Y. Waseda, *The Structure of Non-Crystalline Materials* (McGraw-Hill, New York (1980)).

[11] J. M. Ziman, *Principles of the Theory of Solids, 2nd Ed*, (Cambridge University Press, Cambridge (1972)), p 227.

[12] N.W. Ashcroft in *Density Functional Theory*, ed. E.K.U. Gross and R.M. Dreizler, Plenum, New York (1995).

[13] P.A. Egelstaff, N.H. March and N.C. McGill, Can. J. Phys. **52**, 1651 (1974).

[14] S. Takeda, S. Tamaki and Y. Waseda, J. Phys. Soc. Japan, **54** 2552 (1985); S. Takeda, S. Harada, S. Tamaki and Y. Waseda, J. Phys. Soc. Japan, **55** 184 (1986); *ibid* **55** 3437 (1986), *ibid*, **58**, 3999 (1989), *ibid* **60**, 2241 (1991), *ibid* **63** 1794, (1994).

[15] J. Chihara, J. Phys. F: Met Phys. **17**, 295 (1987),

Chapter 6

Pseudo Atoms and the Quantum Ornstein Zernike Relations

6.1 Introduction: Two Component Electron-Ion Mixtures

As noted in the last chapter, at a near fundamental level, liquid metals are complex binary fluids consisting of ions in a sea of conduction electrons. The ions can usually be treated classically while the electrons are typically degenerate and must be treated quantum-mechanically. The traditional theoretical description of liquid metals simplifies this picture by defining effective potentials (pair and higher) between the ions; in the statistical physics of the ions the electron liquid enters only indirectly through the density dependence of these potentials[1]. The development of *ab-initio* simulation techniques based on a Density Functional Theory (DFT) treatment of the electrons[2] bypasses effective potentials and is capable of treating liquid metals (and other materials) as fundamental mixtures of ions and electrons.

However, because of computational constraints, these simulation techniques are limited to relatively small system sizes and as such have difficulty describing first-order phase transitions such as freezing[3]. Concurrent to the development of the electronic DFT, semi-analytic theories based on approximations to the classical *free-energy* density functional of liquids described by pair potentials have successfully given quantitative theories of *inhomogeneous* liquids, including various first order phase transitions[4]. To date these classical theories have been largely limited to *state-independent* potentials while in systems like liquid metals, where the effective potentials are *state-dependent* (i.e. they depend on a thermodynamic variable) the properties of a first order phase transition clearly depend on the potentials, but these in turn depend on the state of the system through the average density. Thus a treatment of liquid metals based on approximations to the *free-energy* functional of a fully coupled quantum-classical electron-ion system, without the shortcomings of effective potentials in classical DFT (nor the problems of finite system size in electron DFT simulations) would be highly desirable.

A first attempt in this direction by Xu, Hansen and Chandler[6] developed a free-energy functional approach to the melting of an ion-electron plasma; in the binary mixture of (classical) ions and (quantum) conduction electrons, the ions freeze while the electrons remain in itinerant states. Xu *et. al.* used a heuristic approximation to the electron-ion correlation function of the system they studied (essentially monatomic hydrogen at extremely high density) and found large variations in melting predictions depending on which electron-ion theory they used. Although these calculations were outside any known experimental regime, they provided a proof of principle that such theories could be successfully constructed and they clearly demonstrated that the liquid state two-body electron-ion direct correlation function is crucial to quantitative accuracy. A successful development of these techniques depends critically on accurate liquid state correlation functions.

Thus the first step of this ambitious general program entails gaining a more coherent understanding of correlation functions in the full electron-ion mixture. This is the focus of the present chapter.

6.2 Hamiltonian and Free-Energy of a Two Component Electron-Ion Mixture

The Hamiltonian for a non-relativistic two-component mixture of N_I ions of valence $Z = Z$ and N_e electrons interacting through potentials $v_{\alpha\beta}(\vec{r}, \vec{r}')$ is given, for the charge-neutral case $N_e = ZN_I$, by:

$$\hat{H} = \sum_{\alpha=I,e} \left\{ \hat{T}_\alpha + \frac{1}{2} \sum_{\beta=I,e} \int_V d\vec{r} \int_V d\vec{r}' v^{(2)}_{\alpha\beta}(\vec{r} - \vec{r}') \hat{n}_{\alpha\beta}(\vec{r}, \vec{r}') \right\}. \tag{6.1}$$

The two-particle density operator is given by:

$$\hat{n}_{\alpha\beta}(\vec{r}, \vec{r}') = \hat{n}^{(1)}_\alpha(\vec{r}) \hat{n}^{(1)}_\beta(\vec{r}') - \delta_{\alpha\beta} \delta(\vec{r} - \vec{r}') \hat{n}^{(1)}_\alpha(\vec{r}), \tag{6.2}$$

a trace over electron and ion coordinates relates this to the pair-correlation or radial distribution functions:

$$\langle \hat{n}_{\alpha\beta}(\vec{r}, \vec{r}') \rangle = \left\langle \hat{n}^{(1)}_\alpha(\vec{r}) \right\rangle \left\langle \hat{n}^{(1)}_\beta(\vec{r}') \right\rangle g_{\alpha\beta}(\vec{r}, \vec{r}'). \tag{6.3}$$

The long-range nature Coulombic of the potentials requires special attention. First, we rewrite the potentials in terms of a Coulombic part, $\phi_c(\vec{r}, \vec{r}') = e^2/|\vec{r} - \vec{r}'|$, and an excess part $\delta v_{\alpha\beta}(\vec{r}, \vec{r}')$:

$$\begin{aligned} v_{II}(\vec{r}, \vec{r}') &= Z^2 \phi_c(\vec{r}, \vec{r}') + \delta v_{II}(\vec{r}, \vec{r}') & (6.4) \\ v_{eI}(\vec{r}, \vec{r}') &= -Z \phi_c(\vec{r}, \vec{r}') + \delta v_{eI}(\vec{r}, \vec{r}') & (6.5) \\ v_{ee}(\vec{r}, \vec{r}') &= \phi_c(\vec{r}, \vec{r}') + \delta v_{ee}(\vec{r}, \vec{r}'), & (6.6) \end{aligned}$$

where $\delta v_{ee}(\vec{r}, \vec{r}') = 0$. Second, we follow Appendix A of reference [5] and introduce the average densities $n^0_I = N_I/V$ and $n^0_e = ZN_I/V$ as well as two continuous background charge densities of opposite sign, (+en^0_e) and (-Zen^0_I), which allow (6.1) to be recast into the form:

$$\hat{H} = \hat{T}_I + \frac{1}{2}\int_V d\vec{r}\int_V d\vec{r}'\phi_c(\vec{r},\vec{r}')\left\{Z^2\hat{n}_{II}(\vec{r},\vec{r}') - 2Zn_I(\vec{r})n_e + n_e^2\right\} \quad (6.7)$$

$$+ \hat{T}_e + \frac{1}{2}\int_V d\vec{r}\int_V d\vec{r}'\phi_c(\vec{r},\vec{r}')\left\{\hat{n}_{ee}(\vec{r},\vec{r}') - 2n_e(\vec{r})n_e + n_e^2\right\} \quad (6.8)$$

$$- \int_V d\vec{r}\int_V d\vec{r}' Z\phi_c(\vec{r},\vec{r}')\left\{(Z\hat{n}_I(\vec{r}) - n_e)(\hat{n}_e(\vec{r'}) - n_e)\right\}, \quad (6.9)$$

$$+ \delta\hat{H}, \quad (6.10)$$

where $\delta\hat{H}$ denotes the excess part due to deviations from Coulomb's law:

$$\delta\hat{H} = \frac{1}{2}\int_V d\vec{r}\int_V d\vec{r}'\delta V_{II}(\vec{r},\vec{r}')\hat{n}_{II}(\vec{r},\vec{r}') \quad (6.11)$$

$$+ \int_V d\vec{r}\int_V d\vec{r}'\delta V_{eI}(\vec{r},\vec{r}')\hat{n}_{eI}(\vec{r},\vec{r}'). \quad (6.12)$$

The ion-ion term (6.11) is typically small*, but the electron-ion term (6.12) may not be small at all, and has physical significance[1]. Nevertheless, none of the terms in (6.11-6.12) are long-ranged, and so they are expected to be finite. Thus (6.7-6.9) represents the same problem as equation (6.1), but now with rigid backgrounds to ensure charge neutrality. Fluctuations are therefore defined w.r.t these backgrounds. A trace over electron and ion coordinates† gives, by virtue of equations (6.1) and (6.3), the energy in terms of integrals over the pair-correlation functions:

$$E_{tot} = \text{Trace}_{\{eI\}}\left[\hat{H}\right] = \left\langle \hat{H}\right\rangle = < \hat{T}_I > + < \hat{T}_e >$$

* The ion-ion interaction can be well approximated by a Coulomb potential $v_{II}(|\vec{r}-\vec{r}'|) = Z^2/|\vec{r}-\vec{r}'|$ for simple metals. For transition metals with resonant states, the ion is no-longer completely independent of the electron gas and the simple Coulomb form, or even the concept of an ion independent of the electron gas, no longer holds. On the other hand, Gauss' theorem guarantees that the ions do obey a Coulomb interaction law as long as they do not approach close enough for their core-electrons to overlap.

† Again, some care as to ensure the proper electro-neutrality conditions must be taken, see for example appendix A of [5].

$$+ \quad \frac{1}{2}\int_V d\vec{r}\int_V d\vec{r}' n_I(\vec{r})n_I(\vec{r}')v_{II}(\vec{r}-\vec{r}')g_{II}(\vec{r},\vec{r}') \tag{6.13}$$

$$- \quad \int_V d\vec{r}\int_V d\vec{r}' n_I(\vec{r})n_e(\vec{r}')v_{eI}(\vec{r}-\vec{r}')g_{eI}(\vec{r},\vec{r}') \tag{6.14}$$

$$+ \quad \frac{1}{2}\int_V d\vec{r}\int_V d\vec{r} n_e(\vec{r})n_e(\vec{r}')v_{ee}(\vec{r}-\vec{r}')g_{ee}(\vec{r},\vec{r}') \tag{6.15}$$

Similarly the free-energy is given by:

$$F = -k_B T \ln \mathrm{Trace}_{\{eI\}}\left[e^{-\beta\hat{H}}\right]. \tag{6.16}$$

If an adiabatic approximation is made between ions and electrons, this trace simplifies further. The free-energy and can be split up into the ideal (F^0) parts which are independent of interactions, and the excess (F^{ex}) parts which stem from interactions:

$$F = F_I^0 + F_e^0 + F_{II}^{ex} + F_{eI}^{ex} + F_{ee}^{ex}. \tag{6.17}$$

As discussed in Appendix C, the Hohenberg-Kohn-Mermin theorem states that a given *set* of external potentials $\{v_I^{(1)}(\vec{r}), v_e^{(1)}(\vec{r})\}$ there exist a unique *set* of one-particle densities $\{n_I(\vec{r}), n_e(\vec{r})\}$. The free energy (6.17) is a unique functional of the one-body external potentials or equivalently of the equilibrium one-particle densities.

6.3 Derivation of the Quantum Ornstein Zernike Relations

We define the direct correlation functions‡ of an arbitrary two-component mixture in the usual way as functional derivatives of the excess free energy (6.17):

$$\frac{-1}{\beta}C_{ij}(r,r') = \left.\frac{\delta^2 F^{ex}}{\delta n_i(r)\delta n_j(r')}\right|_{\{n_i(r)n_j(r')\}\to\{n_i,n_j\}} \tag{6.18}$$

By manipulating generating functionals for correlation function hierarchies, the direct-correlation functions can be related to the response-functions[5, 7], resulting for a two-component quantum system in a relationship between two 2-by-2 matrices:

$$\frac{1}{\beta}C_{ij} = (\chi_{ij})^{-1} - (\chi^0_{ij})^{-1}, \tag{6.19}$$

which we shall call the **Quantum Ornstein Zernike (QOZ)** relations.

By inverting the QOZ 2 by 2 matrix we find the following relations between matrix components:

$$\chi_{11}(q) = \chi^0_{11}(q)\left(1+\chi^0_{22}(q)C_{22}(q)/\beta\right)/D(q) \tag{6.20}$$

$$\chi_{12}(q) = -\chi^0_{11}(q)\chi^0_{22}(q)\left(C_{12}(q)/\beta\right)/D(q) \tag{6.21}$$

$$\chi_{22}(q) = \chi^0_{22}(q)\left(1+\chi^0_{11}(q)C_{11}(q)/\beta\right)/D(q) \tag{6.22}$$

$$\begin{aligned} D(q) &= \left(1+\chi^0_{11}(q)C_{11}(q)/\beta\right)\left(1+\chi^0_{22}(q)C_{22}(q)/\beta\right) \\ &\quad -\chi^0_{11}(q)\chi^0_{22}(q)C_{12}(q)C_{21}(q)/\beta^2. \end{aligned} \tag{6.23}$$

Note that these are *exact relations* for a two component quantum system. The QOZ relations appear to have been first derived by Chihara[8]. Later Ichimaru *et.*

‡ This is actually the definition of $C(r)/\beta$, a notation that stems from the classical context. At zero-temperature only, this ratio is well defined and given by the relation 6.18, $C(r)$ itself is not.

al. derived similar equations from a two-component linear response formulation[9]. The two formulations are equivalent if the definitions of the direct correlation functions (6.19) are linked in the usual way to the local field factors:

$$\frac{C_{ij}(q)}{\beta} = -V_{ij}(q)(1 - G_{ij}(q)), \tag{6.24}$$

For classical species, the fluctuation- dissipation theorem relates the response functions to density-density correlation functions:

$$\lim_{\hbar \to 0} \chi_{ij}(q, 0) = -\beta (n_i n_j)^{1/2} S_{ij}(q). \tag{6.25}$$

In the limit that both species are classical, the QOZ relations reduce to the usual relations between structure factors[10]. For a mixture of classical ions (I=1) and quantum electrons (e=2), equation (6.25) holds for $\chi_{II}(q)$ and $\chi_{eI}(q)$. From the definitions:

$$S_{II}(q) = 1 + n_I^0 \int d\vec{r} e^{-i\vec{q}\cdot\vec{r}} [g_{II}(r) - 1] \tag{6.26}$$

$$S_{eI}(q) = (n_I^0 n_e^0)^{1/2} \int d\vec{r} e^{-i\vec{q}\cdot\vec{r}} [g_{eI}(r) - 1] \tag{6.27}$$

real-space versions of the QOZ relations can be derived.

6.4 Exact Expressions for the Pseudo-Atom Density

By combining the two QOZ relations (6.20) and (6.21) together with the fluctuation dissipation theorem above, the relation between $S_{eI}(q)$ and $S_{II}(q)$ becomes:

$$S_{eI}(q) = \left(\frac{\chi^0_{ee}(q)}{1 - \chi^0_{ee}(q) C_{ee}(q)/\beta} \right) \frac{C_{eI}(q)}{-\beta} \frac{S_{II}(q)}{(n_I/n_e)^{1/2}}. \tag{6.28}$$

As was done in chapter 5, we write this in terms of a **pseudo atom** by rewriting equation (6.28) as:

$$S_{eI}(q) = \frac{n(q)}{\sqrt{Z}} S_{II}(q), \tag{6.29}$$

from which the pseudo-atom density is defined as:

$$n(q) \equiv \left(\frac{\chi^0_{ee}(q)}{1 - \chi^0_{ee}(q) C_{ee}(q)/\beta} \right) \frac{C_{eI}(q)}{-\beta}. \tag{6.30}$$

If the pseudo-atom density is rewritten as:

$$n(q) = \chi'_{ee}(q) \frac{C_{eI}(q)}{-\beta}, \tag{6.31}$$

then the relation (6.24) between the local-field factors $G_{ee}(q)$ and the direct correlation function $C_{ee}(q)$ allows us to rewrite the new function $\chi'_{ee}(q)$ in the suggestive form:

$$\chi'_{ee}(q) = \frac{\chi^0_{ee}(q)}{1 + \chi^0_{ee}(q) v_{ee}(q)(1 - G_{ee}(q))}. \tag{6.32}$$

If $G_{ee}(q)$ is taken to be independent of ionic correlations (but, through charge neutrality, not of the average density n^0_I) then $\chi'_{ee}(q)$ becomes the well known response function $\chi^{jell}_{ee}(q)$ for jellium[§]. Given a local field factor, equation (6.31) implies that

[§] This can also be seen by taking the appropriate limit of the QOZ relation (6.23).

the electron-ion direct correlation function is directly related to the pseudo-atom density: finding one implies finding the other.

The lowest order approximation for the electron-ion correlation function (low density):

$$C_{eI}(q) = -\beta V_{eI}(q) \tag{6.33}$$

coupled with the jellium approximation for $\chi'_{ee}(q)$ results in the usual linear response pseudo-atom density $n_1(q)$ explored in chapters 4 and 5, i.e.:

$$n_1(q) = \rho_1(q) = \chi_{ee}^{jell}(q) V_{eI}(q), \tag{6.34}$$

which is independent of ionic configuration. Clearly the full pseudo-atom density (6.31) is a functional not only of all orders of electron response, but of ionic-configurations as well, since its correlation function ingredients are coupled together by the QOZ relations.

6.5 Effective One-Component Correlation Functions

By equating $S_{II}(q)$ to an effective one-component liquid structure factor:

$$S_{II}(q) = S(q) = \frac{1}{(1 - n_I^0 C(q))} \tag{6.35}$$

one finds (using the QOZ relation (6.20)) an effective one-component direct correlation function of the form:

$$C(q) = -C_{II}(q) + \alpha(q), \tag{6.36}$$

where $\alpha(q)$ is given by:

$$\alpha(q) = \chi'_{ee}(q)\,(-C_{eI}(q)/\beta)^2 = \frac{(n(q))^2}{\chi'_{ee}(q)} \tag{6.37}$$

The nodal function $\Gamma_{II}(q)$ is given by:

$$\Gamma_{II}(q) = h_{II}(q) - C_{II}(q), \tag{6.38}$$

while the Ornstein-Zernike equation of a one-component system gives:

$$\Gamma(q) = h(q) - C(q), \tag{6.39}$$

Requiring the ion-correlations to be equal in the two-component and effective one-component formulations, (i.e. $h_{II}(q) = h(q)$, where $h(r)$ is related to the pair-correlation function by: $g(r) = h(r) + 1$), together with equation (6.36) relates the two nodal functions:

$$\Gamma(q) = \Gamma_{II}(q) - \alpha(q), \tag{6.40}$$

6.6 Effective Potentials from the Quantum-Percus Identity

The the physics of inhomogeneous and homogeneous classical fluids can be linked by a powerful observation due to Percus[11] who showed that if one particle is fixed at the origin and allowed to interact with the other particles its potential plays the role of an external potential, inducing an *inhomogeneous* one-particle density $n_e(r)$ which in turn is directly related to the two-body correlation function of the *homogeneous* fluid. The quantum-classical generalization of the Percus-identity entails fixing one ion at the origin in the full ion-electron system¶. The surrounding one-body electron density leads to the electron-ion pair correlation function, and the surrounding one-body ion-density leads to the ion-ion pair correlation For the electron density the Percus-identity gives:

$$g_{eI}(0,r) = \frac{n_e(r|I)}{n_e^0}. \tag{6.41}$$

If in addition a Kohn-Sham type approach is employed, reducing the problem to a non-interacting system Euler equation, the pair correlation becomes:

$$g_{eI} = \frac{n_e^0(r|V_{eI}^{MF})}{n_e^0}, \tag{6.42}$$

where V_{eI}^{MF}, the potential of mean-force for the non-interacting electrons, is given by:

$$\beta V_{eI}^{MF}(r) = V_{eI}(r) - \Gamma_{eI}(r) - B_{eI}(r). \tag{6.43}$$

¶ Some care must be taken in adding the requisite number of electrons - i.e. use canonical ensemble and add a fixed ion and Z itinerant electrons. The difference in the Percus-identity between canonical and grand-canonical ensembles disappears in the thermodynamic limit.

and $\Gamma_{eI}(r)$ and $B_{eI}(r)$ are two-component generalizations of the nodal and bridge functions respectively. Similarly for the ions, the Percus identity gives:

$$g_{II}(r) = \frac{n_I(r|I)}{n_I^0} = exp(-\beta V_{II}^{MF}(r)), \tag{6.44}$$

To obtain effective one-component system equations, we require the ion-ion pair correlations to be equal ($h(r) = h_{II}(r)$) which implies that the potentials of mean force are also equal:

$$\begin{aligned} V^{MF}(q) &= V_{II}(q) - \Gamma_{II}(q)/\beta - B_{II}(q)/\beta & (6.45)\\ V_{eff}^{MF}(q) &= V_{eff}(q) - \Gamma(q)/\beta - B(q)/\beta & (6.46)\end{aligned}$$

so that the new one-component effective ion-ion interaction can be identified with

$$V_{eff}(q) = V_{II}(q) - \alpha(q) + (B(q) - B_{II}(q)). \tag{6.47}$$

This pair-potential *exactly* reproduces all pair correlations, and though its definition includes the effect of three-body and higher order potentials. It does not necessarily exactly reproduce higher order correlations though. Another approach would be to start from:

$$C_{II}(q) = -\beta V_{II}(q) + \tilde{C}_{II}(q) \tag{6.48}$$

which together with equation (6.36) results in the following expression for the effective one-component direct correlation function:

$$\begin{aligned} C(q) &= -\beta V_{eff}(q) + \tilde{C}(q) \\ &= -\beta V_{II}(q) + \alpha(q) + \tilde{C}_{II}(q) & (6.49)\end{aligned}$$

so that the effective one-component ion-ion pair interaction can also be identified with:

$$V_{eff}(q) = V_{II}(q) - \alpha(q) + \left(\tilde{C}(q) - \tilde{C}_{II}(q)\right) \tag{6.50}$$

An interesting corollary emerges from the combination of equations (6.47) and (6.50); namely

$$B(q) - B_{II}(q) = \tilde{C}(q) - \tilde{C}_{II}(q). \tag{6.51}$$

If the bridge-functions, or equivalently, the unknown (interaction) parts of the direct correlation functions were equal to each other, this would result in a particularly simple expression for the effective pair potential:

$$V_{eff}(q) = V_{II}(q) - \chi'_{ee}(q) \left(\frac{C_{eI}(q)}{-\beta} \right)^2 \tag{6.52}$$

If in addition to the approximation $B(q) = B_{II}(q)$, $\chi'_{ee}(q)$ is approximated by a jellium form and the classical low density expansion $C_{eI}(q) \sim -\beta v_{eI}(q)$ (see eq(6.33)) is used, this potential reduces to the popular linear response form:

$$V_{eff}(q) = V_{II}(q) + \chi^{jell}_{ee}(q) v_{ei}(q) v_{ei}(-q). \tag{6.53}$$

Clearly improvements in the theory of the pseudo-atom density will lead to improvements in the effective ion-ion potentials; the two are intimately connected.

6.7 Bridge Functions

The one-component ion-ion bridge function is given by the terms beyond second order in the functional Taylor expansion of the direct correlation function $C(r)$:

$$B(r) = \sum_{n}^{\infty} \frac{(n_I^0)^n}{n!} \int dr_1....dr_n C^{(n+1)}(r; r_1...r_n) h^{(2)}(r_1)...h^{(2)}(r_n) \tag{6.54}$$

For the two-component case the generalization is:

$$B_{II}(r) = \sum_{n}^{\infty} \frac{1}{n!} \sum_{l_1=I}^{l_1=e} ... \sum_{l_n=I}^{l_n=e} \left(n_{l_1}^0 ... n_{l_n}^0 \right) \int dr_1....dr_n C_{I,l_1...l_n}^{(n+1)}(r; r_1...r_n) h_{Il_1}^{(2)}(r_1)...h_{Il_n}^{(2)}(r_n) \tag{6.55}$$

Together with the definition of the effective one-component two-body direct correlation function (6.36), it would be tempting to write the the one-component bridge-function as:

$$\begin{aligned} B(r) \quad = \quad & \sum_{n}^{\infty} \frac{(n^I)^n}{n!} \int dr_1....dr_n \left[C_{II}^{(n+1)}(r; r_1...r_n) + \right. \\ & \left. \frac{\delta^{n-1}}{\delta n_I(r_1)..\delta n_I(r_n)} \alpha(r, r_1; r_2..r_n) \right] h_{II}^{(2)}(r_1)...h_{II}^{(2)}(r_n). \end{aligned} \tag{6.56}$$

But this is not quite right. Just because there is a relationship between the *functions* $C(q)$ and $C_{II}(q)$, the homogeneous limits of some functional derivatives, it cannot be concluded that there is also a relationship between the *functionals* and higher order derivatives! However, it may be a reasonable (though uncontrolled) approximation.

6.8 The Quantum Hypernetted Chain Equation (QHNC) à la Chihara.

An important approach to the correlation functions of electron-ion mixtures are the integral equation methods pioneered by Chihara[12] who makes the following approximations in his Quantum Hypernetted Chain (QHNC) equations:

1. The effective electron-ion potential $V_{eI}^{MF}(r)$ in equation (6.43) is approximated by neglecting the electron-ion bridge-function $B_{ei}(q)$.
2. The resultant (one-body) Kohn-Sham equations (in LDA approximation) are solved, resulting in $g_{eI}(q)$.
3. A jellium approximation for $C_{ee}(q)$ is made , (Chihara uses the Geldart-Taylor LFC, which is not consistent with using LDA for $g_{eI}(r)$!).
4. By feeding $g_{eI}(q)$ and $C_{ee}(q)$ into the coupled **QOZ** relations ion-ion correlations are obtained.
5. The above procedure is iterated to self-consistency.

Chihara's approach is an interesting one, but it needs to be more clearly connected to other theories of liquid metals, especially to assess the validity of using a one-center equation for the electronic structure. One improvement may be using liquid-theory approaches to approximate $B_{ei}(q)$ which takes into account ion-correlations beyond the one-center approximation. Chihara also neglects the difference between two-component and one-component bridge functions to obtain equation (6.52) for ion-ion pair potentials. Nevertheless he obtains accurate structure factors with this potential. Perhaps this stems from the small difference between $-C_{eI}(q)$ and $-\beta V_{eI}(q)$, or else because mixing local field factors cancels the errors.

6.9 Making Contact with Linear Response Function Formalism

For a two-component electron-ion system, with a fixed configuration of ions, the electrons can be traced out by the Hellman-Feynman coupling constant method:

$$F_{eI} = \int_0^1 d\lambda < \frac{dH_{eI}}{d\lambda} >_\lambda \tag{6.57}$$

In this case:

$$< \frac{dH_{eI}}{d\lambda} >_\lambda = \frac{1}{\Omega} \sum_{k \neq 0} V_{eI}(k) \hat{n}_I(k) < \hat{n}_e(-k) >_\lambda \tag{6.58}$$

By expanding the average over electron coordinates $<>_\lambda$ in powers of the potential:

$$\begin{aligned} < \hat{n}_e(k) >_\lambda &= \lambda \chi_e(k) V_{eI}(k) \hat{n}_I(k) \\ &+ \lambda^2 \sum_{q1} \sum_{q2} \chi^{(2)}(k, q1, q2) V_{eI}(q1) \hat{\rho}_I(q1) V_{eI}(q2) \hat{\rho}_I(q2) + ... \\ &\equiv \rho^\lambda(-k; [\hat{n}_I]) \hat{n}_I(k) \end{aligned} \tag{6.59}$$

we can define $\rho^\lambda(-k; [\hat{n}_I])$, the "static pseudo-atom density", i.e. the pseudo-atom density for a fixed external configuration of ions, which in turn can be expanded as:

$$\rho^\lambda(k; [\hat{n}_I]) = \lambda \rho_1(k) + \lambda^2 \rho_2(k; [\hat{n}_I]) + ... \lambda^p \rho_p(k; [\hat{n}_I]). \tag{6.60}$$

Note that to first order (linear response), the static pseudo-atom density is independent of ionic configuration. However, at higher orders the actual ionic configuration comes into play. In the Born-Oppenheimer approximation, the coupling constant integration can be trivially carried out for each configuration in (6.59) and obtains:

$$F_{ei} = \frac{1}{\Omega} \sum_{k \neq 0} V_{eI}(k) \hat{n}_I(k) \left\{ \sum (\frac{1}{2} \rho_1(-k) + \frac{1}{3} \rho_2(-k; [\hat{n}_I]) + ... \frac{1}{n} \rho_p(-k; [\hat{n}_I]) \right\} \hat{n}_I(-k) \tag{6.61}$$

So that the "static pseudo-atom density" $\rho^\lambda(k;[\hat{n}_I])$ is really an operator $\hat{\rho}$ that acts on the ionic coordinates, and all of our manipulations so far have been on the level of ionic operators. If we now perform the ionic ensemble average we obtain:

$$\begin{aligned}
< U_{eI} > &= < F_{eI} >_I = \\
&= \left\langle \frac{1}{\Omega} \sum_{k \neq 0} V_{eI}(k) \hat{n}_I(k) \hat{n}_I(-k) \right. \\
&\times \left. \left\{ \sum (\frac{1}{2} \rho_1(k) + \frac{1}{3} \rho_2(k;[\hat{n}_I]) + ... \frac{1}{n} \rho_p(k;[\hat{n}_I]) \right\} \right\rangle_I \\
&\equiv \frac{1}{2} \frac{1}{\Omega} \sum_{k \neq 0} V_{eI}(k) N n(k) S(k)
\end{aligned} \tag{6.62}$$

which defines the **pseudo-atom density** $n(k)$.

One result of this definition is that the exact electron-ion energy in terms of the pseudo-atom densities is given (to all orders in the potential expansion) by:

$$\frac{< U_{eI} >}{N} = \frac{1}{2\Omega} \sum_{\mathbf{q} \neq 0} V_{eI}(q) n(q) S_{II}(q) = \frac{\sqrt{Z}}{2\Omega} \sum_{\mathbf{q} \neq 0} V_{eI}(q) S_{eI}(q) \tag{6.63}$$

which is just the q-space manifestation of equation (6.14)

$$< U_{eI} > \sim (n_e n_I)^{1/2} \int g_{eI}(r) V_{eI}(r) d\vec{r}, \tag{6.64}$$

(the pure structure independent volume-contributions coming from $q = 0$ are not included above), as discussed in chapter 5.

By writing out the energy in the linear response formalism to second order in the potential, and then equating terms proportional to powers of λ, we find the leading order correction to the pseudo-atom density (i.e. the beyond linear response correction). For example: The third order electron-ion energy is:

$$\begin{aligned}
\frac{< U_{eI}^{(3)} >}{N} &= \frac{1}{3\Omega} \sum_{\vec{k} \neq 0} V_{eI}(k) \sum_{\vec{q}} \chi^{(2)}(k, q, |\vec{k} + \vec{q}|) V_{eI}(q) V_{eI}(|\vec{k} + \vec{q}|) \\
&\times \frac{1}{N} < \hat{n}_I(\vec{k}) \hat{n}_I(\vec{q}) \hat{n}_I(|\vec{k} + \vec{q}|) > .
\end{aligned} \tag{6.65}$$

The ionic average above is simply the 3-body structure factor:

$$S^{(3)}(\vec{k},\vec{q}) = \frac{1}{N} < \hat{n}_I(\vec{k})\hat{n}_I(\vec{q})\hat{n}_I(|\vec{k}+\vec{q}|) >= S(k)S(q)S(|\vec{k}+\vec{q}|)[1+n_I^2 C^{(3)}(\vec{k},\vec{q})], \tag{6.66}$$

so that (6.65) can be rewritten as:

$$\begin{aligned} \frac{< U_{eI}^{(3)} >}{N} &= \frac{1}{2\Omega}\sum_{\vec{k}\neq 0} V_{eI}(k)S(k)\frac{2}{3}\sum_{q}\chi^{(2)}(k,q,|\vec{k}+\vec{q}|)V_{eI}(q)V_{eI}(|\vec{k}+\vec{q}|) \\ &\times \; S(q)S(|\vec{k}+\vec{q}|)[1+n_I^2 C^{(3)}(\vec{k},\vec{q})] \end{aligned} \tag{6.67}$$

Comparing this with (6.63) gives the second order pseudo-atom density as:

$$n_2(q) = \frac{2}{3}\sum_{\vec{q}}\chi^{(2)}(k,q,|\vec{k}+\vec{q}|)V_{eI}(q)V_{eI}(|\vec{k}+\vec{q}|)S(q)S(|\vec{k}+\vec{q}|)[1+n_I^2 C^{(3)}(\vec{k},\vec{q})] \tag{6.68}$$

This is somewhat different from the second order object $\rho_2(q)$, the non-linear response function we studied in chapter 4, since it includes 3-body ionic correlations and now obviously depends on structure! In essence this is not surprising, as we expect ionic-correlations to play a role in beyond-linear response terms of the pseudo-atom density. For example the 2nd order response of chapter 4:

$$\rho_2(k) = \sum_{\vec{q}}\chi^{(2)}(k,q,|\vec{k}+\vec{q}|)V_{eI}(q)V_{eI}(|\vec{k}+\vec{q}|) \tag{6.69}$$

only contributes to the 2rd order part of an effective ion-ion pair potential[13]. In an effective one-component system, the pseudo-atom density is part of the effective pair potential, which in turn determines the ionic-correlations; beyond linear response it becomes a self-consistent object.

To go to the first level beyond the linear response to calculate requires two ingredients: (1) second order electron response, which was discussed in chapter 4, and (2) the three-body structure factor $S^{(3)}(\vec{k},\vec{q})$. To find it one needs $C^{(3)}(\vec{k},\vec{q})$, the 3-body direct correlation function, to several approximation schemes exist in the literature[15], although many uncertainties persist. The simplest approximation is the convolution approximation[14] which entails setting the the third-order direct correlation function to zero:

$$C^{(3)}(\vec{k}, \vec{q}) = 0, \tag{6.70}$$

a related but stronger condition than that imposed by HNC approximationm namely:

$$\int d\vec{k} d\vec{q} C^{(3)}(\vec{k}, \vec{q}) = 0. \tag{6.71}$$

HNC is known to perform well for systems with long-range potentials, and we expect the convolution approximation to work best under similar conditions.

6.10 Conclusions

Clearly a better understanding of pseudo-atom densities is paramount to a more coherent theoretical description of coupled inhomogeneous electron-ion systems in general and liquid metals in particular. The content of this chapter was but a small step in that direction: the main results are exact expressions for effective ion-ion potentials (equations 6.47 and 6.50) and an exact expression for the second order pseudo-atom (equation 6.68), but much remains to be explored. For example, ab-initio simulations with new, faster Car-Parrinello[2] codes like VASP[16] would give ab-initio pseudo-atoms which in turn would result in better pair-potentials. While we saw in chapter 4 that the 2nd order electron response captures most of the non-linear electron response, it remains to be seen how well the second-order pseudo-atom captures the full non-linear pseudo-atom when various approximations for the triplet liquid structure are used. Nevertheless, we conclude that techniques from liquid theory can be successfully combined with ideas from electron response theory, leading to new insight into electron-ion mixtures.

Bibliography

[1] For a review, see N.W. Ashcroft and D. Stroud, Solid State Physics **33**, 1 (1978).

[2] R. Car and M. Parrinello, Phys. Rev. Lett. **55** , 2471 (1985).

[3] See for example O. Sugino and R. Car, Phys. Rev. Lett. **74**, 1823 (1996).

[4] See for example R. Evans in *Fundamentals of Inhomogeneous Fluids*, edited by D. Henderson (Marcel Decker, New York 1992) or reference [5].

[5] N.W. Ashcroft in *Density Functional Theory*, edited by E.K.U. Gross and R.M. Dreizler (Plenum Press, New York 1995).

[6] H. Xu, J.-P. Hansen and D. Chandler, Europhys. Lett. **36** 419 (1994).

[7] J-P. Hansen and I. R. McDonald, *Theory of Simple Liquids*, (Academic Press, London (1986)).

[8] J. Chihara, Prog. Theor. Phys. **55**, 340 (1976).

[9] S. Ichimaru, S. Mitake, S. Tanaka and X-Z. Yan, Phys. Rev. A **32**, 1768 (1985).

[10] Y. Waseda, *The Structure of Non-Crystalline Materials* (McGraw-Hill, New York (1980)).

[11] J. K. Percus, Phys. Rev. Lett. **8**, 462 (1962).

[12] see for example: J. Chihara, J. Phys. C: Solid State Phys. **19**, 1665 (1986); J. Chihara, Phys. Rev. A **40**, 4507 (1989), and C. Dharma-wardana and F. Perrot, Phys. Rev. A **26**, 2096 (1982).

[13] J. Hafner, *From Hamiltonians to Phase Diagrams*, (Springer Verlag, Berlin, (1987)).

[14] H.W. Jackson and E. Feenberg, Rev. Mod. Phys. **34** 686 (1962); S. Ichimaru, Phys. Rev. A **2**, 494 (1970); F.Y. Wu and M.K. Chien, J. Math. Phys. **11**, 1912 (1970); L. L. Lee, J. Chem. Phys. **60**, 1197 (1974).

[15] See for example: J. L. Barrat, J. P. Hansen and G. Pastore, Molec. Phys. **63**, 747 (1987); A. Khein and N. W. Ashcroft, preprint (1997); A. Khein, PhD. thesis, Cornell University (1997).

[16] G. Kresse, J. Hafner Phys. Rev. B **47**, RC558 (1993).

Appendix A

Temporal Bell Inequalities

A.1 An Introduction to Temporal Bell Inequalities:

In a paper provocatively entitled "Quantum Mechanics versus Macroscopic Realism: Is the Flux There when Nobody Looks? A. J. Leggett and A. Garg[1] proposed a way to determine whether the magnetic flux of a SQUID (superconducting quantum interference device) was compatible with the postulates:

(A1) *Macroscopic Realism*: "A macroscopic system with two or more macroscopically distinct states available to it will at all times *be* in one or the other of these states."

(A2) *Noninvasive Measurability*: "It is possible, in principle, to determine the state of the system with arbitrary small perturbation on its subsequent dynamics."

The interest in SQUIDS arises because they may perhaps be prepared in "macroscopic" current superpositions, thus testing whether Quantum Mechanics(QM) holds

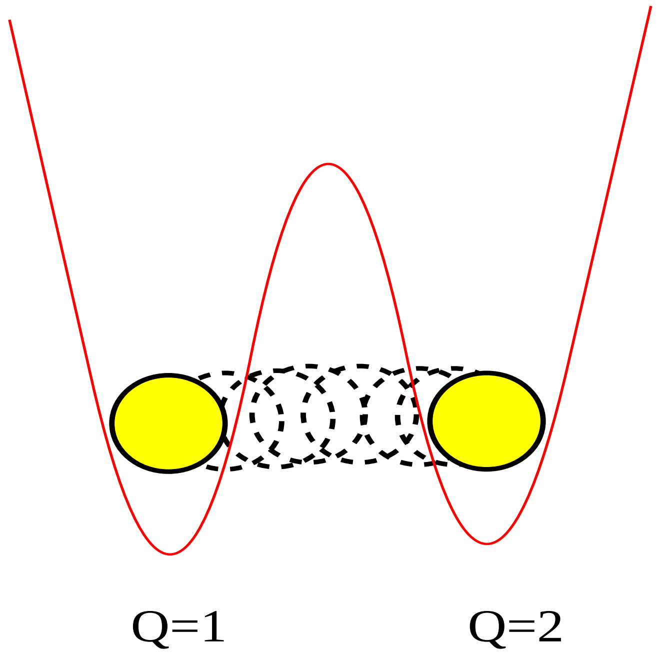

Figure A.1: **double-well potential for a tunneling particle**
A particle tunnels from one well to another. The variable Q measures in which well the particle is situated at a given time t_i.

on the macroscopic level. Let us consider a particle in a double well such as the one depicted in figure A.1 as a simple model.

Define an operator $\hat{Q}(t)$ which takes on the value $+(-)1$ when the particle is measured in the left(right) well. It then follows that for a set of times t_1, t_2, t_3, t_4, the (hypothetical) measurement values (eigenvalues) of the $Q's$ obey the relation:

$$-2 \leq Q(t_1)Q(t_2) + Q(t_2)Q(t_3) + Q(t_3)Q(t_4) - Q(t_1)Q(t_4) \leq 2 \qquad \text{(A.1)}$$

, where $Q(t)$ is a value of the operator $\hat{Q}(t)$. If one assumes *Macroscopic Realism* (A1), then Q(t) takes the meaning of a history or trajectory in some generalized coordinate space, at least if these histories exist in the sense that at any time the particle is one well, the histories Q(t) are an “element of reality”. Armed with this, define correlation functions by averaging over an ensemble of systems following different histories. The two-time correlation functions would be:

$$K_{12} = K(t_1, t_2) = \int [DQ] P[Q(t)] Q(t_1) Q(t_2). \tag{A.2}$$

The integral is over all histories, and $P[Q(t)]$ is the probability of obtaining a certain history in the given ensemble. By averaging the relation between the $Q(t)$'s of equation (A.1) over a given ensemble, we obtain a *Temporal Bell Inequality*:

$$|K_{12} + K_{23} + K_{34} - K_{14}| \leq 2, \tag{A.3}$$

as suggested by Leggett and Garg.

To measure the correlation functions of eq(A.2) one needs the assumption **(A2)** of *Noninvasive Measurability* because for a given history, $Q(t_2)$ is taken to be independent of what the measurement of $Q(t_1)$ gave. In other words, one wants a *conditionally independent representation* of the joint probability distributions. Thus the first analogy with the usual spatial Bell inequalities is that here, noninvasive measurability is similar to locality in space. In other words, the temporal Bell inequalities assume a "locality in time". The time correlation functions K_{ij} are similar to the spatial correlation functions used in the usual Bell inequalities.

But, in quantum theory one cannot assign a definite value to an observable until it has been measured (unless it is in an eigenstate of the measuring apparatus). Thus one cannot consistently define a probability for a given set of histories for time inequalities, and the temporal Bell inequalities can be violated. As a specific example of quantum dynamics consider the double well system of figure 1, but now in the case where it can be accurately approximated by the two-state Hamiltonian[2]:

$$H = -\frac{\hbar}{2} \Delta \sigma_{\mathbf{x}}. \tag{A.4}$$

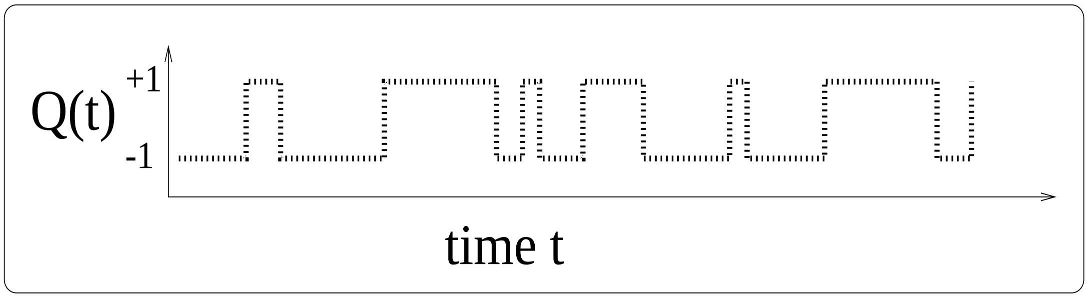

Figure A.2: **A classical history for a particle tunneling between two wells** The operator $\hat{Q}(t)$ takes on the definite value $Q(t) = +(-)1$ when the particle is measured in the left(right) well. Such classical "telegraph noise" histories do not exist for quantum coherent tunneling of the particle.

If the system is prepared in an eigenstate of the σ_z operator, i.e. it is in a definite $Q(t)$ state at time $t = t_1$, then the time correlation is given by:

$$K_{12} = cos(\Delta(t_1 - t_2)) \tag{A.5}$$

so that the time $(t_1 - t_2)$ is analogous to the angle between the polarization measured on each part of an EPR pair. It is not hard to find a set $\{t_1, t_2, t_3, t_4\}$ that violates the inequality (A.3)*. A set of histories such as is depicted in figure A.2 does not exist. Here one sees an immediate contrast to the spatial EPR which is usually formulated in terms of one state (the singlet state for spins or polarizations). In the temporal case, the measurement of any operator which does not commute with H can be made to violate certain inequalities for any initial state. But of course EPR can be formulated for many different states as well, it just has to stay in that state.

* Note that the measurements refer to independent measurements of members of the same ensemble with the same initial preparation at t_1 They are not subsequent measurements on the same system

A.2 Difficulties in Measuring the K_{ij}

The practical measurement of these time correlation functions is complicated by the general rule that an act of measurement in quantum mechanics affects the subsequent dynamics by back-action effects etc... In contrast to the spatial EPR case where special relativity can be invoked to ensure locality in space, no such principle exist to ensure locality in time. Another difficulty arises from the fact that to measure $\hat{Q}(t)$ at a precise time t one must assume an instantaneous "von Neumann" type collapse process, an approximation which may not be valid at all. The K_{ij} are also ensemble averaged, which could be either a large number of identical systems, or one system prepared in the same initial state each time. These difficulties led to some criticism shortly after the Leggett/Garg paper came out.

The critique by L. Ballentine

The first (at least in PRL) to criticize the measuring scheme of Leggett and Garg was Ballentine, who claimed that the contradiction with QM is produced solely by the assumption (A2) of noninvasive measurability[3]. His argument was based on an explicit measurement scheme that showed non violation of the Bell inequalities. But, his analysis was actually totally irrelevant, as he assumed that each system in an ensemble was measured at multiple times, say t_1, t_2, t_3 and t_4. This was then repeated to get an ensemble average. Even in QM the $Q(t_i)$ are taken to be real "elements of reality" when they're actually measured, so that dissipative measuring at say three subsequent times for the same system will give a third order distribution function that will trivially return the second order marginals which in turn determine the correlation functions. The latter will no longer violate the Bell inequalities[4].

The critique by A. Peres

Peres gave a different critique of the specific double well scenario with a semi-classical argument based on the uncertainty principle. It can easily be boiled down to the following:

To measure which well the particle is in, one needs to determine its coordinate with an accuracy $\Delta q \leq Q_0$, where Q_0 is the half the distance between the two wells. Together with the position momentum uncertainty principle $\Delta q \Delta p \geq \hbar$ this gives:

$$\Delta p \geq \hbar / Q_0. \tag{A.6}$$

But to get an appreciable tunneling amplitude:

$$\hbar \Delta \sim \exp - \int_{Q_0}^{Q_0} \frac{p(q)}{\hbar} dq \tag{A.7}$$

the integral in the exponent must not be much smaller than one. Peres approximates the integral by $p_0 Q_0/\hbar$, where p_0 is the classical momentum corresponding to the particle being at the bottom of a well so that one finds the second condition:

$$p_0 \leq \hbar / Q_0, \tag{A.8}$$

from which follows:

$$\Delta p \geq p_0, \tag{A.9}$$

and a measurement of sufficient accuracy to determine the position of the particle is seen to disturb it with enough momentum to kick it over the barrier, i.e. the measurement cannot be approximated by a simple "von Neumann" collapse of the wave function. However, a more careful analysis gives a window where $\Delta p < p_0$[6], so that Peres' argument doesn't hold under closer scrutiny; his approximations were too crude.

Ideal Negative Result Experiment

Both Peres and Ballentine fell prey to the idea that one must measure the particle position at times t_i and t_j separately to determine the joint probability densities. This works fine in the spatial EPR experiments which measure coincidence rates, but is not really necessary. The solution to the measurement problem is simply to measure the joint probability directly. This can be done by "Ideal Negative Result Experiments", an idea Leggett and Garg mentioned in their original paper, and which was worked out in great detail for SQUIDS by Tesche[7]. The basic idea is this: set up a measuring apparatus so it only measures (dissipatively) only one of the two well states (say $Q = 1$) at time t_1, and does a normal dissipative measurement at time t_2. Then one can measure $K_{12}^{-} = K(-, t_1; Q, t_2)$ by only counting those runs in which the first measurement apparatus gave a null result (and, one assumes, didn't affect the system) which corresponds to $Q(t_1) = -1$. The same can be repeated with the opposite arrangement for t_1 to give K_{12}^{+} (but the same ensemble), from which one can easily extract the full correlation function $K_{12} = K_{12}^{-} + K_{12}^{+}$, and see if it violates the Bell inequalities, and thus also the condition (A1) of *Macrorealism*, But even in this scheme, there is one unresolved difficulty, as in general there will be but one system on which to measure repeatedly, and it will be hard to get it into exactly the same initial state each time to insure one is measuring the same ensemble!

A.3 Conclusions

The temporal Bell inequalities are thus shown to be demonstrable in principle, and they have many direct analogies with spatial Bell inequalities. When they are violated as predicted by QM, one cannot assign consistent probabilities to the histories, and the idea of *Macrorealism* is no longer valid. There is nothing conceptually new in this, but the violation of the Bell inequalities has a nice interpretation in that one cannot assign a consistent history (i.e. one cannot represent the position of the particle by telegraph noise such as is depicted in figure A.2), and as such this provocatively demonstrates how classical ideas of reality break down at the quantum level. An additional point of interest would be to measure the violation of these inequalities in SQUIDS where the flux variable can be regarded as macroscopic in itself, but still obey quantum mechanics for its dynamics. However, the condition of "locality in time" is much more difficult to ensure than is "locality in space" due to the difficulties in the measurement problem, and because there is nothing analogous to special relativity to separate the time processes. It may be interesting to generalize the temporal Bell inequalities to the more modern (and spectacular) GHZ type[8, 9] relations, thus avoiding the problem of ensemble preparation. While it is not hard to see how to measure products of more than two observables with the two state system, one cannot measure the analogon of more than one plane of EPR polarization so it is not immediately obvious what system is needed to study GHZ correlations.

Bibliography

[1] A.J. Leggett and A. Garg, Phys. Rev. Lett. **54**, 857 (1985), **54**, 2724 (1985).

[2] This approximation can be justified if the tunneling amplitude $\hbar\Delta$ is much less than the intra-well small oscillation frequency $\hbar\omega_0$ which is in turn much smaller than the well depth V_0. We also assume that the two wells are degenerate in energy.

[3] L.E. Ballentine Phys. Rev. Lett. **59**, 1493 (1987); see also the reply by A.J. Leggett and A. Garg, Phys. Rev. Lett. **59**, 1621 (1987)

[4] This follows from the existence of the third order distribution function. See for example N.D. Mermin, Lecture Notes I, Cornell, Fall '95.

[5] A. Peres Phys. Rev. Lett. **61**, 2019 (1988); see also the reply by A.J. Leggett and A. Garg, Phys. Rev. Lett. **63**, 2156 (1989).

[6] A.A. Louis and J. P. Sethna Phys. Rev. Lett. **74**, 1363 (1995).

[7] C. D. Tesche Phys. Rev. Lett. **64**, 2358 (1990). See also: J. P. Paz and G. Mahler, Phys. Rev. Lett. **71**, 3235 (1993).

[8] D. M. Greenberger, M.A. Horne A. Shimony and A. Zeilinger, Am J. Phys. **58**, 1131 (1990).

[9] N.D. Mermin, Rev. Mod. Phys. **65** 803,(1993).

Appendix B

Coupling of the tunneling atom to Raleigh surface phonons: Ohmic dissipation

Ohmic dissipation occurs when the spectral density $J(\omega)$ is linear in the frequency ω[1], i.e.:

$$J(\omega) = \sum_{\alpha} \frac{(\lambda_\alpha)^2}{m\omega_\alpha} \delta(\omega - \omega_\alpha) \sim \omega. \tag{B.1}$$

A given λ_α is the coupling to the linear coordinate of the environment oscillator (phonon) α in the total Hamiltonian.

In the case of coupling to bulk modes with an external (*monopole*) force[2]*, the coupling goes as:

$$\lambda_k \sim \frac{1}{\sqrt{N}} \tag{B.2}$$

* The use of the word force is an unfortunate misnomer: force is a purely classical concept. Instead this should be the gradient of the potential. However, in keeping with common conventions in the literature, we continue to use the rather akward word force.

where N is the number of atoms. In the case of the bulk waves it is thus independent of k, which gives ohmic dissipation.

For Rayleigh modes there is a penetration depth of $1/\kappa$, where

$$\kappa = \sqrt{k_{||}^2 - \omega^2/c^2} = (\sqrt{1-\xi^2})k_{||}. \tag{B.3}$$

The function ξ can be found in Landau and Lifshitz[3] section (**24**) and depends on one elastic constant only. The momentum parallel to the surface is denoted by $k_{||}$. The number of atoms N that participate in an oscillation are proportional to the number of surface atoms N_s times the penetration depth $1/\kappa$ so that for a given parallel momentum $k \parallel$ the coupling constant goes as:

$$\lambda_k \sim \frac{1}{\sqrt{N_s/\kappa}} \sim \sqrt{k_{||}}. \tag{B.4}$$

When this form of λ_k is plugged into the spectral density (eq B.1) the extra factor k compensates for the 2-dimensional density of states which is proportional to ω.

All this can be put on a firmer footing by writing the displacement field as:

$$\vec{u}(\vec{r}) = \sum_s \sum_k \frac{1}{\sqrt{C}} \sqrt{\frac{\hbar}{2m\omega(\vec{k},s)}} \left(a_{\mathbf{ks}} + a^\dagger_{\mathbf{ks}}\right) \exp\left(i\vec{k}_{||}\cdot\vec{r}\right) \exp\left(\kappa z\right) \exp\left(-i\omega t\right) \tag{B.5}$$

Here $\mathbf{k}$ is the wave vector, and s is a polarization index.

By demanding that each mode α contributes an elastic energy $\hbar\omega a^\dagger_\alpha a_\alpha$, and then by equating two times the kinetic energy to the total energy :

$$2E_{kin} = \int \rho \mid \dot{u} \mid^2 = \sum_\alpha \hbar\omega a^\dagger_\alpha a_\alpha \tag{B.6}$$

one finds the normalization constants C. The coupling term in the Hamiltonian to first approximation is:

$$H_{int} = \vec{F}\cdot\vec{u}(\vec{0}) \tag{B.7}$$

from which the coupling constants $\{\lambda_k\}$ directly follow for the different kinds of modes.

Bibliography

[1] See: A. J. Leggett *et al.*, Rev. Mod. Phys. **59**, 1 (1987)

[2] A.A. Louis and J.P. Sethna, Phys. Rev. Lett. **74**, 1363 (1995).

[3] L.D. Landau and E.M. Lifshitz, *Theory of Elasticity*, Pergamon, London (1959).

Appendix C

Finite Temperature Hohenberg-Kohn-Mermin Theorem for Multi-Component Charged Systems

C.1 Introduction

Two versions of the H-K-M theorem for multi-component charged systems are proven. One for a neutral canonical ensemble, and one for a grand-canonical ensemble. Neither proof needs a Born-Oppenheimer approximation.

C.2 Neutral Canonical Ensemble

Consider a multicomponent system of charged particles at constant volume, and particle numbers, and in contact with an external heat bath - i.e. at constant temperature T. The particle numbers of each component are chosen so that the overall system is neutral.

The equilibrium properties of such a system are governed by the canonical statistical density operator:

$$\hat{\rho}_0 = \exp[-\beta \hat{H}]/Tr\left[\exp[-\beta \hat{H}]\right] \tag{C.1}$$

where the Hamiltonian operator $\hat{H}$ has the form:

$$\hat{H} = \hat{T} + \hat{U} + \hat{V}, \tag{C.2}$$

$\hat{V}$ is a series of one-body terms of the form:

$$\hat{V} = \sum_i \int \hat{n}_i(\vec{r}) v_i(\vec{r}) d\vec{r} \tag{C.3}$$

where the $\{v_i(\vec{r})\}$ are the external potentials and the $\{\hat{n}_i(\vec{r})\}$ satisfy the following neutrality constraint on their integrated ensemble averages:

$$\sum_i Z_i \int n_i(\vec{r}) d\vec{r} = 0. \tag{C.4}$$

The $\{Z_i\}$ are the charges of each constituent and the one particle densities $\{n_i(\vec{r})\}$ are given by:*

$$n_i(\vec{r}) = Tr\left[\hat{\rho}_0 \hat{n}_i(\vec{r})\right]/Tr\hat{\rho}_0, \tag{C.5}$$

where $\hat{\rho}_0$ is the equilibrium density matrix of eq (C.1). Now define the functional:

$$F[\hat{\rho}] = Tr\left[\hat{\rho}\left(\hat{H} + \frac{1}{\beta}\ln\hat{\rho}\right)\right] \tag{C.6}$$

---

* For a canonical system the trace is only over states with the particle number fixed beforehand, so the constraint (C.4) holds at the level of the *operators* $\hat{n}(\vec{r})$ also.

for an arbitrary density operator $\hat{\rho}$ with unit trace. Mermin has shown that at equilibrium, this functional satisfies a minimum property †

$$F[\hat{\rho}] > F[\hat{\rho}_0] \quad \text{for} \quad \hat{\rho} \neq \hat{\rho}_0. \tag{C.7}$$

By equating the minimum of $F[\hat{\rho}]$ with the Helmholtz free energy F:

$$F[\hat{\rho}_0] = -\frac{1}{\beta} \ln Tr \left[\exp\left[-\beta \hat{H}\right]\right] = F, \tag{C.8}$$

contact is made with Thermodynamics.

For a given $\hat{T}$ and $\hat{U}$, the external potential $\hat{V}$ determines the equilibrium density $\hat{\rho}$ - giving the surjective map A:

$$A: \quad \hat{V} \quad \rightarrow \hat{\rho}. \tag{C.9}$$

A given density matrix $\hat{\rho}$ determines the densities $\{\hat{n}_i(\vec{r})\}$ by equation(C.5), giving the map B:

$$B: \quad \hat{\rho} \quad \rightarrow \{n_i(\vec{r}\}, \tag{C.10}$$

which is also surjective.

The H-K-M proof then goes as follows - first we show that both A and B are injective (one to one) and thus bijective (fully invertible)[4].

For a one-component system the injectivity of A can easily be shown, but the statement : a given set $\{v_i(\vec{r})\}$ leads to a unique equilibrium density matrix $\hat{\rho}_0$, while plausible, can't be rigorously proven for multi-component systems such as the

† In the Appendix of his paper[1], Mermin shows the minimum principle for a grand-canonical ensemble. The proof carries through identically for a canonical ensemble. Only very general properties of the density matrix are used (such as positive definiteness), so that the proof also carries over to multi-component systems with no change, except that the density matrix is now understood to carry the information of the full multi-component system

one under consideration, or for that matter, spin-polarized systems with an external magnetic field[4]. We will assume it is true; a proof is lacking.

The injectivity of the map B can be shown by the following argument:

Assume that two different external potential sets $\{v_i(\vec{r})\}$, and $\{v_i'(\vec{r})\}$[‡] with equilibrium densities $\hat{\rho}_0$, and $\hat{\rho}_0'$ give the same set of external densities $\{n_i(\vec{r})\}$. Then:

$$\begin{aligned} F' &= Tr\left[\hat{\rho}_0'\left(H' + \frac{1}{\beta}\ln\hat{\rho}_0'\right)\right] \\ &< Tr\left[\hat{\rho}_0\left(H' + \frac{1}{\beta}\ln\hat{\rho}_0\right)\right] \\ &< F + Tr\left[\hat{\rho}_0\left(V' - V\right)\right] \end{aligned} \tag{C.11}$$

so that:

$$\begin{aligned} F' &< F + Tr\left[\hat{\rho}_0\sum_i\int d\vec{r}\left(v_i'(\vec{r})\hat{n}_i(\vec{r}) - v_i(\vec{r})\hat{n}_i(\vec{r})\right)\right] \\ &= F + \sum_i\int\left(v_i'(\vec{r}) - v_i(\vec{r})\right)n_i(\vec{r}). \end{aligned} \tag{C.12}$$

Simply interchanging the primes (reversing the designation of the two systems) gives:

$$F \;<\; F' + \sum_i\int\left(v_i(\vec{r}) - v_i'(\vec{r})\right)n_i(\vec{r}). \tag{C.13}$$

Adding (eq C.12) and (eq C.13) gives:

$$F + F' < F' + F, \tag{C.14}$$

an evident contradiction, from which it follows that a given density matrix and external potential set $\{v_i(\vec{r})\}$ uniquely determines the density set $\{n_i(\vec{r})\}$, so that the map B is indeed injective.

[‡] Different means more than a constant difference for canonical systems, this is not necessary for a grand-canonical ensemble

Thus for a given $\hat{T}$ and $\hat{U}$ in the original Hamiltonian of equation (C.2) the density matrix is a unique functional of the set of external densities, and the same is true of the free energy functional $F[\{n\}]$, which obeys the minimum principle that the Helmholtz Free energy is given by the set of $\{n_i(\vec{r})\}$ which minimize the functional F. (With the understanding that the $\{n_i(\vec{r})\}$ satisfy the neutrality constraint)

C.3 Grand Canonical Ensemble

The proof for a multi-component charged Grand-Canonical ensemble is quite similar. Simply replace F with Ω, and V with $V - \mu N$, where μ is really a set of chemical potentials. The neutrality constraint (C.4) now holds for the averages only, and no longer at the level of the operators, but that was never necessary for the proof.

One possible subtlety would be if one were to do a constrained trace, i.e. a trace over neutral states. Then the states one traces over will depend on the particular V, and so perhaps different ρ_0's could give identical $\{n_i(\vec{r})\}$'s just because the states change. However, this problem is circumvented by the realization that the constrained trace is equal to the full trace, which is independent of the external potential used (the Lieb-Lebowitz result[5]).

C.4 Some Comments

- Firstly, the proof only goes for a set, so a given one-body density $n_i(\vec{r})$ may be produced by two different sets of external potentials, but the sets $\{n_i(\vec{r})\}$ will be different.

- Secondly, notice that no Born-Oppenheimer assumptions are needed. In the usual electronic H-K theorem, the assumption is that all the $\{n_i(\vec{r})\}$ are externally fixed except the electronic density $n_e(\vec{r})$. This is basically the B-O theorem, the electrons relax while the ions are frozen. Only the potential that couples to the electrons is varied. From the multi-component proof we did it is clear that if all external potentials save one are fixed, the one particle density of that one component must change if it is external potential changes, but there is still a freedom for the other one-particle densities to change. The usual H-K theorem assumes they stay fixed, and are part of the $\hat{T}+\hat{U}$ terms. Similarly in the B-O approximation for classical ions, the ions now have some effective (many-body) interaction $U_{eff}(\{r_i\})$ which may depend on all the ionic coordinates, but as long as it is expressible as a potential, the usual H-K-M theorem goes through. All electronic effects are put into the effective interaction beforehand.

Bibliography

[1] N.D. Mermin, Phys. Rev. **137** A1441 (1965).

[2] P. Hohenberg and W. Kohn, Phys. Rev. **136**, B864 (1964).

[3] N.W. Ashcroft, in *Density Functional Theory*, Edited by E.K.U. Gross and R.M. Dreizler, Plenum Press, New York (1995).

[4] R.M. Dreizler and E.K.U. Gross, *Density Functional Theory* Springer Verlag, Berlin 1990.

[5] E.H. Lieb and J.L. Lebowitz, Adv. in Math. **9**, 316 (1972).

Appendix D

Non-linear response functions

In a homogeneous electron gas with a rigid neutralizing background, a perturbing potential $\lambda v(q)$ induces a charge density:

$$\rho^{ind}(k) = \lambda\chi_1(k)v(k) + \lambda^2 \sum_{\vec{k}_1}\sum_{\vec{k}_2} \chi_2(k, k_1, k_2)v^{ps}(k_1)v^{ps}(k_2) + ..., \tag{D.1}$$

where $\rho^{ind}(k)$ is measured w.r.t. the homogeneous density ρ_0. From the Hohenberg-Kohn-Sham formulation[1, 2] the identical problem can be set-up in terms of the response of non-interacting electrons to the effective potential $\Gamma(q)$:

$$\rho^{ind}(k) = \chi_1^0(k)\Gamma(k) + \sum_{\vec{k}_1}\sum_{\vec{k}_2} \chi_2^0(k, k_1, k_2)\Gamma(k_1)\Gamma(k_2), \tag{D.2}$$

where the effective potential is given by:

$$\Gamma(k) = \lambda v(k) + \frac{8\pi}{k^2}\rho^{ind}(k) + \mu_{xc}(k, [\rho]), \tag{D.3}$$

and the $\chi_i^0(..)$ denote the non-interacting response-functions, which are properties of the *homogeneous* electron gas. The induced density can be expanded in powers of λ:

$$\rho^{ind}(k) = \lambda\rho_1(k) + \lambda^2\rho_2(k) + \lambda^3\rho_3(k) + ... \tag{D.4}$$

and the exchange-correlation potential $\mu_{xc}(q,[\rho])$ can be expanded in powers of the induced density $\rho^{ind}(k)$:

$$\mu(k,[\rho^{ind}]) = \mu_1(k)\rho^{ind}(k) + \sum_{\vec{k}_1}\sum_{\vec{k}_2}\mu_2(k,k_1,k_2)\rho^{ind}(k_1)\rho^{ind}(k_2) + ... \tag{D.5}$$

The full interacting response functions are found by equating powers of λ in (D.1) and (D.2). The first order interacting response function is:

$$\chi_1(k) = \frac{\chi_1^0(k)}{\epsilon(k)}, \tag{D.6}$$

and the second order interacting response function is:

$$\chi_2(k_1,k_2,k_3) = \frac{\chi_2^0(k_1,k_2,k_3) + \frac{1}{2}\mu_2(k_1,k_2,k_3)\chi_1^0(k_1)\chi_1^0(k_2)\chi_1^0(k_3)}{\epsilon(k_1)\epsilon(k_2)\epsilon(k_3)}. \tag{D.7}$$

The third order interacting response function (neglecting the μ_i (i.e. setting them to 0) is

$$\begin{aligned}\chi_3(k_1,k_2,k_3,k_4) &= \Big\{\chi_3^0(k_1,k_2,k_3,k_4) \\ &\quad +2\chi_2^0(k_1,k_2,k_3+k_4)v_c(k_3+k_4)\chi_2^0(k_3+k_4,k_3,k_4)\Big\} / \\ &\quad \{\epsilon(k_1)\epsilon(k_2)\epsilon(k_3)\epsilon(k_4)\}, \end{aligned} \tag{D.8}$$

and so forth. The dielectric function $\epsilon(k)$ is given by:

$$\epsilon(k) = 1 - \left(\frac{8\pi}{k^2} + \mu_1(k)\right)\chi_0^1(k). \tag{D.9}$$

Expressions for the first and second order non-interacting response functions are known: the first order was first derived by Lindhard in 1954[3]:

$$\chi_1^0(k) = \frac{-k_F}{2\pi^2}\left(\frac{1}{2} + \frac{4k_F^2 - k^2}{8k_F k}\ln\left|\frac{k+2k_F}{k-2k_F}\right|\right), \tag{D.10}$$

the second order was first derived by Lloyd and Sholl in 1968[4], and has a much more complex form*. We plot the non-interacting, exchange-correlation, and full

* The full form is too long to put in this thesis, readers can consult reference [4] or alternatively, access the following: "http://www.lassp.cornell.edu/~ardlouis/Thesis/Lloyd_Sholl.html" .

response in figures (D.1 -D.3).

For a given exchange-correlation potential $\mu_{xc}(r,[\rho])$, the functions $\mu_n(r)$ are the functional derivatives :

$$\mu_n(r;r_1..r_j) = \left.\frac{\delta^j \mu_{xc}(r)}{\delta\rho(r_1)..\delta\rho(r_j)}\right|_{\{\rho(r_1)...\rho(r_j)\}\rightarrow\{\rho_0...\rho_0\}} . \tag{D.11}$$

When the LDA approximation to the exchange-correlation potential is employed, the $\mu_i(..)$ reduce to a simple functions of ρ in the homogeneous limit; there is no q dependence.

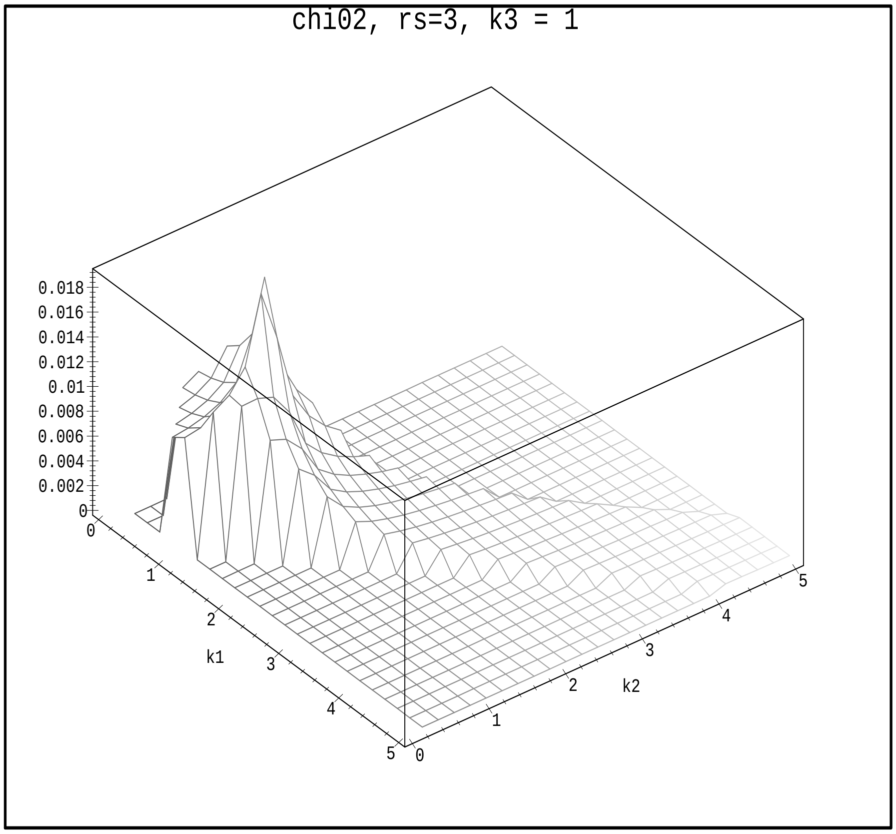

Figure D.1: **Non-interacting $\chi_2^0(k_1, k_2, k_3 = 1)$ for $rs = 3$ and fixed k_3.** The second-order response function $\chi_2^0(k_1, k_2, k_3)$ for non-interacting electrons was taken from reference[4]. As the fixed variable k_3 changes, so does $\chi_2^0(k_1, k_2, k_3)$, but the function remains highly peaked around $k_i = 2k_F$. The function volume is restricted by the limits $(k_3 < k_1 + k_2)$, $(k_1 < k_2 + k_3)$ and $(k_2 < k_3 + k_1)$, which stem from the delta-function constraint 4.15 and must be simultaneously satisfied. Here, $2k_f = 1.28$ a.u.

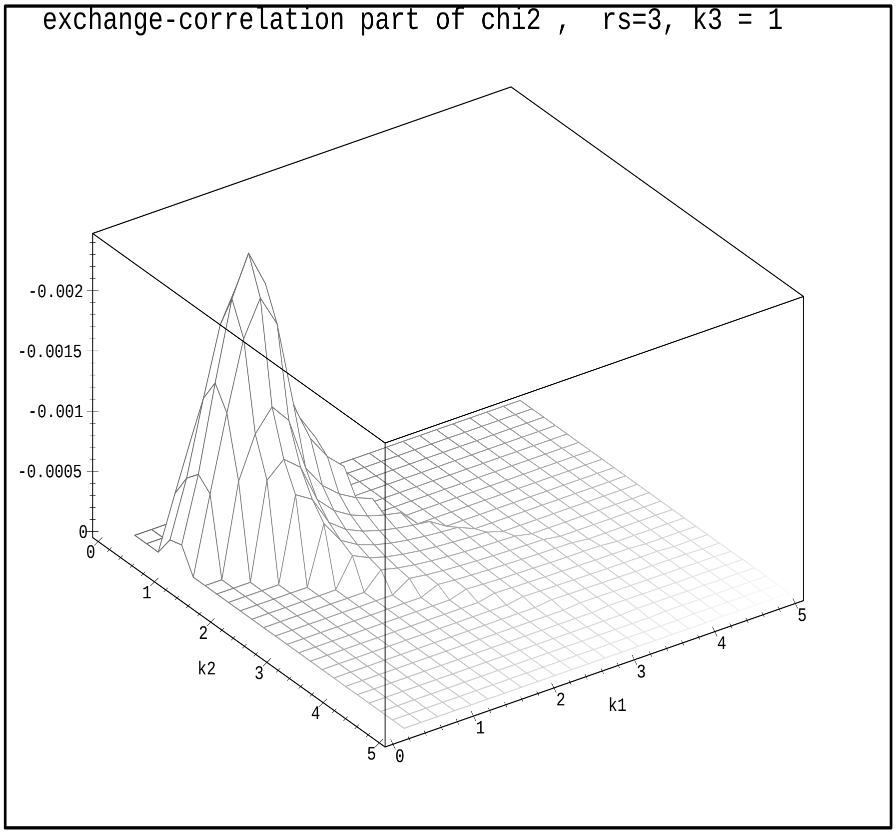

Figure D.2: **LDA exchange-correlation contribution to response for $rs = 3$ and fixed k_3.**
The exchange-correlation contribution to the second-order response function (D.7) has the form:

$$\chi_2^{xc}(k_1, k_2, k_3) = \frac{1}{2}\frac{\mu_2(k_1, k_2, k_3)\chi_1^0(k_1)\chi_1^0(k_2)\chi_1^0(k_3)}{\epsilon(k_1)\epsilon(k_2)\epsilon(k_3)}.$$

We plot it for an LDA form of $\mu_2(k_1, k_2, k_3)$, which has no k dependence; it is a function of density only. Note the inverted axes: this contribution *weakens* the response. The function volume is restricted by the limits $(k_3 < k_1+k_2)$, $(k_1 < k_2+k_3)$ and $(k_2 < k_3+k_1)$, which stem from the delta-function constraint 4.15 and must be simultaneously satisfied. Here, $2k_f = 1.28$ a.u.

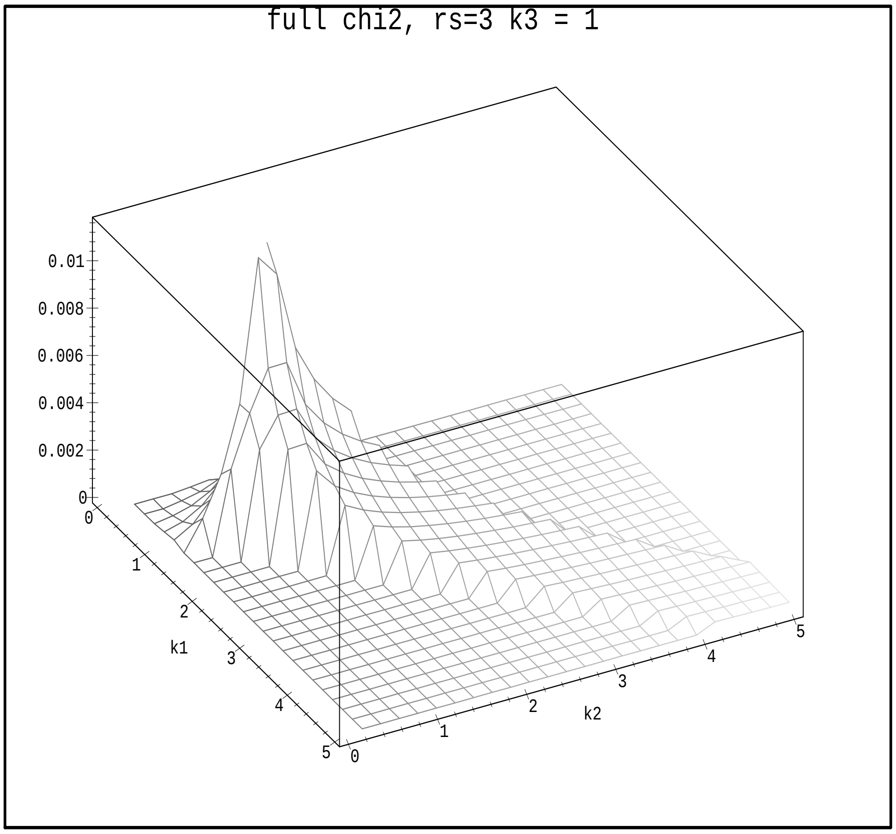

Figure D.3: **Full** $\chi^2(k_1, k_2, k_3 = 1)$ **from (D.7) for** $rs = 3$ **and fixed** k_3**.** As the fixed variable k_3 changes, so does the second order response function $\chi_2(k_1, k_2, k_3)$, but the function remains highly peaked around $k_i = 2k_F$. The function volume is restricted by the limits $(k_2 < k_1 + k_2)$, $(k_1 < k_2 + k_3)$ and $(k_2 < k_3 + k_1)$, which stem from the delta-function constraint 4.15 and must be simultaneously satisfied. Here, $2k_f = 1.28$ a.u.

Bibliography

[1] P. Hohenberg and W. Kohn, Phys. Rev. **136**, B864 (1964).

[2] W. Kohn and L.J. Sham, Phys. Rev. **140**, A1133 (1965).

[3] J. Lindhard, K. Dan. Vidensk. Selsk. Mat. Fys. Medd. **28**, 28 (1954).

[4] P. Lloyd and C. Sholl J. Phys. C **1**, 1620 (1968). see also:E.G. Brovman, Yu. Kagan, A. Holas, Sov. Phys. JETP **34**, 1300 (1972).